

University of Alberta

Odour Perception Model with Concentration Fluctuations

by

Kelly Lisa Hughes



A thesis submitted to the Faculty of Graduate Studies and Research in
partial fulfillment of the requirements for the degree of Master of Science

Department of Mechanical Engineering

Edmonton, Alberta

Spring 2004

UMI Number: MQ96489

INFORMATION TO USERS

The quality of this reproduction is dependent upon the quality of the copy submitted. Broken or indistinct print, colored or poor quality illustrations and photographs, print bleed-through, substandard margins, and improper alignment can adversely affect reproduction.

In the unlikely event that the author did not send a complete manuscript and there are missing pages, these will be noted. Also, if unauthorized copyright material had to be removed, a note will indicate the deletion.

UMI[®]

UMI Microform MQ96489

Copyright 2005 by ProQuest Information and Learning Company.

All rights reserved. This microform edition is protected against unauthorized copying under Title 17, United States Code.

ProQuest Information and Learning Company
300 North Zeeb Road
P.O. Box 1346
Ann Arbor, MI 48106-1346

Abstract

An engineering model is developed for human odour annoyance to predict how odour perception and annoyance will change from breath to breath based on exposure history, odorant type and individual sensitivity. This model uses instantaneous concentration fluctuations, time constants that describe how people detect, desensitize, and resensitize to odours, and a non-linear function for perceived intensity to evaluate current and mean levels of odour annoyance. The model is tested at full-scale atmospheric crosswind and downwind positions using time series of scaled-up fluctuations from laboratory-scale, water channel data. Comparing trends predicted using this model and current regulatory models based on mean concentrations, it is shown that airborne odorants are far more persistent downwind and crosswind than currently predicted by regulatory agencies; consequently the size of area affected by odour annoyance is currently underestimated.

Dedication

For my soon-to-be husband Graeme

Acknowledgements

I would like to thank Dr. David J. Wilson for his guidance and support throughout this project. I will fondly carry his teachings with me.

Additional financial support was provided by the Teagle Foundation and the Government of Alberta, for which I am very grateful.

I would like to thank Trevor Hilderman, Sean Kirkwood and Wayne Pittman for their technical and moral support, as well as the Department of Mechanical Engineering machine shop staff and technicians for their high quality of workmanship and technical assistance.

I sincerely appreciate the love and support my family and friends have given me, without which this would not have been possible. Thank you.

Contents

1	Introduction to Atmospheric Dispersion and Odour Perception	1
1.1	Motivation.....	1
1.2	Background to Odour Perception.....	2
1.2.1	Mechanisms of Human olfaction	2
1.2.2	Psychophysics	3
1.2.2.1	Thresholds.....	3
1.2.2.2	Perceived Intensity	4
1.2.2.3	Adaptation, Habituation and Recovery.....	5
1.2.3	Population Distribution	7
1.2.4	Hyper-sensitivity	7
1.2.5	Summary	8
1.3	Background to Atmospheric Dispersion.....	8
1.3.1	Predicting Plume Concentrations in Atmospheric Dispersion ...	9
1.3.2	Simulating Atmospheric Concentration Fluctuations in Plumes	10
1.4	Odour Annoyance Model.....	11
1.4.1	Overview of Chapter 2 – Model for Human Odour Annoyance.....	11
1.4.2	Overview of Chapter 3 – Predicting Full-scale Concentration Fluctuation Statistics and Water Channel Scale-up Technique	12
1.4.3	Overview of Chapter 4 – Evaluation of Odour Annoyance Model for Neutral Atmospheric Satiability.....	12
1.4.4	Predicting Outcomes of the Odour Annoyance Model	12
1.4.5	Results of Applying the New Odour Annoyance Model	13
2	Introduction to Atmospheric Dispersion and Odour Perception	17
2.1	Introduction	17
2.2	Current Odour Models	17
2.2.1	Concentration, Duration and Frequency	18
2.2.2	Detection Threshold, Perceived Intensity and Tolerance Threshold.....	20
2.2.3	Improving Existing Odour Models.....	22
2.3	Psychophysical Model for Human Odour Annoyance	23
2.3.1	Concentration Fluctuations in the Atmosphere.....	23
2.3.2	Available Concentration	23
2.3.3	Variable Detection Threshold – Desensitization and Resensitization	25
2.3.4	Effective Concentration.....	26
2.3.5	Perceived Intensity	27
2.4	Psychological Model for Human Odour Annoyance.....	29

2.4.1	Memory Window	29
2.4.2	Memory Load	30
2.4.3	Ensemble Average Memory Load.....	31
2.5	Summary	32
3	Predicting Full-Scale Concentration Fluctuation Statistics and Water Channel Scale-up Technique	41
3.1	Introduction	41
3.2	Statistics Currently Used to Model Odour Annoyance	42
3.2.1	Gaussian Dispersion Model	42
3.2.2	Peak-to-Mean Values	43
3.3	Description of Instantaneous Concentration Fluctuations	44
3.3.1	Use of Concentration Fluctuations in Mean Memory Load.....	46
3.3.2	Simulating Full-scale Concentration Fluctuations by Scaling Water Channel Data	48
3.4	Predicting Full-scale Concentration Fluctuation Statistics	48
3.4.1	Mean Concentration	49
3.4.2	Non-dimensional Shear	54
3.4.3	Concentration Integral Time Scale, T_c	58
3.4.4	Concentration Fluctuation Intensity, i	62
3.4.5	Conditional (In-Plume) Concentration Fluctuation Intensity, i_p	64
3.4.6	Intermittency Factor, γ	65
3.4.7	Variation of Plume Statistics with Averaging Time	66
3.4.8	Summary of Calculating Full-scale Plume Statistics	66
3.5	Water Channel Scale-up Techniques	67
3.5.1	Water Channel Experiments	68
3.5.2	Scaling Mean Concentration, C_{avg}	69
3.5.3	Scaling Time Scales	70
3.6	Summary	73
4	Evaluation of Odour Annoyance Model for Neutral Atmospheric Stability	91
4.1	Introduction	91
4.2	Parametric Study of Psychophysical Functions of Odour Annoyance Model	92
4.2.1	Base Detection Threshold	93
4.2.2	Desensitization and Resensitization Time Constants	94
4.2.3	Odour Intensity Exponent	95
4.2.4	Memory Window Length	96
4.2.5	Summary of Psychological and Physical Parameters of Odour Annoyance Model	96

4.3	Predicted Odour Annoyance with Mean Memory Load for Full-scale Case Study	98
4.3.1	Variation in Mean Memory Load with Averaging Time	99
4.3.2	Crosswind and Downwind Variation in Mean Memory Load ...	100
4.3.2.1	Crosswind Mean Memory Load	100
4.3.2.2	Downwind Mean Memory Load	101
4.4	Downwind and Crosswind Comparison with Current Practices	101
4.5	Total and Detectable Memory Loads	103
4.5.1	Crosswind Comparison of Total and Detectable Memory Loads	104
4.5.2	Downwind Comparison of Total and Detectable Memory Loads	105
4.6	Comparison of Odour Load with Toxic Effects	105
4.7	Indoor Sheltering	106
4.7.1	Predicting Time Series of Indoor Concentration Fluctuations ..	106
4.7.2	Mean Memory Loads for Indoor Fluctuations	108
4.8	Summary	108
5	Summary and Conclusions	127
5.1	Summary of Odour Annoyance Model	127
5.2	Conclusions	128
5.3	Future Work	128
	References	130

List of Figures

1.1	Cumulative distribution for percent of population detection, recognition, annoyance and physical irritation by concentrations of hydrogen sulphide	14
1.2	Illustration of desensitization (adaptation/habituation) and resensitization (recovery) processes governing how people react to changing concentration of odorants.....	15
1.3	Gaussian compared with instantaneous profile in the cross-stream direction	16
2.1	Odour unit intensity converts regulatory odour units to perceived intensity, based on Stevens' Law	34
2.2	Variable detection threshold, $c_{th, vary}$, desensitization and resensitization time constants, τ_{de} and τ_{re} respectively. Effective concentration, c_{eff} , is the difference between available concentration and the variable detection threshold, for times when $c_{avail} > c_{th, vary}$	35
2.3	Illustration of the concept of available concentration	36
2.4	Behaviour of the variable detection threshold model. Shaded regions shows detectable odour	37
2.5	Effect of increasing peak and zero concentration periods for equal desensitization and resensitization time constants.....	38
2.6	Illustration and definition for model of perceived intensity, I	39
2.7	Illustration for the calculation of the time varying memory load, L , at three time steps.....	40
3.1	Gaussian distributions with variable averaging times	75
3.2	Cross-section through instantaneous dispersing plume	76
3.3	Parameters describing concentration fluctuations	77
3.4	Typical experimental concentration fluctuation time series	78
3.5	A concentration exposure made up of simple step functions	79

3.6	Variation in crosswind mean concentration normalized with concentration at full-scale reference position 1.0 km downwind from odorant source, on plume centerline	80
3.7	Change in mean concentration profile, C_{avg} , plume spread, σ_z , and convection velocity, U_c , for a ground level source in atmospheric stability class D	81
3.8	Comparison of log-law velocity profile, for neutral stability, with power-law velocity profile	82
3.9	Downwind variation in mean concentration, caused by vertical and crosswind plume spreads for neutral stability and 180 min averaging time.....	83
3.10	Concentration integral time scale, $T_{c, shear}$ levels-off beyond 2.0 km downwind of odorant source.....	84
3.11	Crosswind variation in plume concentration parameters	85
3.12	Downwind variation in plume concentration parameters	86
3.13	Side-view schematic used in the set-up of water channel measurements for the experimental data used in this study.....	87
3.14	Normalized vertical velocity profile, U/U_H , for water channel	88
3.15	Illustration of scaling approach from water channel data to full-scale concentration and time by stretching mean concentrations (a) and concentration integral time scale (b).....	89
3.16	Autocorrelation of streamwise fluctuating velocity for a flow with inertia, R_{uu} , compared to flow without inertia	90
4.1	Insensitivity of mean memory load to base odour detection threshold for full-scale simulations at plume centerline and edge, 1.0 km downwind.....	111
4.2	Sensitivity of mean memory load, L_{avg} , to desensitization (a) and resensitization (b) time constants, τ_{de} and τ_{re} for full-scale simulation on plume centreline, 1.0 km downwind	112
4.3	Sensitivity of mean memory load, L_{avg} , to desensitization and resensitization time constants, τ_{de} and τ_{re} for full-scale simulation on plume centreline (a) and on the plume edge (b), 1.0 km downwind	113

4.4	More than a 550% variation in mean memory load, L_{avg} , for a factor of 4.0 variation in perceived intensity exponent, n , for full-scale simulation at plume edge; compared with less than 5% variation in L_{avg} at plume centerline	114
4.5	Schematic of simulated full-scale crosswind and downwind time series used to evaluate odour annoyance model	115
4.6	Less than 15% variation in mean memory load for a factor of 60 increase in averaging time on simulated full-scale plume centerline	116
4.7	Perceived memory load changes gradually across the plume; compared to rapid decrease in regulatory odour load at plume edge	117
4.8	Perceived odour changes gradually downwind; compared with rapid decrease in regulatory odour load	118
4.9	Crosswind comparison of total and detectable (zero effective concentrations removed) mean odour loads (a), and (b) between odour and concentration intermittencies	119
4.10	Downwind comparison of total and detectable (zero effective concentrations removed) mean odour loads (a), and (b) between odour and concentration intermittencies	120
4.11	Perceived odour is virtually constant downwind; compared with rapid decrease in toxicity and regulatory odour load	121
4.12	Comparison between outdoor and indoor concentration fluctuations for full-scale positions along the plume centreline (a) and at the plume edge (b), assuming one air change per hour	122
4.13	Ratio of concentration fluctuation intensity between centreline and plume edge is maintain from outdoors to indoors	123
4.14	Decreasing air changes per hour (ACH) results in decreasing fluctuation intensities	124
4.15	Comparison between mean memory loads for simulated outdoor and indoor concentration fluctuations	125
4.16	Comparing only times when odour is detectable, mean memory loads are larger outdoor than indoors	126

List of Tables

3.1	Assumed Mixing Layer Heights for Atmospheric Stability	56
3.2	Moni-Obukhov Length Scale L for the Six Pasquill-Gifford Stability Classes	57
3.3a	Concentration integral time scale for variable atmospheric stability class and downstream distance	61
3.3b	Concentration integral time scale for variable atmospheric stability class and roughness height	61
3.4	Change in Plume Characteristics with Averaging Time for Atmospheric Stability Class D	66
3.5	Length scaling factors based on roughness height z_0 and corresponding full-scale distances	71

Nomenclature

C	concentration steady with time, ppm
c	instantaneous concentration, ppm
c'	instantaneous concentration fluctuation $\overline{(c - C_{avg})^2}$ about the mean C_{avg} including the zero concentration periods, ppm
$\overline{c'^2}$	mean-square of mass concentration fluctuations $\overline{(c'^2)}$ about the mean, ppm
C_{avg}	mean concentration including zero concentration periods, ppm
$C_{avg,p}$	conditional (in-plume) mean concentration excluding zero concentration intermittent periods, ppm
$C_{avg,ref}$	mean concentration at reference test position on plume centerline, 1.0 km downwind of source, ppm
C_{avail}	available concentration once filtered by one-breath uptake time, ppm
C_{eff}	$C_{avail} - C_{th,var}$ effective concentration above the variable detection threshold, responsible for perceived intensity of odour, ppm
C_{exp}	exposure concentration equivalent to instantaneous concentration c , ppm
C_{indoor}	indoor instantaneous concentration, ppm
c'_p	standard deviation of the conditional (in-plume) concentration about the conditional mean $C_{avg,p}$ excluding the zero concentration periods, ppm
C_{rms}	root-mean-square $\sqrt{\overline{c'^2}}$ of concentration fluctuations about the mean C_{avg}
$C_{rms,p}$	root-mean-square $\sqrt{\overline{c'^2_p}}$ of conditional (in-plume) concentration fluctuations about the conditional mean $C_{avg,p}$
$C_{th,base}$	base detection threshold, minimum concentration required for detection in 50% of the population, ppm

$c_{th, vary}$	variable detection threshold, greater than or equal to the base detection threshold, time varying threshold governed by the desensitization and resensitization processes of human olfaction, ppm
d	displacement height of the surface roughness, m
H	full-scale mixing layer height, m, water channel mixing layer height, mm
h	total plume height above the ground including source height and final plume rise, m
h_s	source height above ground level, m
I	perceived intensity $(c_{eff} / c_{th, vary})^n$ of effective concentration
i	fluctuation intensity c' / C_{avg} about the mean including zero concentration intermittent periods
$i_{h,ref}$	reference fluctuation intensity at source height h_s
I_{OU}	odour unit intensity $(O_U - 1)^n$ based on steady concentration and base detection threshold
i_p	conditional (in-plume) fluctuation intensity $c'_p / C_{avg,p}$
$I_{Stevens}$	Stevens' power-law for perceived intensity kC^n based on his psychophysical studies of the perception of stimuli
k	constant in Stevens' theoretical power-law for perceived intensity
L	memory load, $\int W_o / t_{mem} \cdot I dt$ based on intensity I , integrated over the memory window t_{mem}
L^*	Monin-Obukhov length, m
L_{avg}	ensemble of memory loads $\langle L \rangle$
$L_{avg,OU}$	ensemble of odour unit memory loads
$L_{avg,d}$	detectable mean memory load
L_{OU}	odour unit memory load
$M_{intensity}$	pseudo-meander parameter, includes internal plume fluctuation in addition to meandering

n	odour intensity exponent
O_U	odour unit, $C_{avg} / c_{th,base}$, regulatory method of assessing odorant concentrations based on steady concentration and base detection threshold
p	exponent used in power-law velocity profile for stream wise mean velocity
S	non-dimensional shear parameter
S_{href}	non-dimensional shear parameter evaluated at source reference height h_{ref}
S_{zref}	non-dimensional shear parameter evaluated at receptor reference height z_{ref}
t	time, s
t_{avg}	averaging time, s
t_{mem}	memory window length, s
t_s	sampling time and total exposure duration, s
t_t	travel time, s
T_c	concentration integral time scale, s
T_u, T_v, T_w	along-wind (x -direction), crosswind (y -direction), and vertical (z -direction) mean velocities, m/s
T_{vel}	total velocity integral time scale, s
U	wind speed, m/s, or mean flow velocity in water channel, mm/s
U_c	convective wind speed, mass convection velocity of a plume passing a position x , m/s
U_H	velocity at the top of the mixed layer, m/s
U_{met}	meteorological wind speed, assumed 3.0 m/s in this study, at a fixed meteorological height z_{met} above ground, m/s
U_{ref}	wind speed at a fixed reference height z_{ref} above ground, m/s
u^*	friction velocity in log-law velocity profile, m/s

w^*	convective scaling velocity, m/s
x	downwind distance from source, m
y	crosswind distance from centreline of source / plume, m
z	height above ground level, m
z_c	reference height above ground where local wind speed U is the same as the plume mass convection velocity U_c , m
z_{met}	meteorological height where meteorological wind speed U_{met} is calculated, assumed to be 10 m in this study, m
z_0	surface roughness height, m
z_{ref}	reference height above ground where the windspeed U_{ref} is measured, m

Greek Symbols

ε	turbulent energy dissipation, m^2/s^3
$\varepsilon_u, \varepsilon_v, \varepsilon_w$	along-wind (x -direction), crosswind (y -direction), and vertical (z -direction) turbulent energy dissipation, m^2/s^3
γ	intermittency factor, fraction of time concentration is non-zero, $c > 0$
γ_{odour}	odour intermittency factor, fraction of time concentration is detectable, $c_{eff} > 0$
κ	von Karman constant = 0.4
Ψ	non-dimensional function of L^* and height z for calculating u^*
σ_0	effective source size, m
σ_y	vertical spread of a gaussian plume, m
σ_z	crosswind spread of a gaussian plume, m
τ	time constant, s
τ_{de}	desensitization time constant, s

τ_{re} resensitization time constant, s

τ_{up} uptake time constant, s

$\tau_{up,building}$ building uptake time constant, s

Commonly Used Subscripts

d detectable conditions excluding periods when odorant concentrations are not detectable

p in-plume conditions excluding zero concentrations in intermittent periods

$noshear$ shear-free statistics

$shear$ shear included statistics

Chapter 1

Introduction to Atmospheric Dispersion and Odour Perception

1.1 Motivation

Odour is one category of air pollution that encompasses both the physiological and aesthetic aspects of air quality. Odour is the major source of air quality complaints to regulatory agencies world wide because people are concerned with the effects odorous airborne pollutants have on their general standard of living and health. This is particularly the case when odours are perceived as being related to a toxic source. Typical industries responsible for such complaints include: refineries, chemical manufacturers, landfills, pulp mills, sewage treatment facilities and agricultural works.

It is well understood by those working in the chemical senses industry that odours can not only act as markers for toxic exposures, but they can also precipitate toxic-like symptoms below toxic levels (Shusterman, 2001). There is a need to regulate airborne odour emissions, not only because they may have health effects, but also because they can “materially interfere” with the normal use and enjoyment of property (Sweeten, 1997).

In order to regulate odorous emissions, it is first important to understand how odours have the potential to annoy and to predict over what range this annoyance could be felt downwind of a source. A tool that predicts the magnitude of potential annoyance, in terms of both the number of people affected and the level of annoyance, could allow users to:

- regulate odorous emissions at the source, and more easily identify the emission source rather than using in-field personnel trained to detect odours
- evaluate tools and practices to mitigate odours without implementing them on a trial basis, which can be counter productive and costly
- separate those people who have been affected by emissions causing adverse health effects from those who are affected by emissions causing annoyance based on their geographical location from a source

There are two distinct components required to predict odour annoyance: the atmospheric dilution, or dispersion, of emissions as they travel downwind in a plume, and the human perception of odours. An atmospheric dispersion model describes how the exposure concentration changes as it is carried downwind. A model for human

perception of odours describes how people perceive and react to different concentrations of odour. Both of these components have engineering importance because atmospheric dispersion is a non-linear function of downwind distance and people's perception of odorous emissions is non-linear with concentration.

Current methods of predicting downwind odour annoyance are based on atmospheric dispersion models that evaluate basic statistics such as mean concentrations. As will be shown in Section 1.3, the predicted mean concentration can be very different from the instantaneous concentration in a plume that fluctuates from instant-to-instant. Yet mean concentration models are widely used despite understanding that to successfully predict odour annoyance the atmospheric dispersion model must be able to predict the fluctuations in concentration at one-breath intervals that affect people downwind (Omerod, 2001).

Current methods of predicting odour annoyance compare the mean exposure concentration to the minimum concentration needed for the odour to be detected. By setting different acceptable ratios of these two concentrations, regulators can account for the differences in odour perception based on who is exposed to the smell and what is being smelled. These approaches need to be improved because they do not directly include the non-linear way in which people perceive intensities of odour, nor do they include the way perception changes based on exposure.

There is room for improvement in current methods used and a need to study whether complicating current methods will produce different predictions than those currently being made. The primary objective of this thesis is to develop a model for human annoyance to airborne odours from agricultural and industrial sources using concepts of human response to odours and the atmospheric dilution of point source emissions. In order for this model to successfully predict odour annoyance, the atmospheric dispersion model must be able to predict the fluctuations in concentration at intervals that are important to the way people detect odour, and the model for human perception must be able to predict how people perceive and react to fluctuations in odour.

1.2 Background to Odour Perception

Engineers often shy away from models that describe the way something is perceived because the word perception implies a qualitative or immeasurable effect. However, the ability to smell is common to almost all people, and concepts that govern how we smell and perceive odours are intuitive. An overview of how the sense of smell operates and how people perceive odours is described in the following sections.

1.2.1 Mechanisms of Human Olfaction

Human olfaction, the process of smelling, operates similarly to the other four senses. A stimulus is introduced into the nasal cavity, which causes receptors in our olfactory bulb to react. Signals are sent from the olfactory bulb to the brain's central nervous system (CNS) and are interpreted by several parts of the brain. Messages such as odour

recognition and perceived intensity are sent back to the olfactory bulb so that it seems to the individual that the stimulus was in fact interpreted in their nose. To be technically correct odour is the sensation, where as odorant is the chemical responsible for sensory activity.

Odorants have several characteristics that are distinguishable through olfaction: detection and recognition thresholds, intensity and hedonic tone (or pleasantness). Shusterman (1992) summarizes various opinions on the differences between odorants that result in their individual characteristics. Some believe that such characteristics are transmitted through the physicochemical properties that influence molecular delivery to the olfactory receptor sites. Others believe that the flexibility of molecular structures or the presence of specific molecular groups determine an odorant's characteristics. These hypothesis have led to several theories to explain how odorant molecules bond with receptors to transmit the information of these characteristics. Jacob (2003), in a review of the various theories, gives detailed explanations of which components of the odorant and nose are responsible for olfaction. The details of such theories are not important in the development of a useful engineering model of olfaction and will not be explored in this study. What is important, however, is that once the message of an odorant is received, a domino effect ensues to open channels of communication. In this way, the smallest amount of odorant effectively opens an extremely large number of communication channels, effectively multiplying its excitation effect, activating the olfactory nerves (Guyton and Hall, 2000). A little odorant goes a long way!

1.2.2 Psychophysics

Psychophysics is a branch of science that strives for an understanding of stimulus-response characteristics of sensory stimuli, including odorants (Shusterman, 1992). Psychophysics strives to describe the two most basic but important concepts in a model for odour annoyance: threshold determination, and perceived intensity. Thresholds allow researchers to describe the minimum concentration required for detection, recognition and annoyance of an odour. Perceived intensity is non-linear with concentration and is altered by the innate human abilities to adapt, habituate and recover from odours. The details of these psychophysical factors are discussed in the following sections.

1.2.2.1 Thresholds

The most important threshold is the detection threshold; without a minimum concentration of odorant, the olfactory sense will not be excited, and the odour will not be detected. The detection threshold is experimentally determined and defined as the minimum concentration of odorant that will be detectable by 50% of the population (CEN, 1998). Like all odorant characteristics, the detection threshold is dependent on the odorant and receptor. Most detection thresholds are very small, in the parts per billion range. For example, in a review of 26 published studies reporting average detection

thresholds for hydrogen sulphide, Amoore (1985) found that thresholds varied from 0.00007 to 1.4 ppm, with a geometric mean of 0.008 ppm.

The recognition threshold is distinguished from the detection threshold as the minimum concentration required for 50% of the tested population to differentiate one particular odour from another. The recognition threshold is slightly larger than the detection threshold as illustrated in Figure 1.1 for H₂S. The detection threshold will be used when evaluating levels of odour annoyance in this study as opposed to the recognition threshold: the detection threshold for the median of the population is also recognizable for a smaller percentage of the population and therefore has the potential for odour annoyance.

Amoore also found that a hydrogen sulphide concentration of 30 ppb would be annoying to 40 % of the population. This annoyance threshold is heavily influenced by the psychological aspects of odour, discussed later in this section. For this reason the range in odour annoyance thresholds is much larger than for the detection and recognition thresholds, as illustrated in Figure 1.1. This is compared to an allowable occupational exposure of 10 ppm over 8 hours according to Alberta Health (1988), which shows that odour sensitivity and annoyance occurs at very low levels.

The maximum perceived intensity is reached once all communication channels to the olfactory nerves are saturated. This level is reached for most odorants at concentrations 100 to 500 times the detection threshold. The dynamic range for the human nose is very small compared to that for the eyes, 500,000 to 1, or the ears, 1 trillion to 1 (Guyton and Hall, 2000). Guyton and Hall conclude that this shows that detection of the presence or absence of odour is more important than the quantitative intensity of that smell.

The human sense of smell is designed to detect changes in odorant concentrations, however, the majority of studies of olfaction and applications for those studies are focused primarily on thresholds, as opposed to the change in perceived intensity. These models will be discussed in more detail in Chapter 2.

A thorough description of how such thresholds are obtained can be found in the European standard for the determination of odour concentration by dynamic olfactometry, (CEN, 1998). Shusterman (1992), points out that there are often large discrepancies between odour detection thresholds reported by different laboratories. The reasons for this include: olfactometer set-up and practices, bias from panellists (e.g. change in health conditions), and odorant sample collection practises.

1.2.2.2 Perceived Intensity

The perceived intensity of odour increases non-linearly as a function of exposure odorant concentration. The relationship between perceived intensity and concentration is dependent on the odorant and receptor in question. This makes the comparison between odorants difficult. In order to overcome this complication, perceived odour intensity is typically measured against an “Odour Intensity Referencing Scale” (OIRS). An example of such as scale is (McGinley *et al.*, 1995):

- 0 = No Odour

- 1 = Very Faint
- 2 = Faint
- 3 = Noticeable
- 4 = Strong
- 5 = Very Strong

The process of “referencing” involves the comparison of an ambient air sample with the odour intensity of a series of concentrations of a reference odorant, typically n-butanol.

The dependence of perceived intensity on exposure stimulus, including odorants, is theoretically described using a variety of equations. Two equations recommended by the European Committee for Standardization (CEN, 1998) for odour regulation are the Fechner log-law and Stevens’ power-law. The logarithmic function for change in perceived intensity according to Fechner is:

$$I = k_w \log \left(\frac{C}{C_o} \right) \quad (1.1)$$

where I is the perceived intensity of sensation, C is the physical intensity (odour concentration), C_o is the threshold concentration, and k_w is the Weber-Fechner coefficient.

The psychophysical power function derived by Stevens (1957, 1960) is:

$$I = k C^n \quad (1.2)$$

where I is the perceived intensity of sensation, C is the physical intensity, n is Stevens’ exponent and k is a constant. The New South Wales Environment Protection Agency (2002) indicates that n ranges from about 0.2 to 0.8 (Stevens, 1960), depending on the odorant. For example, a tenfold reduction in concentration for an odorant with $n = 0.2$ will result in a reduction of odour intensity by a factor of 1.6. Where as a ten-fold reduction in an odorant with $n = 0.8$ will result in a factor of 6.3 reduction in odour intensity. In this study, Stevens’ Law will be used to describe perceived intensity in the development of a model of human odour annoyance.

1.2.2.3 Adaptation, Habituation and Recovery

The non-linear relationship between exposure concentration and perceived intensity is complicated by the innate human ability to adapt/habituate and recover from odours.

To help understand how these concepts work, consider the simple everyday example of cooking with garlic. Initially, there is no garlic odour in the room, but as preparation and cooking of the garlic proceeds the concentration increases allowing us to detect the odorant. At constant concentrations, below irritation levels, human olfactory systems allow for adaptation/habituation to the garlic odorant and the smell fades into the background of the environment. Periods of zero concentration, for example a short period spent outdoors, allow our olfactory system to recover or resensitize to the garlic

odorant. On returning from garlic-free air, garlic can again be detected and recognized in the closed kitchen. This example for how odour works will be used throughout the remainder of the study to add clarity through common experience.

Adaptation and habituation both prevent sensory overload by allowing people to become desensitized to odours, but these processes are governed by very different mechanisms.

It is postulated that after the onset of olfactory stimuli, the central nervous system (CNS) develops a strong feedback inhibition to suppress relaying smell signals through the olfactory bulb (Guyton and Hall, 2000), therefore allowing the brain to adapt to odours. This physiological reduction in perceived odour intensity occurs in response to a constant odorant exposure. Wang *et al.* (2002) found that this response follows an exponential decay and is dependent on the strength of stimulant: the stronger the concentration, the longer it takes to adapt. Physiological adaptation is not complete, but was found by Wang *et al.* (2002) to tend to a plateau; therefore, the exponential decay in response would asymptote at a level higher than zero. Shusterman (1992) points to hydrogen sulphide as an example: at high concentration exposures, H₂S produces rapid and reversible olfactory fatigue or “paralysis”.

Habituation is a psychological process by which cognitive perception of an odour ceases once an individual is exposed to a constant concentration of odorant. Wang *et al.* (2002) found that this process differs from the physiological process of adaptation in that habituation occurs more rapidly and completely. This process allows individuals to ignore constant concentrations of odorants, allowing the specific odour to become part of their background environment.

Studies including models of the subtle differences between habituation and adaptation are in their infancy. As such, the processes of habituation and adaptation are assumed to be included in one process, desensitization.

Desensitization is reversible: in the absence of the exposure odorant, an individual’s olfactory response recovers to sensitivity levels experienced prior to exposure. In this way, odours that had been relegated as unimportant background information can once again be detected at subsequent exposures. In this study, recovery is referred to as resensitization.

The concept of odour desensitization and resensitization has been discussed in the literature for thirty years. Dalton (2002) gives a good review of studies that examine desensitization and resensitization to a wide variety of odorants. She points to Cain (1974) and Berglund (1974) who both showed that the decline in perceived intensity follows an exponential decay function and that the rate and degree of desensitization and resensitization are dependent on the concentration and duration of exposure. These factors suggest the use of a first order function to describe the change in perceived intensity with sensitization. Current regulatory models for odour annoyance do not include these effects. Desensitization and resensitization further validate the assumption that the human sense of smell is tuned to the change in odorant concentrations rather than the concentrations themselves. Extending this concept, it is plausible that the desensitization and resensitization processes act to modify the detection threshold. Exposure to a constant concentration results in a desensitization to that odorant, meaning that a larger exposure concentration is required to be noticed, or equivalently, the

detection threshold increases. Zero-concentration exposures allow a person to resensitize, so that a smaller exposure concentration will be detected, or equivalently, the detection threshold decreases. To account for the time and concentration dependency, the detection threshold will be allowed to vary in this odour model, as illustrated in Figure 1.2. Notice that the variable detection threshold is allowed to vary with changing exposure concentration, and limited at a minimum threshold of the original, or base detection threshold.

As perceived intensity is referenced to the detection threshold, a change in the detection threshold implies a change in the perceived intensity. As these changes follow the changes in exposure odorant concentrations, it is important to accurately predict the concentrations changes that are important to people in order to accurately predict how they will become annoyed by airborne odorants.

1.2.3 Population Distribution

It is no surprise that the psychophysical attributes of individuals varies greatly within a population. Education and previous experience, described above, are among some of the reasons for inter-individual differences in olfactory sensitivity. Additional major reasons for inter-individual differences include:

- Age (the elderly are typically less sensitive)
- Smoking habits (reduce sensitivity)
- Sex (females are typically more sensitive)
- Atopic (allergic) status

Dalton (2002) points out the fact that the variations in responsiveness due to sensitivity factors (for example, gender or age) play a much smaller role than differences in beliefs or attitudes towards the possible consequences of exposure to airborne chemicals.

Regardless of the reasons for differences in sensitivity, the population sensitivity follows a log-normal distribution (Shusterman, 1992). This holds true for odour detection and recognition thresholds, annoyance levels and sensory irritation, shown in Figure 1.1. It is left up to regulatory agencies to decide what portion of the population should be considered when deciding what levels of odour annoyance are acceptable. Opportunity for applying a log-normal distribution to test variation in annoyance levels within a population will be discussed, but the application of such a distribution is not included in the scope of this study.

1.2.4 Hyper-sensitivity

Just as people can desensitize to odorants, they can also develop hyper-sensitivity. Shusterman (1992) indicates that this phenomenon may occur in individuals who live in an environment affected by an industrial odour.

Citing an earlier study he had completed in 1991, Shusterman (1992) indicates that results from a study of hazardous waste site neighbours show that physiological and psychological symptoms of stress were related to both the degree of environmental worry

and the frequency of odour perception. This suggested that acute stress may be induced in individuals who perceive an odour source as a toxicological risk. Such adverse conditioning has been documented in patients after an initial traumatic exposure to a chemical irritant. Patients exposed to this odorant at concentrations below toxic levels experience panic or other stress related symptoms.

This complication is based on past experience and is not easily predicted. For this reason, hyper-sensitivity will not be included as part of the odour annoyance model developed in this study.

1.2.5 Summary

The most important aspects to human odour perception are the detection threshold, perceived odour intensity and the change in perception with sensitization. Consider again the simple example of cooking with garlic. Without a minimum concentration of garlic particles, it would not be detected. Unless trained, people are not aware of what concentration of garlic they are exposed to while cooking, but they can indicate how intense they feel the smell is. Once exposed to the unchanging smell, it will begin to fade into the background as they desensitize. Returning from fresh air, the cooking garlic will once again be noticeable because their noses have resensitized to the smell. Current regulatory models include the concept of a detection threshold, but do not directly account for the non-linearities of how people perceive odours and how that perception is altered through exposure. In order to accurately predict how people will become annoyed to concentration fluctuations of odorant, the complexities of perception must be modelled. A model will be developed in Chapter 2 using mathematical expressions to describe the concepts covered above.

1.3 Background to Atmospheric Dispersion

Airborne odorants emanate from all types of sources ranging from ground-level area sources, such as a lagoon, to elevated point sources, such as a ventilation stack. Odorants are transported downwind by the mean wind velocity in a plume, as illustrated in Figure 1.3. There are three factors, governed by atmospheric dispersion, that are important to predicting human response to a dispersing odorant in a plume:

- **Concentration:** Instantaneous concentration of a dispersing odorant at a specific spatial position and time are dictated by the random nature of the turbulent atmosphere. An example of instantaneous concentration fluctuations across the width of the plume is illustrated in the cross-sectional profile of the plume in Figure 1.3. Exposure concentrations govern how people react to an odour.
- **Duration:** The duration of an odorant (chemical) concentration exposure or odour (sensation) event is also dependent on the random nature of the atmosphere. The duration of an exposure may be hours, days, or years in length, as governed by the variation in large scale meteorological conditions, such as mean wind speed and direction. Over the duration of an exposure event, a person may perceive minute-

by-minute and second-by-second variations in odour that are a function of smaller scale random variations within the atmosphere than those that govern diurnal and annual variations. Odour perception is based not only on concentration, but also duration of odour events within an exposure.

- **Frequency:** The frequency of occurrence of an odour event is governed by a range of atmospheric turbulence scales causing concentration changes that range from minute-by-minute to diurnal to annual variations. The frequency of odour events within an exposure also dictates levels of annoyance.

Dispersion models are designed to evaluate the concentration, duration and frequency of an odour event, as they account for concentration distribution and dilution with downwind position from the source. The time-averaged plume of contaminant can be thought of as having a conical shape originating at the source, as illustrated in Figure 1.3. Barring any chemical reactions, atmospheric dispersion models are based on the basic law of mass conservation: pollution that leaves the source must pass through a plane perpendicular to the plume's travel direction.

1.3.1 Predicting Plume Concentrations in Atmospheric Dispersion

It is relatively easy to model the lower order plume characteristics, such as mean concentration and plume spreads, but much more difficult to predict time series of concentration fluctuations for any given position in the plume. For this reason, dispersion models currently used by regulatory agencies for the purposes of odour assessment do not calculate these instantaneous fluctuations.

As a starting point, models, such as the Gaussian dispersion model, can be used to evaluate the mean exposure concentration. One commonly used, public domain, Gaussian model is the Industrial Source Complex (ISC3) (USEPA, 1995 a&b). This type of model predicts a smooth distribution of ensemble-averaged or time-averaged concentrations in the plume, as illustrated in Figure 1.3.

Factors of safety or a peak to mean ratios are applied to the mean concentration in an attempt to estimate the effect of concentration fluctuations on a more realistic time scale than that provided by the Gaussian model. Best *et al.* (2001) found that peak to mean ratios are independent of atmospheric stability class and are almost only dependent on source type. This type of correction is applied to make a conservative estimate of the strength of odour a person might be exposed to.

The variation in meteorological statistics, such as mean wind velocity, can be used with the mean concentration to evaluate the frequency and duration of minute-by-minute to diurnal to annual variations in odour events. This method is the most common method used by regulatory agencies to predict odour annoyance.

A probability density function (pdf) of concentrations can also be used to predict what percent of the time a person might be exposed to what concentration. Wilson (1995, p 50) recommends the use of a log-normal pdf, as providing a good fit to observed concentration fluctuation data in laboratory-scale and full-scale atmospheric plumes. Higher order plume statistics can also be used to develop a more comprehensive

description of the concentration fluctuations, including duration and frequency, that an individual might be exposed to over the course of an exposure.

Each of these methods only considers the overall statistics of the odour emission, and are unable to predict the instantaneous fluctuations in concentration a person might be exposed to when standing in a dispersing plume of odorant. Hilderman and Wilson (1999) point out that a receptor, located at a fixed position within a plume of dispersing odorant, may be exposed to instantaneous concentrations from zero (background) levels to greater than 20 times the mean concentration, which randomly vary from breath to breath. This natural variation in concentration is due to the random turbulent dilution and dispersion processes. It is recognized by the New South Wales Environment Protection Authority (NEW EPA, Australia) (Omerod, 2001), among other regulating authorities, that people are affected by concentrations that fluctuate within the response time of the human nose, but they continue to use overall statistics rather than fluctuations. For this reason, current methods for predicting human odour annoyance try to fit odour perception models to the few statistics at hand.

1.3.2 Simulating Atmospheric Concentration Fluctuations in Plumes

A simulated time series of instantaneous concentration fluctuations can be used to accurately predict the odour events a person might experience during an entire exposure. An ensemble of these series will automatically contain mean concentrations, higher order statistics, and important information such as true peak concentrations and their probabilities. The use of such a time series does not limit the kind of odour perception model, and will be able to include important effects such as how perception changes with exposure duration and frequency.

The need to use such time series has been recognized by Hilderman (1999 and 2004 a and b). Hilderman uses toxic effects as an example of why simulated time series should be used instead of overall summary statistics. He points out that assumptions of how fluctuations affect outcomes are minimized when outcomes are evaluated directly from the fluctuations. This point is significantly important when modeling odour annoyance: current regulatory models are based on the assumption that mean concentration dictates crosswind and downwind changes in annoyance levels, but it will be shown in this study, through the use of concentration fluctuations, that mean concentration is not as important as zero-concentration intermittency. Hilderman has developed a method to take the basic statistical information about a dispersing plume and generate realistic stochastic time series of concentration fluctuations.

Yamartino *et al.* (1996) and Yamartino and Strimaitis (2000) have developed the Kinematic-Simulation-Particle (KSP) model that has the capacity to predict second-by-second concentration patterns and fluctuations. An instantaneous distribution of the tracer particles yields a “snapshot” of the concentration field and is attained by using mean flow fields and assuming a realistic spectrum of turbulent eddies to transport tracer particles. Though computationally intense, this method is under review by the German EPA for use in situations such predicting odour annoyance.

In this study, laboratory-scale time series will be used to simulate full-scale concentration fluctuations at five crosswind and five downwind ground-level points of interest within a plume. Using these simulations will insure that the results of this study are not biased by ideas of how exposure concentration variation should be related to odour annoyance. Predicted levels and trends in odour annoyance will only be limited by the assumptions used to create the odour annoyance model.

1.4 Odour Annoyance Model

The new odour annoyance model that was developed in this study takes into account the complexities of atmospheric dispersion and of human perception of odours. This new model uses current knowledge of odour perception and instantaneous concentration fluctuations to create an engineering model capable of predicting how odour perception, and therefore odour annoyance, will change from breath to breath based on exposure history, odorant type and individual people's sensitivities. A history of odorant fluctuations will be used in conjunction with a newly developed model for how people detect, desensitize, resensitize and perceive odours to evaluate current and mean levels of odour annoyance.

1.4.1 Overview of Chapter 2 – Model for Human Odour Annoyance

Relying on the ability to predict instantaneous concentration fluctuations, the model for human odour annoyance developed in Chapter 2 is an improvement over current regulatory odour models that rely on simple plume statistics such as mean concentration. This distinction is important in accurately predicting odour annoyance because, as explained in Section 1.2, the human sense of smell is tuned to detect changes in concentration, not a mean exposure concentration. With the ability to predict concentrations that are important to human olfaction, the model developed in Chapter 2 implements the psychophysical intricacies that dictate how people perceive and become annoyed by odours:

- When exposed to concentration fluctuations of an odorant, people adapt and habituate, and resensitize to these concentrations. These processes are modeled in Chapter 2 as a change in detection threshold, as illustrated in Figure 1.2.
- Concentrations above this variable detection threshold are those with potential to annoy and are therefore used in a modified version of Stevens' law, Equation (1.2), to evaluate the perceived intensity of exposure odorant as it fluctuates instant to instant.
- Perceived intensity of an odorant is then used in this model to evaluate current levels of annoyance based on a history of perceived intensity. A linearly-fading memory window is used to capture the perceived intensities of all exposure concentrations, present and remembered.

These steps are used to evaluate a level of odour annoyance that will be used in Chapter 4 to compare between different exposures that occur depending on a person's location in a dispersing plume of odorant.

1.4.2 Overview of Chapter 3 – Predicting Full-scale Concentration Fluctuation Statistics and Water Channel Scale-up Technique

Without minimizing assumptions about which and how concentration fluctuation statistics affect odour annoyance, it is impossible accurately understand how aspects of odour perception interact with different plume characteristics to produce variations in odour annoyance levels. For this reason, laboratory-scale data will be used to simulate full-scale time series of concentration fluctuations for a dispersing plume in a stationary, neutrally-stable atmosphere. Methods of predicting full-scale plume statistics, used to select appropriate laboratory-scale data, will be discussed in Chapter 3. Data were collected in a water channel flume where fluctuations occur much quicker than in the full-scale atmosphere, and at mean concentrations different from those expected in the full-scale atmosphere. For these reasons, methods for stretching laboratory data in time and concentration will be developed and applied in Chapter 3.

1.4.3 Overview of Chapter 4 – Evaluation of Odour Annoyance Model for Neutral Atmospheric Stability

In Chapter 4, a concentration time series representative of selected crosswind and downwind positions will be used to evaluate trends in odour annoyance, and to verify the robustness and realism of the model over a wide range of conditions. These trends will be compared with crosswind and downwind predictions of odour annoyance using the current regulatory method based on mean concentrations.

The model for human odour annoyance will also be compared to a model for the change in toxic effects based on plume statistics. Finally, the model will be adapted to predict indoor concentration fluctuations and compare outdoor and indoor levels of odour annoyance.

1.4.4 Predicted Outcomes of the Odour Annoyance Model

As will be shown in Chapter 3, concentration fluctuations along a plume's centreline are comprised of mostly non-zero concentrations. Considering this, and the process of desensitization, it can be predicted that people will have an opportunity to desensitize when standing along the centreline of an odorant plume. At the edge of the plume, concentration fluctuations are mostly comprised of sudden drops to zero concentration. This intermittency is important to odour modelling because, just as people are able to desensitize to odours, they are also able to resensitize to their original sensitivity levels when given a long enough break between odour events. This ability to resensitize, which

reduces the benefits of desensitization, means that infrequent odour events can be perceived as intensely as if the individual were not exposed to the odorant at all. Walking across the plume from its centreline and considering the periods of zero-concentration versus periods of concentration, it can be predicted that odour events along the plume centreline will be perceived as less intense and therefore have a smaller ability to produce annoyance, than events at the plume's edge.

On average, a person will be exposed to larger mean concentrations on the plume centreline than at the edge of the plume, as illustrated in Figure 1.3. In Chapter 3, it will be shown that mean concentrations vary strongly across the width of a plume. With this in mind, an alternate prediction can be made: odorant concentrations are much larger on the plume centreline than on the edges, therefore people must be more annoyed by odour events when standing on the plume centreline than on the plume's edge.

The intermittency of a plume increases with downwind distance, where as the mean concentration decreases. Both of these trends act to decrease annoyance levels with downwind distance, but the rate of decrease is not easily predicted as intermittency and mean concentration change at different rates.

The hypothesis of this study is that *a balance is struck between mean concentration and intermittency to produce a constant level of annoyance across the plume and to produce levels of odour annoyance that decay at a mean rate between the decrease in mean concentration and increase in intermittency.* Without testing this comprehensive model for human odour annoyance that includes all non-linear complications of odour perception and atmospheric dispersion, it is very difficult to accurately predict variations in odour annoyance levels with crosswind and downwind positions.

1.4.5 Results of Applying the New Odour Annoyance Model

Many regulators are more familiar with how toxic effects vary with position in a plume; therefore, a comparison in downwind decay between toxic effects and odour annoyance is made using the odour annoyance model developed in this study. As expected, it will be shown that odour annoyance is far more persistent than toxic effects, in both the crosswind and downwind directions. This means that regulators can separate who potentially received toxic doses versus annoying doses of chemical odorant within an affected area, but this must be done using two different models; toxic models can not be extrapolated to account for odour annoyance.

This study will also show dramatic differences between crosswind and downwind trends predicted by this new odour annoyance model and current regulatory models. Airborne odorants are far more persistent than are currently being predicted by regulatory agencies; consequently the size of affected areas is being underestimated. Contrary to intuition, it will also be shown that fluctuation statistics, such as intermittency, are far more influential on the outcome of odour annoyance than mean concentration.

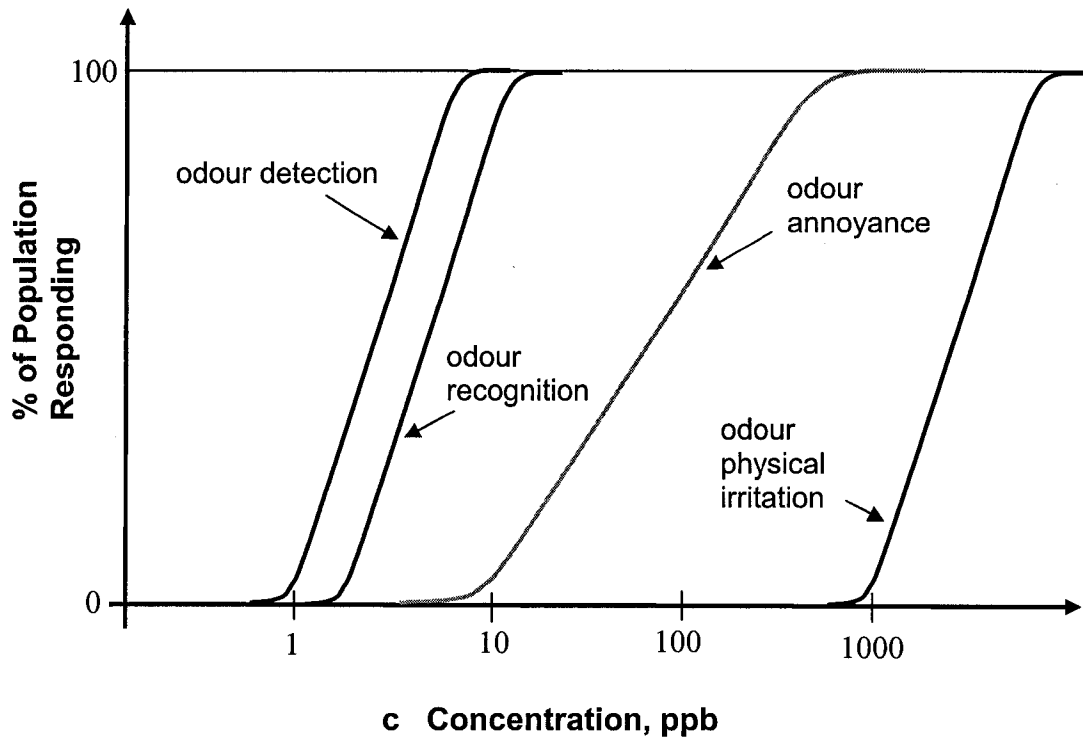


Figure 1.1: Cumulative distribution for percent of population detection, recognition, annoyance and physical irritation by concentrations of hydrogen sulphide. (Following Shusterman, 1992; Flesh and Turk, 1975, Amoore and Hautala, 1983, and Ruth, 1986)

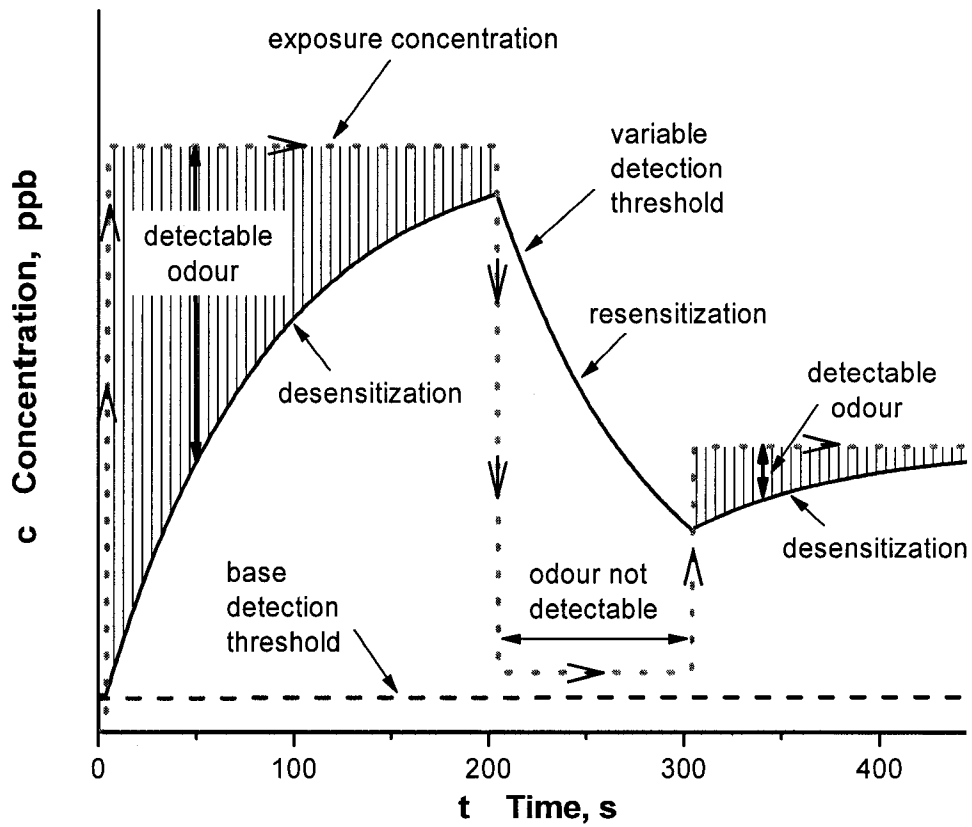


Figure 1.2: Illustration of desensitization (adaptation/habituation) and resensitization (recovery) processes governing how people react to changing concentration of odorants.

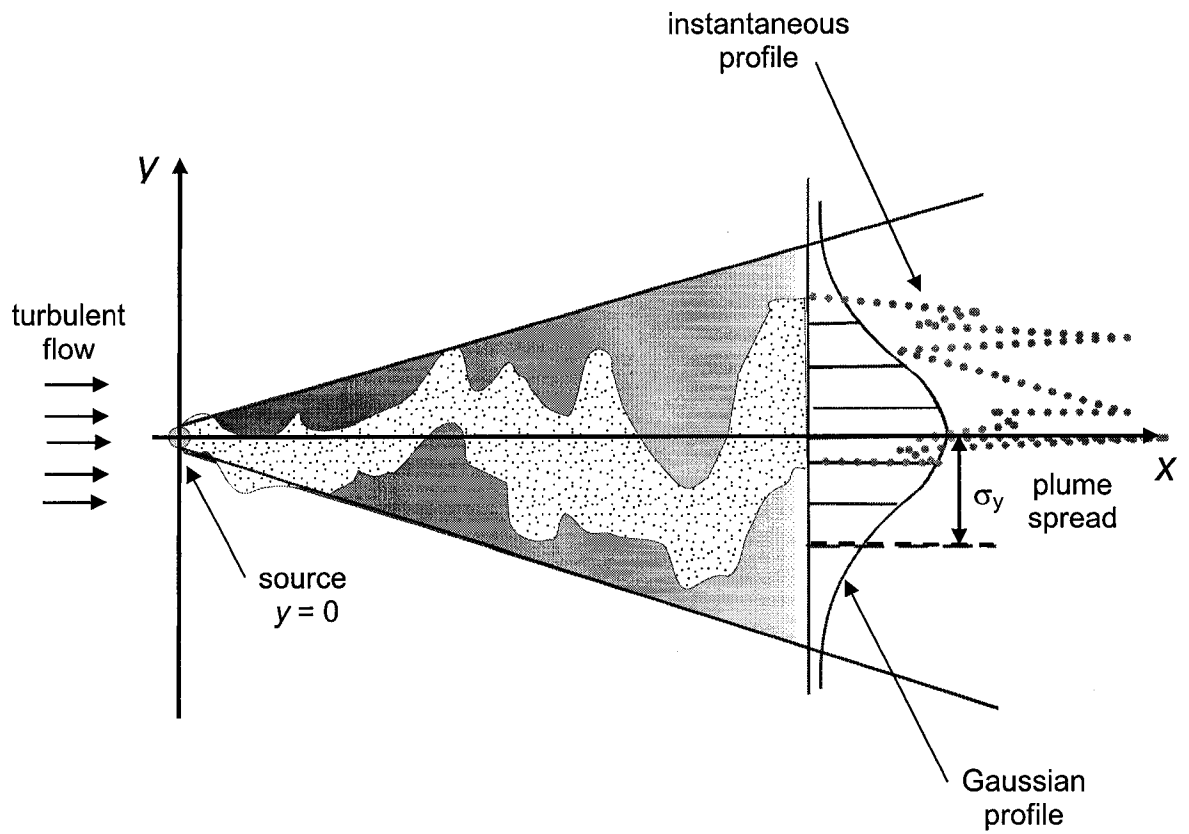


Figure 1.3 Gaussian compared with instantaneous profile in the cross-stream direction; a large ensemble of instantaneous profiles will produce a glassy-smooth Gaussian profile.

Chapter 2

Model for Human Odour Annoyance

2.1 Introduction

A model for human odour annoyance will be developed to allow regulatory agencies to predict how neighbours downwind of an odour source will become annoyed by the odour and how frequently this annoyance will occur. In order for this model to successfully predict odour annoyance, the atmospheric dispersion model must be able to predict the fluctuations in concentration at one-breath intervals. Current models used by regulatory agencies will be reviewed and areas for improvement will be discussed. The new model for human odour annoyance developed for this study takes into consideration the psychophysical principles discussed in Chapter 1 and is based on the ability to predict instantaneous concentration fluctuations at all crosswind and downwind receptor locations within a dispersing odorant plume.

2.2 Current Odour Models

Six factors are important for predicting human response to a dispersing odorant in an atmospheric plume. The first three factors are determined by atmospheric dispersion:

- **Concentration:** Instantaneous concentration of a dispersing odorant at a specific spatial position and a specific time are dictated by the random nature of the turbulent atmosphere. Concentrations above an odorant threshold elicit reactions to the perceived odour.
- **Duration:** The duration of an odorant (chemical) concentration exposure or odour (sensation) event is also dependent on the random nature of the atmosphere. Over the duration of an exposure event, a person may perceive minute-by-minute and second-by-second variations in odour that are a function of a smaller scale of random variations within the atmosphere than those that govern the diurnal and annual variations. Human receptors are able to adapt, habituate and recover to an odorant at rates that depend not only on the exposure concentration but also on the duration of exposure.
- **Frequency:** The frequency of occurrence of an odour event is governed by a range of atmospheric turbulence scales causing concentration changes that range from minute-by-minute to diurnal to annual variations. The new model is based

on the assumption that a frequently perceived odour event is just as, if not more annoying than an infrequent event of larger perceived odour.

Predicting the concentration, duration and frequency of a dispersing odorant helps solve part of the problem of predicting human response. The remaining three factors are directly related to the psychology and physiology of human olfaction (the way people detect and perceive odorants).

- **Detection Threshold:** The detection of an odorant is accomplished by the olfactory system in a human receptor. For an odorant to be detected, a receptor must be exposed to a minimum threshold concentration of odorant. This minimum concentration is dependent on the odorant and receptor in question.
- **Perceived Intensity:** Perceived odour intensity is a psychophysical function dependent on the concentration and duration of exposure of current and past exposures, as well as the sensitivities of the human receptor. The major complication in describing what a human receptor experiences is that perceived intensities of odours are non-linear with odorant concentrations.
- **Tolerance Threshold:** The tolerance threshold is dependent on physiological, psychological and social factors and is a determinant for the odour intensity that causes annoyance. People may find that the initial perception of an offensive odour is intolerable, for example rotting meat, while other odours, such as perfume, are acceptable unless presented in high concentrations. Most odorant are capable of evoking a negative reaction; the strength or concentration that will be viewed negatively is dependent on the particular odorant and receptor's sensitivity.

The detail with which these three psychological and physiological factors are modeled is dependent on the detail with which atmospheric dispersion (including concentration, duration and frequency) is predicted. Each of these six factors is important to predicting human reaction to a dispersing odorant in an atmospheric plume.

2.2.1 Concentration, Duration and Frequency

Current methods of determining and predicting acceptable airborne odorant concentrations used by regulatory agencies world-wide are based on predicting only the mean concentration and using peak-to-mean factors to estimate the worst case odour level. These methods estimate the duration and frequency of time-averaged concentrations, but are unable to predict the instantaneous fluctuations that are important to the way humans detect and respond to odours. Specific examples of models used by Australian (NSW EPA, 2001) and Austrian (Schauberger, 2000) will be used to illustrate current regulatory approaches for evaluating odorant plume statistics.

Airborne odorants emanate from sources ranging from large ground-level area sources, such as a lagoon, to elevated point sources, such as a ventilation stack. Odorants are transported by the mean wind and randomly diluted and diffused producing time-varying instantaneous concentration fluctuations, illustrated in the cross-sectional profile of the plume in Figure 1.3.

It is relatively easy to model the time-averaged characteristics of this process, such as mean concentration and plume spreads, but much more difficult to predict time series of concentration fluctuations for any given position in the plume. For this reason, many dispersion models for odour exposures are based on simple Gaussian profiles of mean concentration over a few minutes to a few hours. Some models, for example the Austrian Odour Dispersion Model (AODM) (Schauberger, 2000), incorporate diurnal or annual changes in meteorological conditions to determine changes in mean concentration. For example, a position downwind of a refinery in the morning might be upwind in the afternoon with the diurnal variations in meteorology. These variations in meteorology are then used to predict odour event frequency, but only on time scales of hours and days rather than seconds.

Odour acceptability is determined by comparing the predicted mean concentration to the base detection threshold, which is the minimum concentration required for 50% of the population to detect the odour. Odour units (O_U) indicate the severity of the odour (Mahin, 2001):

$$O_U = \left(\frac{C_{avg}}{c_{th,base}} \right) \quad (2.1)$$

where C_{avg} is the mean concentration for a given averaging time and $c_{th,base}$ is the base detection threshold. One odour unit is, by definition, the detection threshold. Any O_U measure greater than 1.0 is detectable by at least 50% of the population.

Mahin (2001) highlights odour regulations and guidelines in Europe, Asia, Australia, New Zealand and North America. Comparison of regulatory standards can be difficult because some odour guidelines are given in units of O_U/m^3 while others use O_U . The emission rate, expressed as $O_U \cdot m^3/s$, can be calculated by multiplying the odour units at the source by its flow rate.

Odour exposure guidelines are usually defined as the number of O_U (or O_U/m^3) for a given averaging time permitted for certain percentage of the year. The standard range for compliance is $1.0 < O_U < 7.0$. The standard averaging times range from $1.0 \text{ min} < t_{avg} < 1.0 \text{ hr}$ with 98% to 99.9% annual compliance.

The averaging time over which the odour fluctuations are observed is an important parameter for calculating mean concentrations—and will be discussed in further detail in the following chapter. The longer the averaging time, the more the instantaneous concentration fluctuations are filtered and the less realistic the exposure prediction. In addition, modellers typically use a Gaussian profile, for example, to calculate concentrations across the width and height of a plume as an ensemble of instantaneous profiles, as illustrated in Figure 1.3.

A good example of a regulation based on odour units is the one used in New South Wales (Australia) (NSW EPA, 2001) which permits odour concentrations in urban areas of $2 O_U/m^3$, for a one-second averaging time, with 99.5% compliance. This means that industries may only exceed $2.0 O_U/m^3$ for 44 hours in a year, or equivalently that neighbours of odour emitting industries can expect to be annoyed a maximum of 44 hours in a year. If the 44 hours of exceedence are all in a row, people would be annoyed

for a little less than two days. However, an emitter could also meet the regulatory standard with many one-second events spread over an entire year, which would mean that people would be annoyed once every 3.3 minutes. These two results, both of which are compliant with regulations impact the public in very different ways.

It is reasonable to assume that humans respond to one-breath (approximately one second) changes in concentration, as implied in the New South Wales regulation. Hilderman *et al.* (1999) point out that a receptor, located at a fixed position within a plume of dispersing odorant, may be exposed to instantaneous concentrations from zero (background) levels to greater than 20 times the mean concentration due to the random turbulent dilution and dispersion processes. Although ensemble mean concentrations can be calculated for a one-breath averaging time, the ensemble does not indicate what a human receptor may experience from one breath to the next. As explained in Chapter 1, humans are sensitive to the changes in odour information so it is the sequence time-varying fluctuations, not the ensemble of one-second mean concentrations, that is important.

A few atmospheric dispersion models enable the prediction of the variance and intermittency of concentrations within a plume that allows odour modellers to determine the range of concentrations a receptor will experience. The most sophisticated level of dispersion modelling is to simulate second-by-second variations in concentration. These simulations can be accomplished through computationally intensive models, or experimentally (as will be used later in this study). Simulated second-by-second exposure time series provide the information needed to directly address the concentration, duration and frequency components that are important to predicting human annoyance to airborne odorants. Methods of calculating higher order concentration statistics and producing simulated time series will be discussed in Chapter 3.

2.2.2 Detection Threshold, Perceived Intensity and Tolerance Threshold

Current methods of predicting acceptable airborne odorant concentrations used by regulatory agencies world-wide are based on the odour unit method: a comparison of the detection threshold to the mean concentration of odorant an individual might be exposed, described in Equation (2.1). Using the odour unit method, regulators are able to account for the differences in perceived intensities, based on the receptor and odorant, through different acceptable limits in mean concentrations. For example:

- New South Wales (Australia) Environment Protection Authority (NSW EPA, 2001) recommends different acceptable O_U values based on an affected rural or urban population to acknowledge that perception is based on social background.
- Agricultural Operation Practices Act for Alberta (2002) offers different O_U limits depending on the type of odorant to acknowledge the fact that different odorants are perceived differently.

It is the perception aspect of human odour annoyance that is the most enigmatic piece of the puzzle. Human perception is governed by not only physiological parameters (such as the detection threshold) but also by psychological and social complexities (such

as education and age). People who think of an odour as being dangerous to their health will be more sensitive to exposures of that odorant and will be more likely to complain about a perceived odour than those who have no preconceived ideas (Shusterman, 2001). Odour units are an attempt to quantitatively describe degrees of odour perception. In a report on experimental work at the Centre for Water and Wastewater Treatment (CWWT) at the University of New South Wales and in Germany, Jiang and Sands (2000) indicate that concentrations below 3.0 O_U are not likely to be offensive, even though they are detectable. This indicates that concentrations less than 3.0 times the detection threshold will not be perceived as offensive, and are unlikely to cause an odour complaint.

The confusion in trying to account for perception is apparent in the large range of odour unit limits for the regulatory agencies reviewed by Mahin (2001) (i.e. from 1.0 to 7.0 O_U for a range of averaging times from 1.0 min < t_{avg} < 1.0 hr with 98% to 99.9% annual compliance, as mentioned in the Section 2.2.1). Varying O_U limits are necessary because the O_U method does not inherently account for non-linearities in odour perception. A twofold increase in O_U does not imply a twofold increase in perceived intensity, and the perceived intensity of a twofold increase in O_U for one odorant is not equivalent to the perceived intensity of a twofold increase in O_U for another odorant.

It has been recognized for over forty years (Stevens, 1957) that people do not sense absolute concentrations of odorant (unless trained to do so), but rather the perceived intensity of an odour. The European Committee for Standardization (CEN, 1998) describes two psychophysical models for predicting the perceived intensity of an odorant concentration, the Fechner log-law and Stevens' power-law (Stevens,1957). Stevens' law is the only model explored in detail because it is easily modified for the purposes of this study, as will be shown later in this chapter. Stevens' law calculates a perceived intensity of a sensation, $I_{Stevens}$, as a function of the physical intensity, C (odorant concentration), to a power n (Stevens' exponent):

$$I_{Stevens} = k C^n \quad (2.2)$$

where k is an odorant-dependent constant. The New South Wales Environment Protection Authority (Australia) indicates that n ranges from about 0.2 to 0.8, depending on the odorant (NSWEPA, 2002). For an odorant with $n = 0.2$, a doubling of concentration will result in an increase of odour intensity by a factor of 1.1. For an odorant with $n = 0.8$, a doubling of concentration will result in a factor of 1.7 increase in odour intensity. The psychophysical approach of Stevens' law is an improvement over odour units as it attempts to account for the non-linearities in human response with the use of a power-law with exponent n . A 2.0 on Stevens' scale of perceived intensity is actually twice as bad as 1.0, while it is not clear how much worse the effect of 2.0 O_U is compared to 1.0 O_U .

The difficulty with Stevens' model for perceived intensity is in it's application to the existing odour unit method. People do not perceive the mean concentration of odorant that they are exposed to, but rather the change in concentration that occurs from breath to breath. The odour unit approach is unable to take advantage of perception models, such as Stevens' power-law, because it makes use of a mean concentration and not the instantaneous fluctuations in concentration that a person is exposed to when

standing outside in a dispersing plume of odorant. The new odour annoyance model developed in this chapter will improve on the current odour unit approach by being able to account for the instantaneous fluctuations in odorant concentration.

Odour perception is more complicated than Equation (2.2) might lead one to believe: the perceived intensity of a concentration of odorant can change in time as perception is based on history of exposure, governed by the processes of adaptation, habituation and recovery. The ideas of adaptation, habituation and recovery have been discussed in literature for the past 30 years. Dalton (2000), Cain (1974) and Berglund (1974) found that perceived intensity follows an exponential decay function and that the rate and degree of adaptation, habituation and recovery are dependent on the concentration and duration of exposure. To help understand how these psychophysical parameters affect people's tolerances, consider the simple everyday example of cooking with garlic, which was first introduced in Chapter 1. Initially, there is no garlic odour in the room, but as preparation and cooking of the garlic proceeds the concentration increases allowing us to detect the odorant. At constant concentrations, below irritation levels, human olfactory systems allow for adaptation and habituation to the garlic odorant and the smell fades into the background of the environment. Periods of zero concentration, for example a short period spent outdoors, allows our olfactory system to recover or resensitize to the garlic odorant. Upon returning from garlic-free air, garlic can again be detected and recognized in the closed kitchen.

The process of adaptation, habituation and recovery are very important to predicting odour annoyance because they affect perception of odorant concentrations and therefore, the tolerance or acceptable threshold of the odorant. It is difficult to incorporate these processes into the current odour unit method as it is based on a mean concentration, where as adaptation, habituation and recovery are based on the instantaneous fluctuations in concentration. The new model for human odour annoyance developed in this chapter will incorporate these ideas into a variable detection threshold that changes with the fluctuations in exposure concentration (see Section 2.3.3 for details).

2.2.3 Improving Existing Odour Models

Several improvements can be made to the existing methods for predicting human reactions to odorant concentrations in the atmosphere. For the remainder of this chapter it will be assumed that the instantaneous concentration fluctuations can be predicted, so the psychophysical aspects of perceived intensity, habituation and adaptation, and recovery can be applied to these fluctuations in order to more completely describe human olfaction and predict odour annoyance. In the following sections a model for perceived odour intensity is developed using the six concepts of concentration, duration, frequency, detection threshold, perceived intensity and tolerance threshold.

2.3 Psychophysical Model for Human Odour Annoyance

The problem of describing human perception and response to concentration fluctuations of an airborne odorant are addressed by evaluating a normalized effective concentration, c_{eff} , and normalized perceived intensity, I . The parameters are explained in greater detail in this section.

- A base detection threshold, $c_{th,base}$, is applied to the exposure concentration fluctuations. Below this threshold, odour cannot be perceived by the median human receptor.
- An available odour concentration, c_{avail} , is calculated for all concentrations above the base detection threshold using an uptake time constant τ_{up} .
- The concepts of adaptation, habituation and recovery are incorporated in a variable detection threshold, $c_{th,vary}$, that is calculated from the effective odour concentration using a de-sensitization (adaptation and habituation) time constant τ_{de} and re-sensitization (recovery) time constant τ_{re} .
- The effective odour concentration is calculated as the difference between the available concentration and the variable detection threshold.
- The effective concentration is then normalized with the variable detection threshold and this ratio is used in the Stevens' Law Equation (2.2) to calculate the perceived intensity of the exposure concentration.

The key features of the proposed psychophysical model for human odour annoyance are the variable detection threshold $c_{th,vary}$ and the effective concentration c_{eff} . The model incorporates psychophysical concept that have yet to be included in regulatory models: an uptake time constant τ_{up} , a desensitization time constant τ_{de} and a resensitization time constant τ_{re} . (Similar ideas, such as the τ_{up} , have already been incorporated in a model for human toxicology presented by Hilderman and Wilson (1999).)

2.3.1 Concentration Fluctuations in the Atmosphere

A receptor, located at a fixed position within a plume, will be exposed to an entire range of concentrations which vary from instant to instant throughout an exposure. Figure 2.2 is an illustration of these exposure concentrations, c_{exp} .

2.3.2 Available Concentration

Available concentration, c_{avail} , determines how much of the exposure concentration is available for perception by the receptor, is a function of the exposure concentration, c_{exp} , the uptake time constant τ_{up} and the base detection threshold $c_{th,base}$, as shown in Figure 2.3. The uptake time constant accounts for the lag between exposure, inhalation and physiological response and acts as low-pass filter for the concentration fluctuations. The

base detection threshold is an odorant dependent concentration above which concentrations elicit an olfactory response. Both of these concepts are described in detail below.

Uptake Time Constant

Inhalation and the complex absorption of the chemical odorant, is approximated by a simple first order response to exposure concentration c_{exp} with uptake time constant τ_{up} :

$$\frac{dc_{avail}}{dt} = \frac{c_{exp} - c_{avail}}{\tau_{up}} \quad (2.3)$$

The uptake time constant filters the exposure concentration fluctuation time series by attenuating the concentration changes in c_{exp} , creating a lag between the available concentration and the exposure concentration. This is identical to the way a house (or any enclosed volume) acts to dampen concentration fluctuations; however the time constant for a house is on the order of an hour.

The uptake time constant τ_{up} is primarily a function of the inhalation rate, which at rest is 2.0 to 3.0 seconds per breath. The time required for olfactory receptors to detect an airborne odorant, activate the olfactory nerves, transmit information to the central nervous system (CNS), process that information, and return this information to the olfactory bulb is considered to be almost instantaneous (Guyton and Hall, 2000). New South Wales Environment Protection Authority (NSW EPA), among other regulating authorities, recommend the use of a 1.0 second nose-response time that includes both the breathing rate and olfactory response factors. (Omerod, 2001). This is conservative because it is shorter than the time of a typical inhalation and will provide less attenuation of the exposure concentration fluctuations than a longer τ_{up} . It is also assumed that the temporal resolution of the exposure concentration fluctuations is sufficient to resolve the one-second time constant effect.

Detection Threshold

The detection threshold $c_{th,base}$ is defined as the minimum concentration of odorant that will elicit a physiological response in 50% of the population. For the purposes of this study, all exposure concentrations below the base detection threshold will be considered unimportant.

As the available concentration is the concentration capable of eliciting a response, it is redefined here as having a minimum value equal to the base detection threshold as shown in Figure 2.3

$$\frac{dc_{avail}}{dt} = \frac{c_{exp} - c_{avail}}{\tau_{up}} \quad \text{for } c_{exp} \geq c_{th,base}$$

$$c_{avail} = c_{th,base} \quad \text{for } c_{exp} < c_{th,base}$$
(2.4)

The available concentration is defined in this manner because it is the driving force behind the variable detection threshold, which must be equal to or greater than the base detection threshold, as will be described in the Section 2.3.3. Figures 2.2, 2.4 and 2.5 show exposure concentrations with time scales of fluctuations much slower than one second. With $\tau_{up}=1.0$ seconds, the available concentration is approximately equivalent to the exposure concentration for the slowly fluctuating exposures shown in these figures.

2.3.3 Variable Detection Threshold - Desensitization and Resensitization

Adaptation and habituation are the physiological and psychological reduction in perceived odour intensity as a function of exposure time (Dalton, 2000). As explained in Chapter 1, it is postulated that after the onset of an olfactory stimulus, the central nervous system (CNS) develops a strong feedback inhibition to suppress relaying odour signals through the olfactory bulb. This physiological adaptation is believed to be a means to sharpen one's ability to distinguish between odorants (Guyton & Hall, 2000). In a study to correlate physiological and psychological responses to odour stimulation, Wang et al. (2002) recorded the olfactory event-related potentials (OERP) from human subjects in conjunction with cognitive responses of perceived odour intensity. They concluded that in the presence of a constant odorant, the physiological response decays to approximately half the original response in only a few breaths. The time to full adaptation was dependent on the strength of the odorant. Wang et al. (2002) also concluded that psychological habituation decays exponentially, but declines more rapidly and completely to zero compared with physiological adaptation.

For a simplified engineering model, the processes of adaptation and habituation are described by the single process of desensitization. Desensitization is the process that causes the effective odour detection threshold to gradually increase and level off with constant exposure. The human nose works like a high-pass filter that gradually removes slowly changing components but passes high frequency fluctuating components that are of interest. Consider again the simple example of cooking with garlic. Throughout the preparation and cooking of the garlic the smell gradually fades into the background. Breaking another clove of garlic to add to the food, the pungent odour will be perceived, but as cooking continues the increase in garlic odour will again fade into the background. It is only an increase in garlic odour that will be noticed. This desensitization process is illustrated in Figure 2.2 for time $t = 0$ to 200 s where the increase in the variable detection threshold allows a receptor to incorporate the odorant as part of the background odours. The effective odour concentration, c_{eff} , is the difference between the variable detection threshold and the current exposure concentration. In Figure 2.2 c_{eff} decreases for time $t = 0$ to 200 s, so the expected human response will also decrease.

When the exposure concentration is removed, people recover or resensitize to the odorant. Without resensitization, a long constant exposure would permanently inhibit people's ability to smell an odorant at concentrations equal to and below the initial exposure concentration and everyone would become anosmic, insensitive to olfactory

stimuli. Continuing with the garlic cooking odour analogy from above, leaving the kitchen for a breath of fresh air, shown in Figure 2.2 for time $t = 200$ to 300 s, causes the detection threshold to decay. This resensitization allows a person to notice the odour upon returning to the kitchen at $t = 300$ s, even though the exposure concentration is well below the variable detection threshold at the previous exposure.

Desensitization and resensitization will be modelled as a first order response function. A variable detection threshold concentration is calculated from the available concentration, c_{avail} , as:

$$\begin{aligned} \frac{dc_{th, vary}}{dt} &= \frac{c_{avail} - c_{th, vary}}{\tau_{de}} & \text{for } \frac{dc_{avail}}{dt} &\geq 0 \\ \frac{dc_{th, vary}}{dt} &= \frac{c_{avail} - c_{th, vary}}{\tau_{re}} & \text{for } \frac{dc_{avail}}{dt} &< 0 \end{aligned} \quad (2.5)$$

where $c_{th, vary}$ is the variable detection threshold concentration, c_{avail} is the available concentration, and the sensitization time constant τ_{de} or τ_{re} is used for desensitization and resensitization processes respectively. If c_{avail} is increasing or constant τ_{de} is used, otherwise τ_{re} is used as shown in Equation (2.5). The variable detection threshold $c_{th, vary}$ has a lower limit of $c_{th, base}$. The longer the sensitization time constants τ_{de} and τ_{re} , the longer it takes the variable threshold to respond to the available concentration.

2.3.4 Effective concentration

The effective concentration, c_{eff} , is the concentration above the detection threshold that produces the perceived odour sensation. It is the difference between the variable detection threshold, $c_{th, vary}$, and the available concentration, c_{avail} :

$$\begin{aligned} c_{eff} &= (c_{avail} - c_{th, vary}) & \text{for } c_{th, vary} &< c_{avail} \\ c_{eff} &= 0 & \text{for } c_{th, vary} &\geq c_{avail} \end{aligned} \quad (2.6)$$

As illustrated in Figure 2.2, when $c_{eff} > 0$ the odour is detectable, and when $c_{eff} \leq 0$ the odour is not detectable.

It can be shown from (2.6) and Figure 2.2 that the effective concentration is dependent on the sensitization time constants τ_{de} and τ_{re} . For a longer desensitization time constant, the effective concentration increases and in some cases, the duration over which the concentration is perceived also increases. Another interesting effect demonstrated in Figure 2.2. is that only an increase in concentration above the current variable detection threshold will produce a detectable effective concentration, $c_{eff} > 0$ once c_{eff} has dropped to zero. Had the exposure concentration not dipped below the

constant concentration for times 200 to 300 s, the resensitization process would not have been started, and then the concentration step at $t = 300$ s would not have crossed the variable detection threshold, and therefore its effects would not have been detected

Figure 2.4 shows two cases for exposure concentration fluctuations that are slightly more complicated than the step function in Figure 2.2. These two cases further demonstrate the behaviour of the effective concentration and the variable detection threshold. Figure 2.4(a) shows that c_{eff} decreases for both a decreasing and a constant exposure. However, when exposed to an increasing exposure concentration with a constant slope, c_{eff} levels off to a constant concentration, when the variable detection threshold follows the slope of the exposure, as demonstrated in Figure 2.4(b) for times 200 to 300 s. Complete desensitization is not attainable for the case of a constant rate of increase, “ramp” function exposure concentration.

The effect of change in frequency of peak concentration and zero concentration periods is demonstrated in Figure 2.5(a) and (b) respectively where variable periods of peak and zero concentrations result in variable amounts of desensitization and resensitization. Long zero-concentration intermittent periods and short peak concentration periods, typical of exposures in the outer fringes of a dispersing plume, produce large effective concentrations. Alternatively, long peak concentration periods and short zero concentration periods, typical of exposures near the plume centreline, produce comparatively small effective concentrations. These two observations support the idea that highly intermittent odorant exposures could be equally annoying as frequent exposures.

It is clear from Figures 2.2, 2.4 and 2.5 that human olfaction is function of the concentration exposure time series and is not adequately described by just a mean concentration estimate. Even attempts to improve the temporal resolution of mean concentration by using short averaging times (e.g. NSW EPA who suggest the use of a 1.0 second averaging time (Omerod, 2001)) do not provide any information on the sequence of the exposure concentrations and cannot include complex time dependent effects as described above.

2.3.5 Perceived Intensity

The concepts of effective concentration and a variable detection threshold, based on the exposure concentration and duration, cannot be incorporated directly into the current standard for predicting human odour annoyance, O_U . The current odour unit method relies on a concentration that is calculated from an ensemble of concentrations, such as the Gaussian, as opposed to concentration that fluctuates second-by-second. Applying the sensitization time constants to a constant concentration results in an effective concentration that decays to zero, and does not recover from zero unless the mean concentration changes by means of change in wind direction, for example. The deficiency in the odour unit model is that sensory perception, which is non-linear with exposure concentration, is not included. A modified definition for odour units will be used with Stevens’ law, Equation (2.2), to create a new psychophysical function for the

prediction of perceived intensity of an exposure concentration while including the concepts of an effective concentration and a variable detection threshold.

Combining the concepts of odour units and Stevens' law for perceived intensity, Equation (2.2) becomes

$$\text{Perceived Intensity} = O_U^n = \left(\frac{C_{avg}}{c_{th,base}} \right)^n \quad (2.7)$$

Equation (2.7) is equivalent to Equation (2.2) where $k = (1/c_{th,base})^n$. When O_U , is greater than 1.0, the odour is detectable. Using Equation (2.7), intensity is only perceived over the range $1.0 < \text{Perceived Intensity} < \infty$. A shift in starting point for the intensity to zero is more logical; using this range, an $\text{Perceived Intensity} > 0$ would indicate that a receptor is able to detect the odorant. In order to achieve this effect, the base in Equation (2.7) is replaced by $O_U - 1$ to form the odour unit intensity, also shown in Figure 2.1:

$$I_{OU} = (O_U - 1)^n = \left(\frac{C_{avg} - c_{th,base}}{c_{th,base}} \right)^n \quad (2.8)$$

In order to incorporate the desensitization and resensitization processes, a new time-dependent intensity I is defined as the ratio of effective concentration, c_{eff} , to the variable detection threshold, $c_{th,vary}$, as illustrated in Figure 2.6:

$$I = \left(\frac{c_{eff}}{c_{th,vary}} \right)^n \quad (2.9)$$

where n is Stevens' exponent, with a range from 0.2 to 0.8 for odorants (NSW EPA, 2002, Stevens, 1957). The effective concentration c_{eff} as defined in Equation (2.6) is $c_{avail} - c_{th,vary}$ for $c_{avail} > c_{th,vary}$, and $c_{th,vary}$ is governed by the sensitization processes with values greater than or equal to $c_{th,base}$. For these reasons the intensity I is defined using (2.9) for a range $0 < I < \infty$, where an intensity $I > 0$ can be detected and therefore, has potential for annoyance. Equation (2.9) will be used as the definition for intensity for the remainder of this study. This intensity, I , is akin to the odour unit intensity, I_{OU} ; these two measures of intensity will be compared later in Chapter 4.

The intensity I varies with time, so an input time series of odorant concentration fluctuations produces a time series of perceived intensities. Methods for comparison between perceived odour intensity time series will be examined in Section 2.4.

2.4 Psychological Model for Human Odour Annoyance

The problems of accounting for differences in human perception and response to concentration fluctuations of airborne odorants are addressed by evaluating a memory load, L .

- A linearly-fading memory window is used to capture the perceived intensities, I , of all exposure concentrations, present and remembered. The variation in odour sensitivity within a population is accounted for through a variable memory window length, t_{mem} , where more sensitive people can recall odour events over a longer time.
- Memory load, L , is calculated from the sum of I over a person's memory window at any given time during an exposure.
- Mean memory load, L_{avg} , is calculated from an ensemble of memory loads throughout an odour exposure and is normalized in such a way to allow for comparison between odour exposures over different durations, for different odorants, and for varying sensitivity in exposed people.

The mean memory load is an indication of the odour annoyance an individual might experience during an odour exposure: L_{avg} greater than zero indicates that the odour was detected (and therefore has potential for annoyance), and increasing L_{avg} is indicative of increasing odour annoyance.

2.4.1 Memory Window

It can be assumed that sensitive people who are easily annoyed by an odour can remember odour events for a long time. Conversely, insensitive people have a shorter memory of the previous odour events. This effect will be modelled with a moving memory window to isolate the effects of the current and remembered odour events. The sensitivity of individuals can be accounted for through the length of memory window, t_{mem} .

Odour sensitivity differs among individuals in a population. Dalton (2003) showed that among all factors the differences in beliefs or attitudes towards the possible consequences of exposure to airborne chemicals plays the largest role. Without performing a community survey, the differences among individuals are difficult to predict. Like most natural processes, the differences in individuals, including odour sensitivity, follow a log-normal distribution (Shusterman, 1992). Conceivably, an array of t_{mem} with a log-normal distribution of memory window times could be used to test the sensitivities of individuals in a population. This type of activity is beyond the scope of this study and will be left for future research.

It is logical to assume that for two events of equal magnitude, the first having just occurred and the second having occurred an hour ago, the first event would be perceived as having a larger effect than the second. A linear window time weighting function, $W_o(t)$, is used to simulate this decaying memory of past events. The window starts at zero

percent at a fixed time in the past, and ramps up to 100 percent at the present time, shown as “Window Weighting” in Figure 2.7. The window remains at a constant size and moves in time so that previous events are eventually forgotten.

2.4.2 Memory Load

The concept of an integrated load has been used when describing the cumulative effect of a toxic exposure, for example see Hilderman *et al.*, (1999). In the proposed odour model this load concept is extended to human olfaction to predict a person’s annoyance level.

At any given time, a person’s level of tolerance for an odorant is a function of the current perceived intensity of that odorant, and the perceived intensities of the odour events that have occurred within his/her memory window, including the weighting effect of the window. The instantaneous memory load, L , is calculated at the present time step, $t = 0$:

$$L = \int_{t=-t_{mem}}^{t=0} W_o(t) \left(\frac{c_{eff}(t)}{c_{th, vary}(t)} \right)^n dt \quad (2.10)$$

Where $c_{eff}(t)$ is the effective concentration as a function of time t which is normalized by the variable detection threshold $c_{th, vary}$, multiplied by the window weighting, $W_o(t)$, and integrated over the duration of the memory window from $t = -t_{mem}$, to the present time $t = 0$.

Figure 2.7 demonstrates the procedure for calculating the integrated memory load. At time $t_0 = 0$ minutes, the normalized effective concentration is zero and the integral load is zero. When a receptor is not currently being exposed to an odorant and he/she can not recall having been exposed to an odorant, their odour load is zero. The memory load only increases above zero when a person is exposed to an odorant concentration above their current detection threshold, i.e. $c_{eff} > 0$. This is illustrated in the first column ($t_1 = 10$ minutes into the exposure) of Figure 2.6. The second column ($t_2 = 30$ minutes into the exposure) in Figure 2.6 demonstrates that for an effective concentration step change the maximum instantaneous load occurs at the moment when the entire load has just entered their memory window. This maximum annoyance level is a function of the linearly weighted memory time window. Other memory window weighting functions may produce different results. As the step change effective concentration passes into memory and the current effective concentration is once again zero, the instantaneous load decreases. The receptor “forgets” about the odour event, as illustrated in the third column ($t_3 = 60$ minutes into the exposure) of Figure 2.7. Extrapolating this concept of a memory window, it is easy to see that for an identical effective concentration time series, longer memory windows will produce larger instantaneous memory loads.

A long memory window will produce a larger memory load than a short memory window, but it is uncertain how long or short the memory window should be for a given receptor. The comparison of individual receptors’ sensitivities, using varying t_{mem} , is beyond the scope of this study; but it is important to evaluate trends in this human odour

annoyance model for different plume characteristics. To reduce the complications of individual receptor sensitivities, Equation (2.10) is normalized by the length of the memory window, t_{mem} :

$$L = \int_{t=-t_{mem}}^{t=0} \frac{W_o(t)}{t_{mem}} \left(\frac{c_{eff}(t)}{c_{th,vary}(t)} \right)^n dt \quad (2.11)$$

Equation (2.11) can also be written in terms of the perceived intensity I :

$$L = \int_{t=-t_{mem}}^{t=0} \frac{W_o(t)}{t_{mem}} I(t) dt \quad (2.12)$$

Of all parameters used in this model, the psychological t_{mem} parameter has the least amount of certainty associated with it and is the least amenable to engineering analysis. By normalizing the memory load using t_{mem} the complications of this psychological parameter are minimized.

Because intensities greater than zero are detectable (see Section 2.3.5), memory loads $L > 0$ indicate a potential for annoyance. Equation (2.11) will be used throughout the remainder of this study to calculate the memory load as a measure of odour annoyance.

2.4.3 Ensemble Average Memory Load

The instantaneous odour load is calculated for each time step, as illustrated in Figure 2.7, and therefore fluctuates as the concentration fluctuates in time. In order to compare the effects of different concentration exposures, an ensemble average memory load, L_{avg} , is calculated from the instantaneous odour loads through the exposure or sampling time.

$$L_{avg} = \langle L(t) \rangle$$

or

$$L_{avg} = \left\langle \int_{t=-t_{mem}}^{t=0} \frac{W_o(t)}{t_{mem}} \left(\frac{c_{eff}(t)}{c_{th,vary}(t)} \right)^n dt \right\rangle \quad (2.13)$$

By taking an ensemble average, the mean odour load, L_{avg} , is effectively normalized by the exposure or sampling time, t_s , allowing for comparison of mean odour loads between exposures of varying length. Mean odour loads greater than zero indicate a potential for odour annoyance, and larger mean odour loads indicate larger levels of annoyance.

One of the key assumptions in this study is that human olfaction is tuned to detect change. Odour annoyance must correlate to the number of times a change is detected,

which is the number of times the exposure concentration exceeds (up-crosses) the variable detection threshold $c_{th, vary}$. This correlation is inherent in the model because without a concentration greater than $c_{th, vary}$ the odour load does not exceed zero; and as the number of up-crossings increases so to does the number of times c_{eff} is greater than zero and therefore, the magnitude of L_{avg} also increases. In addition, another assumption of this study is that highly intermittent odorant exposures can be equally annoying as less intermittent odorant exposures. The ensemble average memory load L_{avg} of Equation (2.13) will be used to demonstrate that the mean memory load can be greater for concentration fluctuations that are highly intermittent, than for less intermittent exposures.

The application of Equation (2.13) requires the use of a backward difference numerical method for calculation of the memory load at each time step within an ensemble. Programming optimization techniques were required to reduce computation time, depending on the length and number of time series in an ensemble. With proper optimization, computation times were reduced by a factor of 1000.

2.5 Summary

The plume dispersion models used to describe odorant exposures limit current regulatory models for human olfaction. Typical dispersion models use smooth ensemble averages, such as a Gaussian plume profile, to predict mean concentrations of odorant for a given averaging time. These simple models do not take into consideration the time- and concentration-dependent psychophysical processes of sensitization, but instead use only predicted exposure concentrations and detection thresholds that are constant in time, to produce a single odour unit O_u value as shown in Equation (2.1). Odour unit predictions do not include the random nature of turbulent dilution and dispersion that cause wide fluctuations in the instantaneous concentrations of odorant including periods of zero (background) concentration, periods of concentrations greater than twenty times the mean concentration, and all of the fluctuations in between.

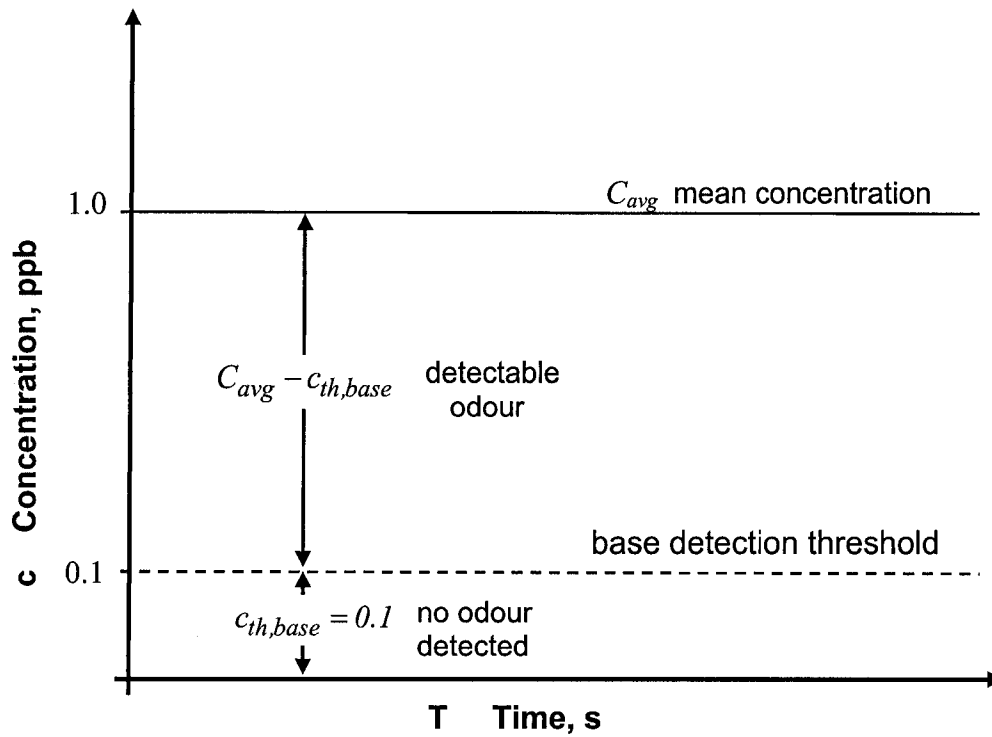
A new odour model has been developed by considering the complex physics involved in atmospheric dispersion and psychophysical factors that affect human perception of odorants.

- The model proposed here incorporates the time-dependent nature of concentration fluctuations in the atmosphere and the known ability for people to adapt and habituate (desensitize) and recover (resensitize) from odours, to create the time- and concentration-dependent variable detection threshold, $c_{th, vary}$, in Equation (2.5). This variable detection threshold is used in Equation (2.6) to determine the effective concentration c_{eff} for producing an olfactory response.
- People are known to perceive odour in terms of intensity rather than concentration. Using the concept of a psychophysical function for perceived intensity derived by Stevens (Equation (2.2), CEN, 1998), Equation (2.9) has been developed for perceived intensity, I , based on the variable detection threshold $c_{th, vary}$ and the effective concentration c_{eff} . In this manner, the odour annoyance

model takes into account the non-linearities between perceived intensity and exposure concentration.

- Borrowing the concept of integrated load from toxicology and using a linearly-fading memory time window, the effective intensity for a person's present and recent past odour exposures has been developed in terms of the odour load in Equation (2.11). An ensemble average of these odour loads, as in Equation (2.13), allows for comparison between different exposures. A memory load greater than zero is detectable, and an increasing memory load leads to higher annoyance levels. These comparisons will allow regulatory agencies to compare emission events and assess the relative annual odour exposures, from which annoyance occurrences can be predicted.

This odour annoyance model incorporates the complexities of both the atmospheric dispersion of airborne odorants and the psychophysical principles that govern human perception of odorant stimuli in an improved engineering model that accounts for the non-linearities of odour perception.



odour units are defined as:

$$O_U = \left(\frac{C_{avg}}{c_{th,base}} \right)$$

odour unit intensity is defined as:

$$I_{OU} = \left(\frac{C_{avg} - c_{th,base}}{c_{th,base}} \right)^n = (O_U - 1)^n$$

typically: $0.2 < n < 0.8$

Figure 2.1: Odour unit intensity converts regulatory odour units to perceived intensity, based on Stevens' Law.

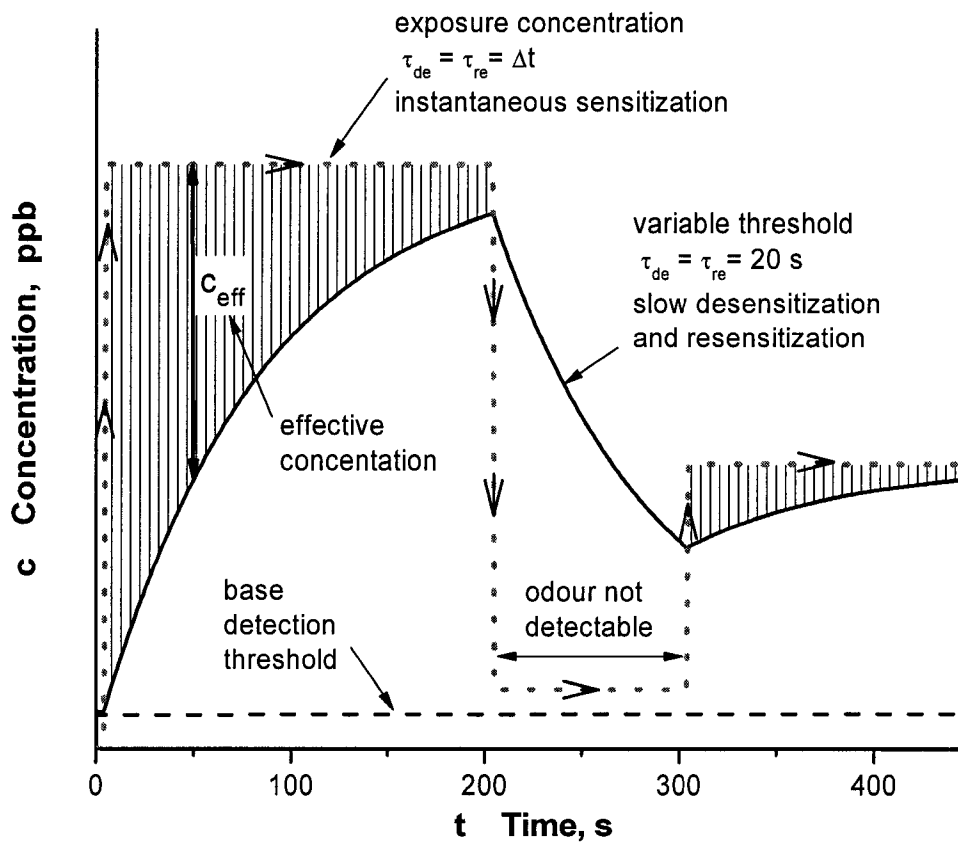


Figure 2.2: Variable detection threshold, $c_{th, vary}$, desensitization and resensitization time constants, τ_{de} and τ_{re} respectively. Effective concentration, c_{eff} , is the difference between available concentration and the variable detection threshold, for times when $c_{avail} > c_{th, vary}$. Shaded regions shows detectable odour.

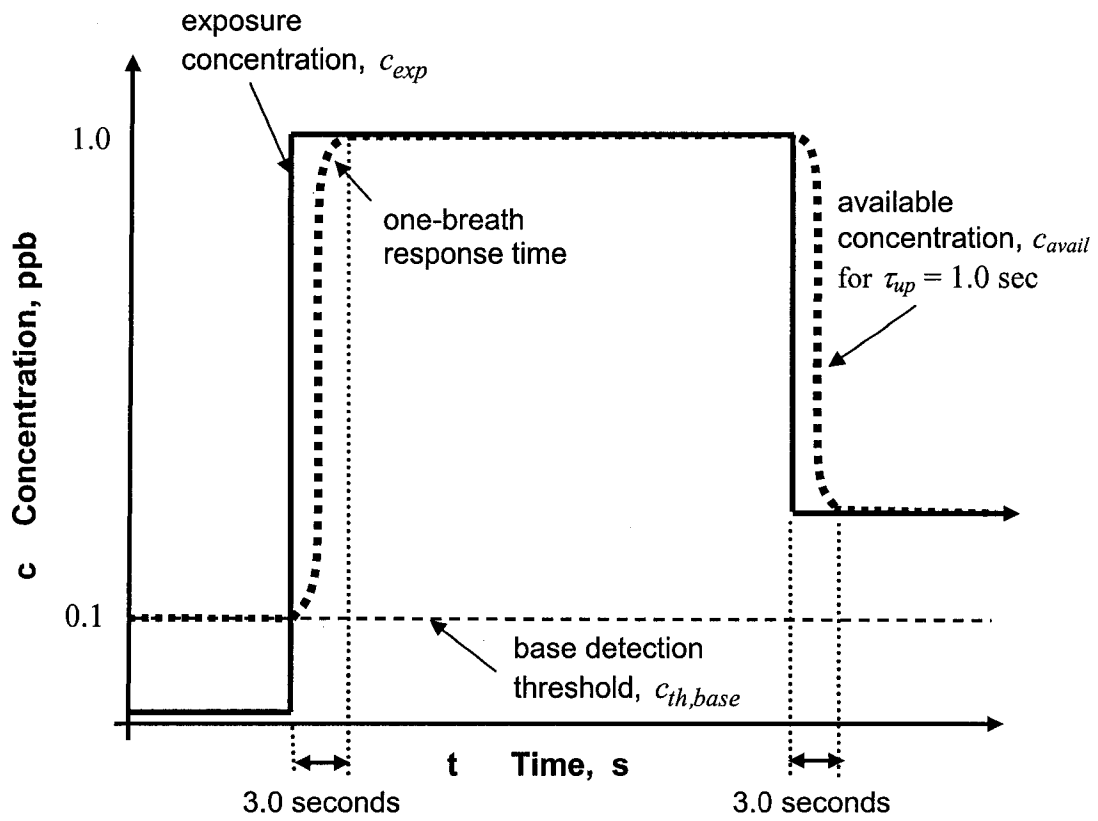
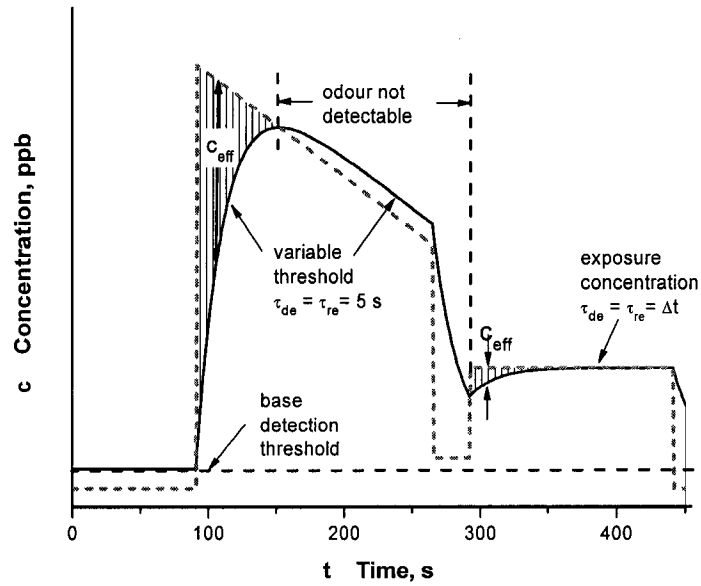
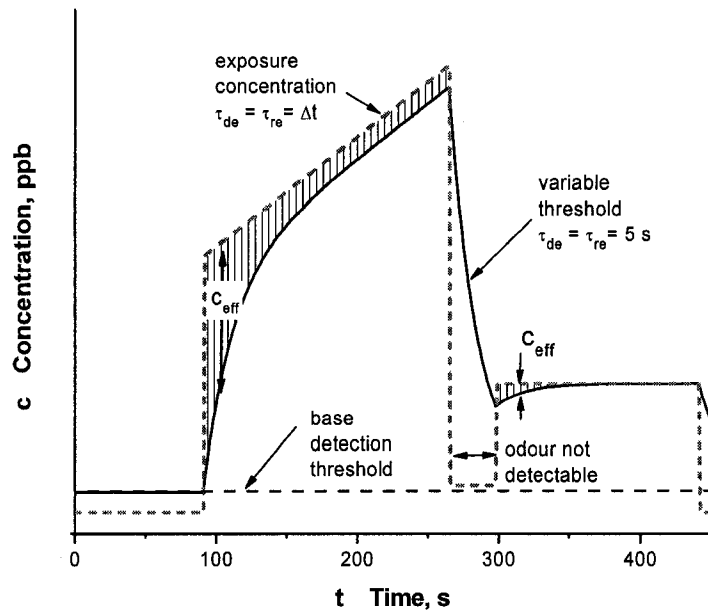


Figure 2.3: Illustration of the concept of available concentration. (Delay is typically 2τ to 3τ time scales in length.)

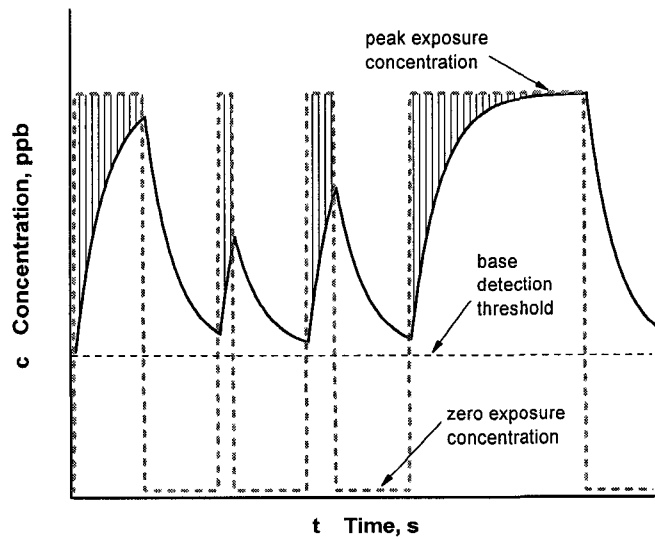


(a)

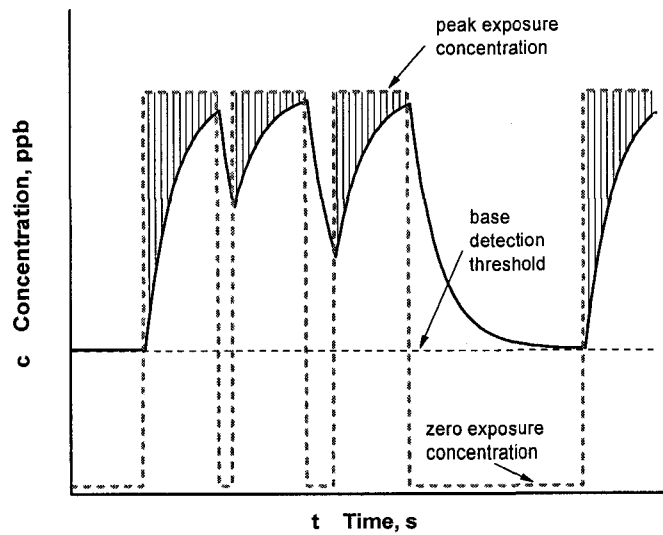


(b)

Figure 2.4: Behaviour of the variable detection threshold model. Shaded regions shows detectable odour.

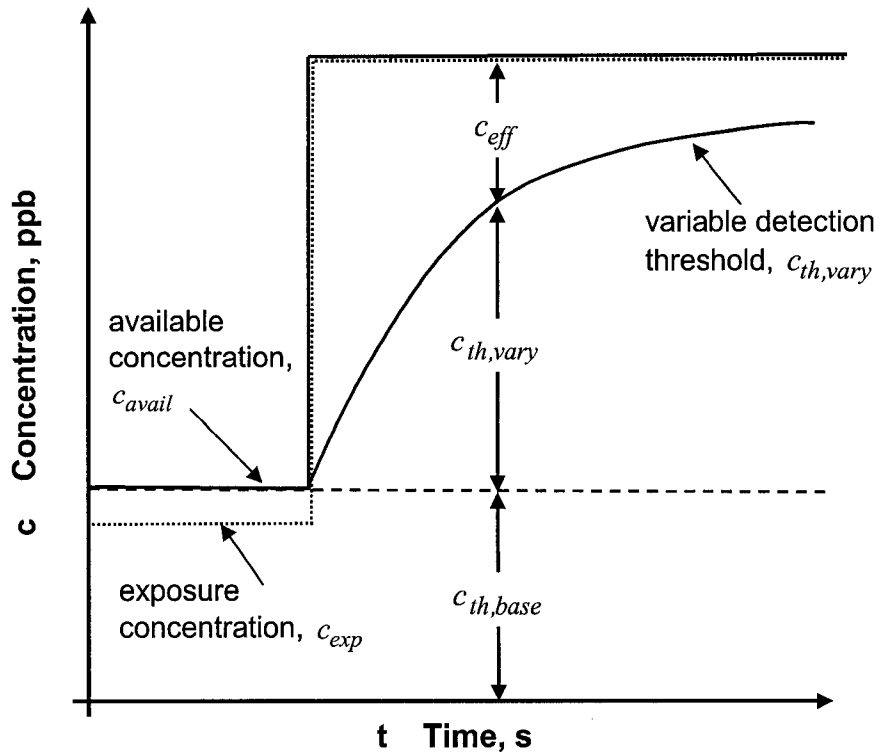


(a)



(b)

Figure 2.5: Effect of increasing peak, figure (a), and zero, figure (b), concentration periods for equal desensitization and resensitization time constants. Shaded regions shows detectable odour.



Model Definition:

normalized odour intensity

$$I = \left(\frac{c_{eff}}{c_{th,vary}} \right)^n$$

typically: $0.2 < n < 0.8$

Figure 2.6: Illustration and definition for model of perceived intensity, I , developed in this study to predict human response to airborne odorants. Effective concentration, c_{eff} , shows detectable odour.

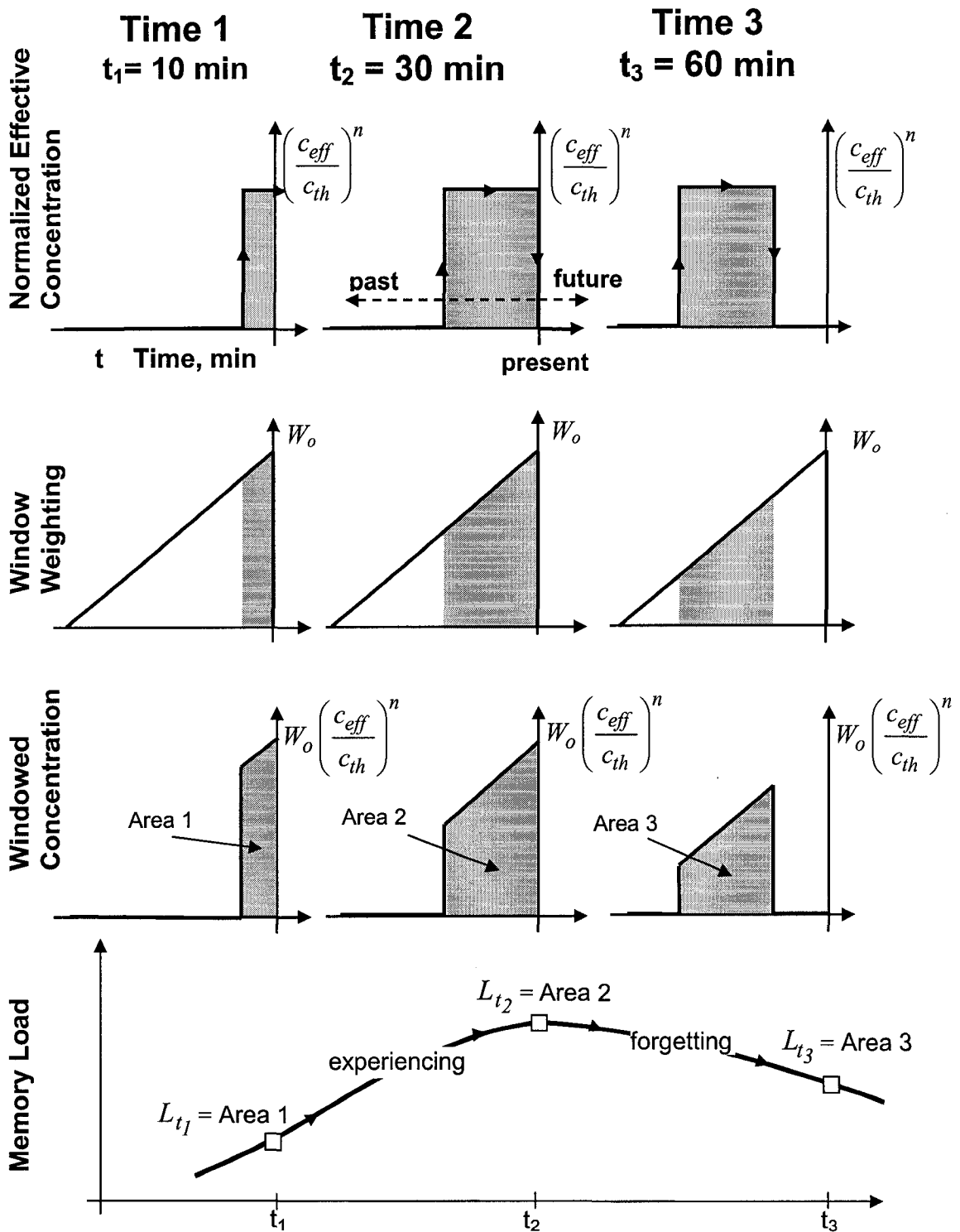


Figure 2.7: Illustration for the calculation of the time varying memory load, L , at three time steps. The load reaches a maximum when the entire event is first present in the window, and then decays as the step concentration passes through the memory window.

Chapter 3

Predicting Full-Scale Concentration Fluctuation Statistics and Water Channel Scale-up Technique

3.1 Introduction

Random turbulent motion in the atmospheric mixing layer produces high frequency concentration fluctuations ranging from zero (background) concentration to greater than 20 times the mean concentration are expected at a receptor location within the dispersing plume. This chapter focuses on producing simulated full-scale concentration time series at downwind and crosswind points of interest, by scaling laboratory water channel data to match predicted full-scale plume characteristics. The mechanics of plume dispersion in the atmosphere must be understood to properly scale the data and produce time series with the correct the exposure concentration, duration and frequency. These time series are then used as inputs to the psychophysical and psychological model presented in Chapter 2.

Typical regulatory Gaussian plume dispersion models predict several minute to several hour mean concentrations. In the regulatory approach, these mean values are then transformed with peak-to-mean concentration factors into “instantaneous” peak concentrations representative of a single breath averaging time. However, simple dispersion models based on mean downwind and crosswind concentrations cannot predict the time series of instantaneous concentration fluctuations produced in the atmosphere. As discussed in the development of the odour model in Chapter 2, detailed knowledge of these concentrations fluctuations is required for the accurate prediction of human reaction to airborne odours.

Simulated full-scale time series of instantaneous concentration fluctuations will be produced from a library of data from small scale water channel plumes scaled to match the following five parameters:

- mean concentration C_{avg}
- fluctuation intensity i
- intermittency factor γ
- conditional fluctuation intensity i_p
- integral time scale of concentration fluctuations T_c

Normalized parameters such as the conditional fluctuation intensity i_p and intermittency factor γ are not affected by scale, so i_p and γ evaluated for each full-scale position will be used to choose specific time series from the experimental data set. The concentration will be scaled to match the mean concentrations at respective full-scale positions. The elapsed time of the water channel data series will also be scaled by comparing measured concentration integral time scales T_c for each experimental data set to the expected ground level concentration integral time scales calculated from a model developed by Hilderman (2004, Chapter 3). A key feature of the time scale-up method used is that fluctuations are assumed to have no inertia, so that even short time steps scale kinematically with the mean flow velocity and length scale-up factor.

The contribution of the present study is the application of existing concentration fluctuation models to scale up the author's small-scale water channel measurements to simulate full-scale odour perception in the atmospheres. This scale-up process relies heavily on the concentration fluctuation models developed by Wilson (1995), Hilderman and Wilson (1999), and refined in Hilderman (2004). In Sections 3.2 and 3.3, their methods for estimating concentration fluctuation statistics are described, and adapted to generate the necessary scale-up.

Later, in Chapter 4, these scaled up downwind and crosswind time series will be used to evaluate the model for human odour annoyance developed in Chapter 2 to establish trends in mean odour load for a dispersing plume of odorant in a neutrally stable atmosphere.

3.2 Statistics Currently Used to Model Odour Annoyance

In this section, the basic concepts of Gaussian plume dispersion models and regulatory application for predicting human reaction to odorants, will be examined. The Austrian odour dispersion model (AODM) (Schauberger *et. al*, 2000) will be used as an example of the application of peak-to-mean ratios to correct some of the shortcomings of a basic (mean concentration only) Gaussian model.

3.2.1 Gaussian Dispersion Model

One commonly used, public domain, Gaussian dispersion model is the Industrial Source Complex (ISC3) (USEPA 1995 a, b). This type of model predicts an ensemble average of all of the concentration fluctuations in the plume to produce a smooth distribution of concentration, illustrated in Figure 1.1. It also assumes constant meteorological conditions over the travel time from the source to the receptor, and is applicable for event durations of 3 minutes to a few hours (Wilson, 1995, Best *et al.*, 2001).

The Gaussian model provides a general description of the footprint of a dispersing plume. It predicts time-averaged mean concentrations for positions downwind of the source as well as crosswind from the plume mean centreline. The averaging time plays an important role in the mean centreline direction and the estimated mean concentrations. The plume centreline (or convective direction) is a function of averaging time: the longer

a plume is observed (i.e. the longer the averaging time), the larger the eddy sizes which affect the plume, and the more the plume meanders.

Assuming statistically stationary turbulent flow in the atmosphere, Figure 3.1 illustrates the effects of increasing averaging time on plume characteristics. Longer averaging times produce larger plume spreads as the plume meanders over a larger footprint. A simple mass balance shows that if the same amount of mass is spread over a larger cross-sectional area the result is a smaller centreline mean concentration and a larger mean concentration at the plume edges. The longer the averaging time for the mean the greater the difference between the mean and the instantaneous peak concentration. For this reason, the New South Wales Environment Protection Authority in Australia (NSW EPA), among other regulating authorities, recommend the use of nose-response based one-second averaging time in odour models, (Omerod, 2001).

Even with a short averaging time, the smooth concentration profiles predicted using a Gaussian model do not account for the instantaneous turbulent concentration fluctuations, including zero periods, within the plume. This shortcoming of regulatory models is evident when comparing the glassy-smooth Gaussian profile to an instantaneous profile for a downstream position in the plume, shown in Figure 1.1. It is this shortcoming that limits the ability of the odour unit approach to accurately describe the time and concentration varying ways that people respond to odours.

3.2.2 Peak-to-Mean Values

In an attempt to overcome the inability of the Gaussian model to predict realistic instantaneous concentrations, Schauburger *et al.* (2000) made peak-to-mean corrections in the AODM. Peak-to-mean ratios are usually calculated from the following power law relationship:

$$\frac{C_{avg,p}}{C_{avg,m}} = \left(\frac{t_m}{t_p} \right)^q \quad (3.1)$$

Where $C_{avg,m}$ is the mean concentration for an averaging time of t_m and $C_{avg,p}$ is the peak concentration for an averaging time of t_p . As reviewed by Schauburger *et al.* (2000), Smith (1973) gives values of the exponent q that range from 0.35 for stable conditions to 0.65 for unstable conditions. Schauburger *et al.* give a more sophisticated method for calculating a peak-to-mean ratio that decrease with downwind distance from the source. This ratio is a function of the ratio in Equation (3.1) and the Lagrangian time scale. Best *et al.* (2001) offer a different approach used by the NSW EPA that is based on the concentration fluctuation intensity (a measure of peak concentrations) correlated to the source type and indicate that these ratios can be used with an hourly average concentration prediction. The reasons for and values of peak to mean ratios can vary greatly between methods used.

The assortment of peak-to-mean calculation schemes indicate that this method of predicting plume concentrations is a crude and uncertain estimate of the random time-

varying concentrations within a dispersing plume. Even if realistic peak concentrations could be estimated, it is not always clear what this peak is meant to describe: the 90th percentile, the 99th percentile, the once per event peak, or the worst case peak. These methods tend to be vague and certainly do not provide a complete description of time-varying fluctuations of a dispersing plume.

To help understand why the fluctuations are important to predicting odour effects consider the simple everyday example of cooking with garlic. Initially, there is no garlic odour in the room, but as pressing and cooking of the garlic proceeds the concentration increases, allowing us to detect the odour. At a constant concentration, below irritation levels, our olfactory system adapts/habituates to the garlic odorant and the smell fades into the background of the environment. Periods of zero concentration, for example a short period spent outdoors, allows our olfactory system to recover or resensitize. Upon returning from a garlic-free air, the garlic smell is recognized in the closed kitchen once more. A dispersion model that predicts only the peak garlic concentration in the kitchen is not an accurate model of even this simple event because it does not provide a picture of the changing odour events is not sufficient for a model for human olfaction with time and concentration varying parameters.

3.3 Description of Instantaneous Concentration Fluctuations

Instantaneous concentration fluctuations are caused by a range of turbulent eddy sizes that distribute energy and matter, including odorants, in the atmosphere. Eddies that are approximately the width of the plume, and larger, are responsible for meandering the plume back and forth about a mean plume centreline. A downstream 1-D slice through an instantaneous snapshot of a plume in Figure 3.2 shows that these large eddies are responsible for large pockets of concentrations greater than zero, shown at position four, and long periods of zero concentration, shown at position three. Eddies much smaller than the plume disperse smaller pockets of concentration within the meandering plume as illustrated in positions one and two of Figure 3.2.

For a human receptor at a fixed distance downstream of the source, it is more appropriate to think of the concentration fluctuations changing in time. From this Eulerian (receptor at a fixed position on the ground) point of view, long periods of zero concentration are indicative of the plume meandering away from the receptor, while long periods of time when the concentration is above zero indicate that the plume is directly overhead. For a position on the mean centreline the receptor will experience mostly non-zero concentrations. For a position at the edges of the plume, the receptor will experience peaks of concentration amongst long periods of fresh air.

Plumes can be characterized using five parameters.

- **Mean concentration** C_{avg} is a function of either sampling time (as will be used in this study) or equivalently averaging time (as used by regulatory agencies to calculate peak concentrations)
- **Fluctuation intensity** i , is a measure of concentration fluctuations about the total mean, illustrated in Figure 3.3, and is defined as:

$$i = \frac{c'_{rms}}{C_{avg}} \quad (3.2)$$

where $\overline{c'^2}$ is the variance of the concentration and the standard deviation or the root mean square fluctuation is $c'_{rms} = \sqrt{\overline{c'^2}}$. (The conventional notation for indicating the instantaneous concentration, c , in terms of the fluctuation, c' , from the mean concentration C_{avg} , is $c = C_{avg} + c'$).

- **Intermittency factor γ** is the fraction of exposure time the atmospheric concentration of odorant is greater than zero, as illustrated in Figure 3.3. Plume intermittency leads to the definition of two kinds of statistics; total concentration statistics include the zero concentration periods and conditional statistics include only periods when the plume is present, excluding the zero concentration periods. Conditional statistics are denoted by a subscript “p” for in-plume.
- **Conditional fluctuation intensity i_p** is an indication of the peak-concentration fluctuations when the plume is present, i.e. odorant concentrations are greater than zero:

$$i_p = \frac{c'_{rms,p}}{C_{avg,p}} \quad (3.3)$$

where $\overline{c_p'^2}$ is the conditional concentration variance and $C_{avg,p}$ is the conditional mean concentration. The total and conditional (in-plume) fluctuation intensities are related to the intermittency factor through the exact algebraic definition (Wilson et al., 1985, Equation (8)):

$$\gamma = \frac{1+i_p^2}{1+i^2} \quad (3.4)$$

- **Integral time scale of concentration fluctuations T_c** provides an indication of how quickly changes in concentration occur within the dispersing plume. The shorter T_c , the faster the fluctuations occur. Hilderman (2004) explains that the timescale can be calculated from the one-dimensional power spectra of the concentration time series. The intercept, $E_c(0)$, is calculated by extrapolating the spectrum to zero frequency and T_c is found from the following definition:

$$T_c = \frac{E_c(0)}{4\overline{c'^2}} \quad (3.5)$$

As Hilderman (2004) explains, the highly sheared flow at ground level produces large differences in plume characteristics compared to a plume dispersing in more homogenous

turbulence well above ground level. The non-dimensional shear, S , developed by Hilderman will be used to correct full-scale predicted γ , i , i_p and T_c for this effect following the methods prescribed in his 2004 thesis.

Figure 3.4 shows two examples of typical concentration exposure time series. Short bursts of high concentration with long periods of no concentration are characteristic of plumes with low intermittency factors and large conditional fluctuation intensities, as shown in Figure 3.4a. Small changes about the mean concentration and short periods of no concentration are characteristics of plumes with high intermittency factors and small conditional fluctuation intensities, shown in Figures 3.4b.

3.3.1 Use of Concentration Fluctuations in Mean Memory Load

The concept of memory load was developed in Chapter 2 to account for both the physiological and psychological aspects to odour annoyance. The mean memory load, L_{avg} , calculated using Equation (2.13), is a tool to compare the perceived intensities of odour for different memory window lengths and odorant concentration exposures. The perceived odour intensity I developed for this study is a function of the effective concentration to a power n ; where the effective concentration varies in time with the atmospheric concentration fluctuations and the exponent has a range $0.2 < n < 0.8$. Effectively, the mean odour load can be thought of as a function of time-varying concentrations to the power n and averaged, $\overline{c^n}$. It is of interest to explore the difference between $\overline{c^n}$ and C_{avg}^n . If there is little difference between the two, instantaneous concentration fluctuations are not necessary to describe the mean memory load. However, for powers n much different than unity, as in the case of odour, there is a large difference between the two. This can be easily shown through the following numerical example.

Assume a concentration exposure made up of simple step functions, where the non-zero concentrations are four times the mean concentration, $c = 4C_{avg}$, and the fluctuations are greater than zero for $\gamma = 0.25$. Figure 3.5 is an illustration of such an exposure. Using the fluctuation notation discussed above,

$$\begin{aligned} \overline{c^n} &= \overline{(C_{avg} + c')^n} \\ \text{or} & \\ \overline{c^n} &= C_{avg}^n \left(1 + \frac{c'}{C_{avg}} \right)^n \end{aligned} \tag{3.6}$$

Making use of the intermittency factor, γ , and the conditional concentration fluctuations, c_p ,

$$\overline{c^n} = C_{avg}^n \left[(1-\gamma) \left(1 + \frac{c'}{C_{avg}} \right)_{c=0}^n + \gamma \left(1 + \frac{c'}{C_{avg}} \right)_{c>0}^n \right] \quad (3.7)$$

Assuming a Steven's exponent $n = 0.4$, and using the assumed values and lengths of the peak and zero concentrations, (3.7) becomes:

$$\begin{aligned} \overline{c^{0.4}} &= C_{avg}^{0.4} \left[0.75(1-1)^{0.4} + 0.25(1+3)^{0.4} \right] \\ &= C_{avg}^{0.4} [0 + 0.435] \end{aligned} \quad (3.8)$$

Finally,

$$\overline{c^{0.4}} = 0.435 C_{avg}^{0.4} \quad (3.9)$$

In this simple example, $\overline{c^n} > C_{avg}^n$. This simple example holds true because the square wave time series must produce the correct mean value in relation to the intermittency factor, γ , and peak concentration, c , such that

$$C_{avg} = (\gamma - 1)(0) + \gamma(c) \quad (3.10)$$

or,

$$c = \frac{C_{avg}}{\gamma} \quad (3.11)$$

This illustrative example can't be applied to all values of intermittency (for a square wave, the peak concentration c would have to change to reflect γ according to Equation (3.11)). Equation (3.11) does not apply to a log normal probability distribution of concentration fluctuations, where the peak concentration is interpreted as the value exceeded only 1.0% of the time. However, for exponents less than unity, $\overline{c^n} < C_{avg}^n$. Applying an exponent $n < 1.0$ to a time series effectively "drags" all concentrations greater than zero closer to the mean concentration, and reduces the effect of the fluctuations about the mean. The mean concentration will over-estimate of the effect of the fluctuations.

Regardless, it is the instant-to-instant variation in concentrations that dictate the effective odour concentration, c_{eff} , that is responsible for human response, and without a time series of fluctuations, human response can not be predicted. This will be illustrated in the following chapter when a highly intermittent time series at the edge of the plume is compared to a time series along the plume centreline with mostly non-zero concentrations with an equivalent mean concentration. Intermittent versus non-intermittent time series result in very different mean memory loads. The mean of the exposure concentrations is not enough information to adequately describe the dilution of odorants in the atmosphere,

nor is it enough information to test the odour annoyance model. Time series of concentration fluctuations are necessary to test the odour annoyance model.

3.3.2 Simulating Full-scale Concentration Fluctuations by Scaling Water Channel Data

In the following sections of this chapter, details of mapping five different plume characteristics in the downwind and crosswind directions from an odorant source will be explored.

- Change in mean concentration crosswind and downwind will be evaluated assuming a Gaussian mean profile with respect to a reference receptor location. This map of relative mean concentrations will then be used to linearly stretch experimental data to represent full-scale concentration fluctuations.
- Assuming inertialess fluctuations the concentration integral time scale can be used to scale experimental data in time to produce plausible atmospheric fluctuation rates.
- The conditional fluctuation intensity, i_p , gives a clear indication of the peaks in concentration compared to the mean when the plume is present. In comparison, the total fluctuation intensity, i , is less informative and more difficult to interpret: a large i could indicate large peak concentrations, or a small intermittency factor γ , or a combination of both. Considering that the conditional fluctuation intensity is easier to interpret, i_p is used in conjunction with γ as the parameters to characterize a plume.

These characteristics will be used to map the concentration fluctuations expected in a dispersing plume measured at ground level for various downwind and crosswind receptor positions. This map will be used to select experimental water channel concentration fluctuation data sets.

3.4 Predicting Full-scale Concentration Fluctuation Statistics

In order to choose appropriate concentration fluctuation time series from the water channel experimental data, the full-scale concentration fluctuation statistics must be predicted.

- Normalized mean concentrations will be evaluated based on the dispersion of a Gaussian plume for downwind and crosswind positions centred about and normalized by a position an $x = 1$ km downwind of the odorant source along the plume centreline ($y = 0$).
- The non-dimensional wind shear parameter, S , developed by Hilderman (2004, Chapter 3) will be used in this study to correct the following four plume characteristics to account for wind shear effects in which dU/dz smears out and reduces concentration fluctuations near ground level where most odour receptors are located.

- The concentration integral time scale, T_c , is used to describe the length of time between concentration fluctuations, and therefore, odour events. T_c will be calculated using S for each of the downwind and crosswind positions.
- The predictions for the concentration fluctuation intensity, i , are based on Wilson's (1995) pseudo-meandering plume model, and will be adjusted for shear using the non-dimensional shear S .
- The conditional concentration fluctuation intensity and the intermittency factor will be calculated from i , and, as such, will be corrected for shear effects. The conditional intensity and intermittency pair calculated for each downwind and crosswind position will be used in the following section to select the appropriate water channel data series.
- These series will then be scaled with mean concentration and concentration integral time scale to produce time series of concentrations fluctuations representative of those expected in the full-scale atmosphere. These scaled time series will then be used in the following chapter to evaluate the odour annoyance model.

3.4.1 Mean Concentration, C_{avg}

The mean concentration C_{avg} is the average concentration over the entire exposure time. The conditional mean concentration $C_{avg, p}$ does not include zero periods and is related to the total mean concentration and the intermittency factor by $C_{avg, p} = C_{avg} / \gamma$. For highly intermittent plumes, γ is small and conditional mean concentrations will be much larger than total mean concentrations. This is apparent when comparing C_{avg} and $C_{avg, p}$ between Figures 3.4a and 3.4b.

For this study, it is assumed that the dispersing steady-state plume follows a Gaussian profile. For a continuous release, Pasquill and Smith (1983) show that the mean concentration, C_{avg} , of a plume, in kg/m^3 , with convection windspeed U_c , is given by the reflected Gaussian profile:

$$C_{avg} = \frac{Q}{2\pi U_c \sigma_y \sigma_z} \exp\left(\frac{-y^2}{2\sigma_y^2}\right) \left[\exp\left(\frac{-(z-h)^2}{2\sigma_z^2}\right) + \exp\left(\frac{-(z+h)^2}{2\sigma_z^2}\right) \right] \quad (3.12)$$

where σ_y and σ_z are the cross-stream and vertical plume spreads respectively, Q is the pollutant emission rate (kg/sec), h is the plume effective source height (including source height and plume rise), z is the measurement height above the ground and y is measured from the crosswind plume centreline at $y = 0$.

Pasquill and Smith (1983) show that the plume spreads, σ_y and σ_z , can be approximated by power law functions.

$$\sigma_y = D_y x^{a_y} \quad (3.13)$$

$$\sigma_z = D_z x^{a_z} \quad (3.14)$$

The coefficients D_y , D_z , a_y , and a_z are based on atmospheric stability class and roughness height z_0 . Wilson (1994) derived these coefficients from Smith's correlations in Pasquill and Smith (1983). For the purposes of this study, the following meteorological conditions and surface roughness are assumed:

- neutral atmospheric stability class (D)
- $U_{met} = 3$ m/s at $z_{met} = 10$ m (typical meteorological station height)
- full-scale surface roughness $z_{0,full} = 10$ cm

Neutral stability was chosen as it is a common atmospheric stability in Alberta, and the water channel experimental data was taken under neutrally stable-conditions. U_{met} was chosen as it is possible to have a mean wind speed of 3 m/s for any atmospheric stability class. The surface roughness is consistent with rural areas in southern Alberta, where agricultural practices are prevalent, and provides a conservative estimate of the dilution that would take place in urban areas where z_0 is typically 1.0 m.

Using Smith's correlations to roughness height and stability class from Pasquill and Smith (1983), and assuming $z_{0,full} = 10$ cm in stability class D the crosswind and vertical plume spreads are:

$$\sigma_y = 0.16 x^{0.88} \quad (3.15)$$

$$\sigma_z = 0.20 x^{0.76} \quad (3.16)$$

Wilson (1981, Equation (14)) shows that the convection velocity U_c , should be calculated for a convection height z_c . The convection height is a function of effective source height, h , (including the source height and final plume rise) and vertical plume spread σ_z :

$$z_c = h + 0.17 \sigma_z \quad (3.17)$$

Notice that the convection velocity is a function plume spread, where $\sigma_z \propto x$ and increases with downwind distance.

Reference Position

For the purposes of this study, a reference position was chosen to normalize all mean concentrations:

- crosswind position $y_{ref} = 0$ m (plume centreline)
- downwind position $x_{ref} = 1000$ m from the odour source
- reference height above ground $z_{ref} = 2.0$ m
- averaging time $t_{avg, ref} = 180$ min = 3.0 hours
- mean concentration $C_{avg, ref} / C_{avg, ref} = 1.0$

The downwind position $x_{ref} = 1000$ m was chosen as an appropriate distance when considering the odour annoyance of those living "close" to an agricultural facility. The 180 minute averaging time was chosen because three hours is commonly considered the

longest time over which meteorological conditions can be assumed stationary in Alberta. The reference crosswind position and mean concentration were chosen for simplicity.

Variation in Mean Centreline Concentration with Averaging Time

Averaging time affects the crosswind plume spread, but not the vertical plume spread. Vertical mixing in the atmosphere is restricted by mixing layer depth, and therefore, the size of eddies in this direction are also restricted. Vertical spreads will increase for averaging times from zero up to about 3 minutes after which they are approximately constant. Hanna et al. (1996, pp 108) use this explanation to justify a limited vertical dispersion coefficient, σ_z , and state that σ_z is not influenced by the larger meandering eddies that cause the crosswind spread to increase with averaging time beyond 3 minutes. Equation (3.16) for the vertical spread is accurate for all averaging times greater than 3 minutes (Wilson, 1994).

Cross-wind plume spreads are effectively unrestricted and continue to increase as averaging time increase. There are many methods for correcting the crosswind plume spreads: from the simple 0.2 power law recommended by Hanna et al. (1996, Equation (6.1)) typically used by regulatory agencies, to a complicated model based on the Lagrangian integral velocity fluctuation time scale and plume travel time presented by Wilson (1995, Equation (3.12)) and corrected by Hilderman (2004, Chapter 2). As per the recommendation of Hanna et al., the widely-used 0.2 power law will be adopted in this study.

$$\frac{\sigma_{y1}}{\sigma_{y2}} = \left(\frac{t_2}{t_1} \right)^{0.2} \quad (3.18)$$

Examining the Gaussian dispersion Equation (3.12), it is clear that mean concentrations along the plume centreline are inversely proportional to the crosswind spread (assuming all other parameters are constant). Applying Equation (3.18) to Equation (3.12) the ratio of mean concentrations with averaging time is:

$$\frac{C_{avg,y=0,1}}{C_{avg,y=0,2}} = \left(\frac{t_2}{t_1} \right)^{0.2} \quad (3.19)$$

Downwind Variation in Mean Concentration

The downwind variation in mean concentration is evaluated using the Gaussian dispersion Equation (3.12), with the reference position $x_{ref} = 1000$ m used to normalize all downstream mean concentrations. The ratio of centreline, mean concentration at a distance x to the centreline, mean concentration at $x = 1000$ m is in general:

$$\frac{C_{avg,x}}{C_{avg,ref}} = \frac{(U_c \sigma_y \sigma_z)_{ref}}{(U_c \sigma_y \sigma_z)_x} \quad (3.20)$$

The convection wind speed U_c is calculated in terms of the convection height z_c , which is a function of the vertical plume spread, as per Equation (3.17). Figure 3.7 illustrates how U_c , z_c , and σ_z change, resulting in a decrease in centreline mean concentration with downstream position.

Recall that the mean wind speed is assumed to be $U_{met} = 3$ m/s at the meteorological station $z_{met} = 10$ m. A power-law profile for the change in velocity with height above ground can be assumed:

$$\frac{U}{U_{met}} = \left(\frac{z}{z_{met}} \right)^p \quad (3.21)$$

The power law exponent p is given by Irwin (1979) for varying atmospheric stability classes and varying terrain roughness z_0 . It is important to note that it is equally appropriate to use a log-law velocity profile for neutral atmospheric stability:

$$U = \frac{u_*}{\kappa} \ln \left(\frac{z-d}{z_0} \right) \quad (3.22)$$

where u_* is the friction velocity, the von Karman constant is $\kappa = 0.4$, d is the zero-plane receptor height, and z_0 is the roughness height. Equation (3.22) is only appropriate for neutral stability; the mean velocity is a much more complicated function for stable and unstable atmospheric stabilities. The power p in (3.21) is derived by matching the slopes of (3.21) and (3.22) at a desired height z_{match} . The slope of the power law is:

$$\frac{\partial U}{\partial z} = \frac{Up}{z} \quad (3.23)$$

The slope of the log law is approximated by:

$$\frac{\partial U}{\partial z} = \frac{u_*}{\kappa z} \quad (3.24)$$

Equating these two slopes results in an equation for p :

$$p = \frac{u_*}{U\kappa} \quad (3.25)$$

Substituting for U from the power law and letting $z - d = z_{match}$, Equation (3.25) becomes:

$$p = \frac{1}{\ln \left(\frac{z_{match}}{z_0} \right)} \quad (3.26)$$

Using this approach, the power law is matched to the log law in both the mean velocity U and the slope $\partial U/\partial z$ at z_{match} , as illustrated in Figure 3.8. From Irwin (1979), assuming a full-scale surface roughness $z_{0\ full} = 10$ cm and a neutral atmospheric stability the exponent is $p = 0.16$. This is equivalent to a match height of $z_{match} = 50$ m, which is reasonable when examining dispersing plumes from slightly elevated sources. The power-law does not describe the velocity profile as accurately as the log-law, however it is more convenient to use as it simplifies calculations. Keeping with conventions, the power law profile will be used to describe the velocity profile in full-scale and Irwin's result for the exponent $p = 0.16$ in neutral stability will be used in the study.

Equation (3.21) is used to calculate the convective mean wind speed, U_c . In the case of the convective velocity and height, the effective source height h , from Equation (3.17) is not known because the final plume rise is unknown. A typical odour source is likely near ground level with minimal vertical momentum or buoyancy. In other words it is assumed, for simplification purposes, that $h \ll 0.17 \sigma_z$, and therefore $U_c \propto \sigma_z$ only. The ratio of convective wind speeds in (3.20) becomes:

$$\frac{U_{ref}}{U_c} = \frac{U_{met} \left(0.17 \sigma_{z,ref} / z_{met} \right)^{0.16}}{U_{met} \left(0.17 \sigma_z / z_{met} \right)^{0.16}}$$

or

$$\frac{U_{ref}}{U_c} = \left(\frac{\sigma_{z,ref}}{\sigma_z} \right)^{0.16}$$
(3.27)

Using Equations (3.20) and (3.27), and substituting cross-wind and vertical plume spread relationships of Equations (3.13) and (3.14), then the ratio of mean concentration at downstream position x to the reference mean concentration is:

$$\frac{C_{avg,x}}{C_{avg,ref}} = \frac{\left(D_z x_{ref}^{a_z} \right)^{1.16} \left(D_y x_{ref}^{a_y} \right)}{\left(D_z x^{a_z} \right)^{1.16} \left(D_y x^{a_y} \right)}$$
(3.28)

The crosswind plume spread is adjusted for averaging time effects using Equation(3.18).

Assuming $C_{avg, ref} = 1$ for $x = 1000$ m, the range of normalized mean concentrations is $11.5 < C_{avg, x} / C_{avg, ref} < 0.1$ for a range of downstream positions $0.2 \text{ km} < x < 4 \text{ km}$, as illustrated in Figure 3.9. This is a factor of 115 difference in normalized mean concentrations on the centreline for these positions. At this point, it is anticipated that the mean concentration will play the dominant role in affecting odour annoyance parameters with downstream position.

3.4.2 Non-dimensional Shear

Hilderman (2004) explains that people are typically exposed in the highly sheared flow at ground level, where there are large differences in plume characteristics as compared to a plume dispersing in more homogenous turbulence well above ground level. For this reason, the non-dimensional shear, S , developed by Hilderman (2004, Chapter 3) is essential to the calculation of the following four characteristics of a dispersing plume: the concentration integral time scale, T_c , the fluctuation intensity, i , the in-plume fluctuation intensity, i_p , and the intermittency factor, γ .

The state-of-the-art methods for accounting for shear in the flow developed by Hilderman (2004, Chapter 3) will be used throughout the remainder of this study. The shear models developed by Hilderman (2004, Chapter 3) rely on plausible arguments and laboratory scalar concentration statistics, but do agree with the small selection of full-scale data that are currently available. The reader may refer to Hilderman (2004, Chapter 3) for a more in-depth discussion of these calculations.

Using his observations that local shear effects vary with travel time and source position, Hilderman (2004, Chapter 3) derived S as:

$$S = \frac{w'_{rms} t_t}{U} \left(\frac{\partial U}{\partial z} \right) \quad (3.29)$$

where w'_{rms} is the root mean square (rms) vertical velocity fluctuation, t_t is the travel time, $U(z)$ is the mean stream-wise velocity and $\partial U / \partial z(z)$ is the shear all evaluated at an appropriate height z_{ref} that accounts for both the source height and the receptor height.

The shear profile can be calculated by taking the derivative of the vertical power law velocity profile, Equation (3.21):

$$\frac{dU_{ref}}{dz} = \frac{p U_{met}}{z_{met}^p} z_{ref}^{p-1} \quad (3.30)$$

where U_{ref} is the velocity at height z_{ref} , U_{met} is the known velocity at z_{met} , typically at a 10 m meteorological station, and p is the power of the velocity profile. In this study, we will assume a $U_{met} = 3$ m/s for a height $z_{met} = 10$ m. The power law exponent p is given by Irwin (1979) for varying atmospheric stability classes and varying terrain roughness z_0 .

The average non-dimensional shear S_{avg} is evaluated at the reference source position h_{ref} and the reference receptor position z_{ref} :

$$S_{avg} = \frac{S_{z_{ref}} + S_{h_{ref}}}{2} \quad (3.31)$$

where the reference source position h_{ref} and the reference receptor position z_{ref} are based on the effective source height h and receptor height z respectively:

$$z_{ref} = z + 0.1\sigma_z \quad (3.32)$$

$$h_{ref} = h + 0.1\sigma_z \quad (3.33)$$

Hilderman (2004, Chapter 2) notes that if either z_{ref} or h_{ref} get too small there can be problems with (3.31) in overestimating shear effects. He recommends then a minimum z_{ref} or h_{ref} of $5z_0$ or 2.0 m should be used. In this study, specifics of the source including final plume rise are unknown, therefore the source is assumed to be a low momentum, zero buoyancy source near ground level, appropriate for a typical source in the agricultural industry. It will be assumed that $z_{ref} \approx h_{ref}$, for a receptor height of 2 m and calculate σ_z using (3.16) from Smith's correlations of plume spreads to roughness height and stability class (Pasquill and Smith, 1983). The average non-dimensional shear S_{avg} is then equivalent to S_{zref} .

In order to calculate S from Equation (3.29) the root mean square vertical velocity fluctuation w'_{rms} must be estimated. For calculations made near ground level where $z \ll H$ (mixing height) we can approximate w'_{rms} by:

$$w'_{rms} = 1.3u_* \quad (3.34)$$

where u_* is the friction velocity. Kerschgens et al. (2000, Equation (4.1)), provide the following more complicated expression for w'_{rms} under neutral and unstable conditions:

$$w'_{rms} = \left[\left(1.3u_* \exp\left(-\frac{z}{H}\right) \right)^3 + \left(1.3\left(\frac{z}{H}\right)^{1/3} \left(1 - 0.8\left(\frac{z}{H}\right) \right) w_* \right)^3 \right]^{1/3} \quad (3.35)$$

and for stable atmospheric conditions:

$$w'_{rms} = 1.3u_* \exp\left(-\frac{z}{H}\right) \quad (3.36)$$

where H is the mixing height, described below, and the convective scaling velocity w_* is calculated using the Monin-Obukhov length L_* :

$$w_* = u_* \left(-\frac{H}{\kappa L_*} \right)^{1/3} \quad (3.37)$$

This height, H , is governed by the surface heat flux due to ground level warming, and is dependent on what day and what time of the day we may be observing this temperature gradient in the atmosphere.

There is a wide range of methods in the literature to calculate the mixing layer height H for varying stability classes. Van Ulden and Holtslag (1985) offer a formula based on the friction velocity, u^* and a Coriolis parameter. Hilderman (2004, Chapter 3) uses a formula provided by Kerschgens et al. (2000) based on the Monin-Obukhov L^* and the friction velocity, u^* . More formulas for mixing layers based on stability class can also be found in Wilson (1994). These methods give a wide range of H between 250 m and 1100 m in the case of neutral and stable conditions (D through F) and at a maximum of 1900 m for unstable (A through C) classes.

In the present study, typical mixing layer heights were assumed depending on whether this layer is governed by convective turbulence and/or mechanical turbulence. The following table gives the estimates of these heights, consistent with the governing physics of the problem, and a brief explanation for the three stability classes examined in this study.

Table 3.1 – Assumed Mixing Layer Heights for Atmospheric Stability

Stability	Governing Turbulent Process	Driving Force	Mixing Layer Height H
A (unstable)	Convective turbulence	Large surface heat flux	1200 m
D (neutrally stable)	Convective & mechanical turbulence	Past history of stability	600 m
F (stable)	Mechanical turbulence	Monin-Obukhov length scale L^*	300 m

It will be shown later in this study that variations in H affect only w'_{rms} and have only a small impact on the non-dimensional shear S that mostly affects the concentration integral time scale. The concentration fluctuation time scale T_c has little effect on odour annoyance, and so the specific mixing layer height used has little effect on the outcome of this study.

The turbulent friction velocity u^* is calculated using the equation of van Ulden and Holtsag (1985):

$$u^* = \frac{\kappa U_{met}}{\ln\left(\frac{z_{met}}{z_0}\right) - \Psi_M\left(\frac{z_{met}}{L^*}\right) + \Psi_M\left(\frac{z_0}{L^*}\right)} \quad (3.38)$$

where $\kappa = 0.4$ is the von Karman constant, z_{ref} is the reference height at which the velocity U_{ref} is known, z_0 is the surface roughness, and L^* is the Monin-Obukhov length. This function provides an accurate estimate of the velocity profile as it is affected by

mechanical turbulence and other atmospheric mixing mechanisms. The function Ψ_M for unstable conditions, for stability classes A through C, is given by van Ulden and Holtsag (1985):

$$\Psi_M = \left(1 - 16 \frac{z}{L_*}\right)^{1/4} - 1 \quad (3.39)$$

and for stable conditions, stability classes E and F:

$$\Psi_M = -17 \left(1 - \exp\left(-0.29 \frac{z}{L_*}\right)\right)^{1/4} - 1 \quad (3.40)$$

For neutral stability conditions, i.e. class D, both of the above reduce to:

$$\Psi_M = 0 \quad (3.41)$$

Where the function Ψ_M is calculated using the z/L_* ratio given in Equation (3.38).

The Monin-Obukhov length, L_* , is a function of the velocity profile, as it relates to the atmospheric stability class, and is independent of measurement height. For these reasons, this length scale is indicative of the height of the mechanical turbulent mixing layer. Hanna et al. (1996, p.16) recommend the following Monin-Obukhov lengths according to the Pasquill-Gifford Stability Classes:

Table 3.2 : Monin-Obukhov Length Scale L_* for the Six Pasquill-Gifford Stability Classes

Pasquill-Gifford Stability Class	Monin-Obukhov Length L_*
A	-10 m
B or C	-50 m
D	> 100 m, $\rightarrow \infty$
E	50 m
F	10 m

Hilderman provides a robust fit for the correction of no-shear plume characteristics to include shear effects using the non-dimensional shear. This fit was created using concentration fluctuation data taken over a large range of heights above ground level in a water channel. Hilderman suggests that:

$$\frac{\text{shear statistic}}{\text{no-shear statistic}} = (1 + 5 S_{avg})^B \quad (3.42)$$

where the exponent B is based on the specific plume statistic being corrected. In the following sections, the non-dimensional shear S will be used to calculate the concentration integral time scale, T_c , the fluctuation intensity, i , the in-plume fluctuation intensity, i_p , and the intermittency factor, γ , while accounting for shear effects. It is important to notice that S changes with downwind position, as it is a function of σ_z , but is predicted to be a constant with crosswind position.

3.4.3 Concentration Integral Time Scale, T_c

The definition of the concentration integral time scale T_c is the area under the auto-correlation curve for the concentration fluctuation time-series. T_c provides an indication of the rate of concentration fluctuations, and the time over which these fluctuations are correlated. The shorter T_c is, the faster the fluctuations occur.

Returning to the analogy of cooking with garlic, it is easily to see why the rate of concentration fluctuations is important. Consider the periods of time when the odorant is present. If a receptor is exposed to garlic odorant for a short period of time, his olfactory system may not have long enough to adapt. For longer, constant exposures, he adapts to the smell and it fades into the background of the environment. Consider also the periods of time between exposures. Stepping outside into garlic-free air for just a moment may not be long enough to allow the nose to become resensitized to the odour. In this case, he would not notice the strong odour in the kitchen. Leaving the kitchen for an extended period of time will certainly allow the receptor's nose to zero, or return to his original sensitivity to garlic odorant. Therefore, upon entering the kitchen once more, the smell of garlic is noticed. The rate at which odorant concentrations change, including periods of zero concentration, is important to how people smell odours, and therefore important to how receptor's perceive odorants and become annoyed.

The concentration integral time scale will be used to stretch the water channel data in time, to ensure that the fluctuation rate accurately simulates the full-scale atmosphere.

Time scale using shear-free integral time scale

The definition for the concentration integral time scale T_c is the area under the autocorrelation curve $R_c(t)$ is:

$$T_c = \int_{-\infty}^{\infty} R_c(t) dt \quad (3.43)$$

where the autocorrelation for a time delay τ is defined as:

$$R_c(\tau) = \frac{\overline{c(t)c(t+\tau)}}{c^2} \quad (3.44)$$

Following Hinze (1975, pp. 62-65) the timescale is calculated from the one-dimensional power spectra of the concentration time series. The power spectrum is the Fourier transform of the autocorrelation, where the area under the one-sided spectra is defined in this study as the variance of the concentration fluctuations:

$$\int_0^{\infty} E_c(f) df = \overline{c'^2} \quad (3.45)$$

The concentration integral time scale T_c is found from the following equation:

$$T_c = \frac{E_c(0)}{4\overline{c'^2}} \quad (3.46)$$

where $\overline{c'^2}$ is the variance of concentration fluctuation from the mean concentration C_{avg} . The intercept, $E_c(0)$, is calculated by extrapolating the spectrum to zero frequency. It is important to note that this can be different from $E_c(0)$ at the zero frequency, which is a measure of the mean of the autocorrelation. There can be a discrepancy between the $E_c(0)$ and $E_c(0)$ extrapolated because the autocorrelation function can be poorly behaved especially for large time delays, τ . Using an extrapolation provides a better estimate of $E_c(0)$ in these cases, and this is the same reason that spectral extrapolation is used to estimate T_c rather than directly measuring the integral of the the autocorrelation Equation (3.43).

In order to estimate the concentration integral time scale, Hilderman (2004, Chapter 3) developed a robust boundary layer model from shear-free water channel data. He compared the total velocity time scale T_{vel} to the concentration time scale in this data and found that for the shear-free case, the ratio of T_c to T_{vel} is a constant across the plume and with downstream position:

$$T_{c,no\,shear} \approx 0.8T_{vel} \quad (3.47)$$

The total velocity time scale was derived by drawing a parallel between the scalar turbulent energy dissipation ε and the scalar velocity time scale. The total turbulent energy dissipation is the sum of the three components of dissipation:

$$\varepsilon = \varepsilon_u + \varepsilon_v + \varepsilon_w \quad (3.48)$$

Given that $\varepsilon \propto$ velocity variance / timescale, and following this model for adding scalars, it is expected that the velocity time scales should add as inverses:

$$\frac{1}{T_{vel}} = \frac{1}{T_u} + \frac{1}{T_v} + \frac{1}{T_w} \quad (3.49)$$

If the velocity fluctuations of a flow field are known, the total velocity time scale can be calculated the no-shear concentration integral time scale can be calculated using Equation (3.47). Hilderman points out that T_c is variable with height. Considering that the length scale, L_c , is more consistent with height, it is convenient to use L_c as a model of how the concentration fluctuations change. Assuming frozen turbulence (i.e. turbulent scales are convected with the mean flow) and using (3.47):

$$L_{c,no-shear} = T_{c,no-shear} U_{no-shear} = 0.8 T_{vel} U_{no-shear} \quad (3.50)$$

Hilderman (2004, Chapter 3) refers to the work of Counihan (1975) to develop a simplified model for $T_{c,no-shear}$, in the absence of detailed flow information, i.e. T_{vel} . Based on Counihan, Hilderman states that the no-shear streamwise integral length scale $L_{u,no-shear}$ is approximately $\frac{1}{2}$ the maximum L_u expected at $\frac{1}{3}$ the mixing height H , or:

$$L_{u,no-shear} \approx \frac{H}{6} \quad (3.51)$$

Assuming that the smallest scale will dominate (3.49), it is proposed that

$$T_{vel,no-shear} \approx T_w \approx T_u / 5 \quad (3.52)$$

In the absence of detailed flow information, a model for the no-shear concentration integral time scale was proposed by Hilderman (2004, Chapter 3) using Equations (3.50), (3.51), and (3.52):

$$T_{c,no-shear} \approx \frac{H}{40 U_{no-shear}} \quad (3.53)$$

where H is the mixing layer height, following Table 3.1, and $U_{no-shear}$ is the velocity at H , the top of the boundary layer. This approximation is based on experimental work done in a water channel that was used as a scale model of neutral atmospheric stability, and is designed to be used when detailed measurements of vertical, crosswind and downwind velocity fluctuations are not available.

Time scale using shear affected concentration integral time scale

In a comparison of concentration fluctuation data in shear-free and shear flow, Hilderman (2004, Chapter 3) developed a relationship between the concentration integral time scale in shear-free flow, $T_{c,no-shear}$, and the concentration integral time scale in shear flow, $T_{c,shear}$, using the non-dimensional shear in Equation (3.42):

$$\frac{T_{c,shear}}{T_{c,no-shear}} = \frac{U_{no-shear}}{U_{zref}} (1 + 5 S_{avg})^{1/3} \quad (3.54)$$

Where S_{avg} is calculated following the steps described earlier, $U_{no-shear}$ is evaluated at the height of the mixing layer, H , and U_{zref} is measured at the reference height z_{ref} , where z_{ref} (Hilderman 2004, Chapter 3):

$$z_{ref} = z + 0.1\sigma_z \quad (3.55)$$

A matrix of stability classes, roughness heights z_0 , and downstream distances x_{full} for wind speeds and reference heights calculated using the power law for appropriate power p based on a wind speed of $U_{met} = 3$ m/s at $z_{met} = 10$ m was used to calculate concentration integral time scales in shear flow, $T_{c,shear}$. The integral time scale was consistently high for stability class F (very stable) and low for class A (very unstable), with stability class D at the median $T_{c,shear}$. The range of $T_{c,shear}$ for varying roughness height and downstream distance is listed in Table 3.3a and 3.3b.

Table 3.3a – Concentration integral time scale for variable atmospheric stability class and downstream distance

Pasquill-Gifford Stability Class	$T_{c,shear}$		
	$z_0 = 0.1$ m $x_{full} = 2000$ m	$z_0 = 0.1$ m $x_{full} = 1000$ m	$z_0 = 0.1$ m $x_{full} = 200$ m
F	18.6 s	18.4 s	14.7 s
D	14.5 s	14.2 s	12.0 s
A	18.7 s	18.3 s	16.7 s

Table 3.3b – Concentration integral time scale for variable atmospheric stability class and roughness height

Pasquill-Gifford Stability Class	$T_{c,shear}$	
	$z_0 = 0.1$ m $x_{full} = 200$ m	$z_0 = 0.01$ m $x_{full} = 200$ m
F	14.7 s	14.0 s
D	12.0 s	9.8 s
A	16.7 s	14.0 s

For this study, a neutral class D atmospheric stability class with a mixing layer height $H = 600$ m and a surface roughness $z_0 = 0.1$ m are assumed. For these terrain and atmospheric conditions, Figure 3.10 is a plot of the $T_{c,shear}$ model and chosen downwind positions used in this study. Notice that the model predicts a levelling off of $T_{c,shear}$ beyond approximately 2 km downwind of the source. This levelling off is driven by the decreasing change in the shear $\partial U/\partial z$ as z_{ref} grows with downstream position. This is

similar to the way z_c grows with downstream position in Figure 3.7. $T_{c, shear}$ is a constant with crosswind position.

The shear concentration integral time scale is constant with averaging times long enough that the vertical plume spread is a constant, i.e. for averaging times greater than about three minutes. This is discussed further in Hilderman (2004, Chapter 3).

The shear concentration integral time scale will be used later in this study to stretch the time series of concentration fluctuations from water channel experiments in order to achieve a plausible frequency of odour events receptors might be exposed to while standing outside in a dispersing odorant plume.

3.4.4 Concentration Fluctuation Intensity, i

The total fluctuation intensity, including zero concentrations, is defined as $i = c'_{rms} / C_{avg}$, where c'_{rms} is the standard deviation of the concentration, shown in Figure 3.3. In his 1995 book, Wilson offers a pseudo-meandering plume based Equation for the change in centreline fluctuation intensity. The meandering plume model first proposed by Gifford (1959), assumes that the total plume spread σ_y is composed of two components, a uniform non-fluctuating instantaneous plume spread σ_{yi} that is flapped back and forth by a meandering spread σ_{ym} . Wilson's 1995 study expands on this idea by including internal fluctuations in the instantaneous non-meandering component, as developed by Wilson and Zelt (1990).

Wilson (1995, Equation (6.3)) gives the following formulae for calculating the reference fluctuation intensity $i_{h, ref}$ (that accounts for shear) at a source height h_s , with downstream distance x , for a reference sampling time of $t_{ref} = 2$ minutes:

$$i_{h, ref} + \left(i_{h, ref}^2 + 1 \right)^{1/2} = \frac{10.0 \left(\frac{\sigma_e}{L_e} \right)}{\left(\frac{\sigma_e}{L_e} + 3.0 \left(\frac{\sigma_o}{L_e} \right)^{2/3} \right)^{3/2}} \quad (3.56)$$

This relationship was derived using data taken in shear flow, where:

$$\sigma_e = \left(\sigma_y \sigma_z \right)^{1/2} \left(1 + \frac{8.0 p x}{h + 0.02 \sigma_z} \right)^{1/2} \quad (3.57)$$

and p is the power law velocity profile exponent in (3.21), and the turbulence length scale L_e is defined as:

$$L_e = L_v + 0.03 \sigma_e \quad (3.58)$$

The Eulerian length scale L_v of a crosswind velocity is roughly estimated with:

$$L_v = 0.6(h + \sigma_o) \quad (3.59)$$

For the purposes of this study it is assumed that $h \approx z_{receptor} = 2$ m as discussed earlier, and $\sigma_o = 0.6$ m is the effective plume spread caused by the source size and is based on an assumed source diameter of 1.0 meters and effective source size equations developed in the Wilson *et al.* 1998 ASHRAE report. A sensitivity study was performed to determine that both of these assumptions have little bearing on $i_{h,ref}$ except at downwind positions very near the source.

The averaging time effects on centreline fluctuation intensity are related to the ratio crosswind plume spreads by (Wilson, 1995, Equation (6.9)):

$$\frac{i_h^2 + 1}{i_{h,ref}^2 + 1} = \frac{\sigma_y}{\sigma_{y,ref}} \quad (3.60)$$

Using this relationship and the 0.2 power law, $\sigma_y \propto t_s^{0.2}$, the total fluctuation intensity at the plume centreline can be scaled for sampling time by:

$$\frac{i_h^2 + 1}{i_{h,ref}^2 + 1} = \left(\frac{t_s}{t_{s,ref}} \right)^{0.2} \quad (3.61)$$

Fluctuation intensities can be calculated across the width of the plume using a model developed by Wilson (1995, Equation (6.8)):

$$i^2 + 1 = (i_h^2 + 1) \left[\exp \left(\frac{(z-h)^2}{\sigma_z^2} + \frac{y^2}{\sigma_y^2} \right) \right]^{1+2M_{intensity}} \quad (3.62)$$

where $y = 0$ is defined as the plume centreline, and $M_{intensity}$ is the 2-dimensional pseudo-meander parameter developed from Sawford and Stapountzis (1986) by Wilson (1995, Equation (6.10)):

$$M_{intensity} = i_h^2 + (i_h^4 + i_h^2)^{1/2} \quad (3.63)$$

For vertical positions other than at h_{ref} , the following equation, developed by Hilderman (2004, Chapter 3), must be used to calculate $i_{no-shear}$ for use in Equations (3.62) and (3.63). Using the no-shear intensity fluctuations, $i_{no-shear}$, predicted above and the dimensionless shear S , Hilderman (2004, Chapter 3) offers the following model for calculating fluctuation intensities corrected for shear, i_{shear} :

$$\frac{i_{shear}}{i_{no-shear}} = \frac{1}{\left(1 + 5 S_{z_{ref}}\right)^{1/3}} \quad (3.64)$$

This equation is then reapplied to evaluate the shear fluctuation intensity.

Following the above procedure, concentration fluctuation intensities were calculated as $i_{shear} = 0.3, 1.1$ and 1.3 for 3 minute, 60 minute and 180 minute sampling times respectively at the centreline reference position, 1.0 km downwind from the source. A map of expected concentration fluctuation intensities across the plume and downwind from the source was created for a 180 minute sampling time. The map of shear corrected intensities consists of crosswind positions $0 < y/\sigma_y < 3$, at $x = 1$ km, shown in Figure 3.11 (b), and downwind, centreline positions $200 \text{ m} < x < 4$ km, shown in Figure 3.12 (b).

3.4.5 Conditional (In-plume) Concentration Fluctuation Intensity, i_p

The conditional fluctuation intensity is $i_p = c_{rms,p}' / C_{avg,p}$ where $c_{rms,p}'$ is the conditional (in-plume) standard deviation of the non-zero concentrations. Wilson (1995) relates the conditional fluctuation intensity and total fluctuation intensity to each other using the intermittency factor by the definition in Equation (3.4).

The conditional fluctuation intensity, i_p , is a measure of how large the concentration fluctuations are when zero (background concentration) intermittent periods are excluded from the analysis. A large i_p indicates large peak concentrations and therefore a higher exposure concentration and a larger chance of annoyance from the odorant. The total fluctuation intensity, i , is less informative and more difficult to interpret. A large i could indicate large peak concentrations, or a small intermittency factor γ , or a combination of both. Considering that the conditional fluctuation intensity is easier to interpret, i_p is therefore used in conjunction with γ as the primary parameters of interest to characterize a plume.

Equation (3.4) demonstrates how the conditional in-plume fluctuation intensity i_p and the intermittency factor i are related to the total fluctuation intensity; however a relationship between the two fluctuation intensities, independent of γ , is useful when the intermittency factor is unknown. An empirical relationship between the total and conditional fluctuation intensities was constructed by Wilson (2003):

$$i_p = \frac{i}{\left(1 + \left(\frac{i}{i_{p,\infty}}\right)^3\right)^{1/3}} \quad (3.65)$$

where $i_{p,\infty}$ was originally thought to be a constant. Hilderman (2004, Chapter 3) examined concentration fluctuation data to find that $i_{p,\infty}$ was in fact a function of the non-dimensional shear S . Applying the shear function (3.42):

$$i_{p,\infty} = \frac{1.9}{(1 + 5S_{avg})^{1/6}} \quad (3.66)$$

The non-dimensional shear S is a function of downwind position, but does not vary with crosswind position; therefore, $i_{p,\infty}$ is only a function of downwind position as well (for constant terrain and meteorological conditions).

The in-plume fluctuation intensity at infinity is then used in conjunction with the fluctuation intensity, i , in (3.65) to calculate the shear corrected in-plume fluctuation intensity, i_p . As with i , a map of expected in-plume, concentration fluctuation intensities across the plume and downwind from the source was created for a 180 minute sampling time. The map of shear corrected intensities consists of crosswind positions $0 < y/\sigma_y < 3$ at $x = 1$ km, shown in Figure 3.11 (c), and downwind, centreline positions $200 \text{ m} < x < 4$ km, shown in Figure 3.12 (c).

3.4.6 Intermittency Factor, γ

The intermittency factor γ is defined as the fraction of total exposure time when the concentration is greater than zero. A concentration of zero is defined as the limit of the measurement instrument, in the case of experimental work, and as the atmospheric background concentration of the particular odorant when applying this model to a realistic situation.

Hilderman and Wilson (1999) first proposed that the probability density function of concentration fluctuations should look like a clipped log-normal distribution for the fraction of time with non-zero concentrations with a delta function for the fraction of time with zero concentrations. This is illustrated in Figure 3.3. This model is important when thinking of taking an individual sample of concentration in a plume. At the edge of the plume, the intermittency factor is small and therefore the modal concentration value is zero. Taking one sample at the edge of the plume, it can be concluded that a trained observer would likely not be able to smell the odorant. At a position along the plume mean centreline, the modal value will be a moderate concentration. Taking one sample at this position, close to the source, a trained observer will likely be able to smell the dispersing odorant.

Using the shear corrected total and conditional fluctuation intensities, i and i_p respectively, the intermittency factor is determined using Equation (3.4). Following the map created for i and i_p , the variation in γ is determined for crosswind positions $0 < y/\sigma_y < 3$, at a position $x = 1$ km, shown in Figure 3.11 (a), and downwind position $200 \text{ m} < x < 4$ km along the plume centreline, shown in Figure 3.12 (a).

3.4.7 Variation of Plume Statistics with Averaging Time

The variation in the intermittency factor, γ , fluctuation intensity, i , conditional fluctuation intensity, i_p , shear concentration integral time scale, $T_{c, shear}$, and normalized mean concentration, C_{avg} , with averaging time are shown in Table 3.4. For averaging times greater than three minutes, the vertical plume spread is constant, but the crosswind plume spread varies. This increase in crosswind plume spread results in an increase of i and i_p , and a decrease in γ . The time scale is a function of the vertical plume spread, and therefore does not change with averaging times beyond three minutes. With increasing plume spread, the concentration of the plume at any downwind position is spread over a greater cross-sectional area, resulting in a decrease in normalized mean concentration.

Table 3.4 Change in Plume Characteristics with Averaging Time for Atmospheric Stability Class D

t_{avg}	i	i_p	γ	$T_{c, shear}$	$C_{avg}/C_{avg, ref}$
3 min	0.38	0.38	0.998	14.2 s	2.3
60 min	1.0	0.93	0.896	14.2 s	1.3
180 min	1.3	1.1	0.815	14.2s	1.0

Where $C_{avg, ref} = 1.0$ for stability class D, at plume centreline, $y/\sigma_y = 0$, and downwind position $x = 1000$ m.

3.4.8 Summary of Calculating Full-scale Plume Statistics

Full-scale parameters were predicted based on the following topographical and meteorological assumptions:

- neutral atmospheric stability class (D)
- $U_{met} = 3$ m/s at $z_{met} = 10$ m (typical meteorological station height)
- full-scale surface roughness $z_{o, full} = 10$ cm
- power-law velocity profile with power $p = 0.16$ (from Irwin, 1979)
- mixing layer height $H = 600$ m (from Counihan, 1975)

and a reference position, time, and concentration of

- crosswind position $y_{ref} = 0$ m (plume centreline)
- downwind position $x_{ref} = 1000$ m from the odour source
- averaging time $t_{avg, ref} = 180$ min
- mean concentration $C_{avg, ref} / C_{avg, ref} = 1$

The five characteristics of the full-scale were then determined.

- The normalized mean concentration was evaluated based on the dispersion of a Gaussian plume for downwind and crosswind positions centred about and normalized by a position an $x = 1$ km downwind of the odorant source along the plume centreline ($y = 0$).

- The concentration fluctuation intensity, i , was calculated using Equation (3.62) and was corrected for the non-dimensional shear, S (of Equation (3.29)) in Equation (3.64).
- The conditional fluctuation intensity, i_p , was calculated from i using Equation (3.65), and corrected for S using Equation (3.66).
- The intermittency factor, γ , is defined as a function of i and i_p through Equation (3.4), and as such is inherently corrected for shear effects. The conditional intensity and intermittency pair calculated for each downwind and crosswind position will be used in the following section to select the appropriate water channel data series.
- The concentration integral time scale, T_c , is used to describe the average length of time between concentration fluctuations, and therefore, odour events. T_c was calculated using S in Equation (3.54) for each of the downwind and crosswind positions.

The variation in intermittency factor, γ , fluctuation intensity, i , conditional fluctuation intensity, i_p , and normalized mean concentration, C_{avg} , with crosswind position relative to the plume mean centreline, $y = 0$, are shown in Figure 3.11. From section 3.3.3, the concentration integral time scale, T_c , a measure of the frequency of odour events, is predicted to be a constant across a dispersing plume. This figure, which shows the overall statistical measures, illustrate the complications in trying to predict a trend in memory load from odour as the receptor travels from the plume centreline to the plume fringes (at $y/\sigma_y > 2$), given that i and i_p increase, γ and C_{avg} decrease, and T_c remains a constant across the plume. The odour annoyance model developed in Chapter 2 must be tested with complete time series of concentration fluctuations to determine which factor/factors contribute the most to the change in memory load and what trend is expected across the width of the plume.

The downwind variations of plume statistics are much more gradual than those in the crosswind direction. The variations in intermittency factor, γ , fluctuation intensity, i , conditional fluctuation intensity, i_p , and normalized mean concentration, C_{avg} with downwind position relative to the plume mean centreline, $y = 0$ are shown in Figure 3.12. Figure 3.10 shows the variation in concentration integral time scale, T_c , with downwind position. Beyond $x = 200$ m, one might expect a decrease in odour annoyance with downwind position based on the decrease in γ , i , i_p , and dramatic decrease in C_{avg} with downstream position. However, T_c shows a distinct increase in the time scale and then a levelling off beyond $x = 1.5$ km. It is unclear whether the mean concentration or the concentration fluctuations will have the greatest affect on odour annoyance; therefore, as with the crosswind variation, the odour annoyance model must be tested with downwind position.

3.5 Water Channel Scale-up Technique

In Section 3.3 plume statistics for a range of downwind, centreline positions and crosswind positions at a reference 1.0 km downwind in full-scale were determined. To apply this information to the human odour annoyance model developed in Chapter 2

simulated full-scale concentration fluctuation time series in the present study were generated by scaling up water channel experiments to match the full-scale statistics.

All of the water channel time series data used in this study were obtained using the linescan, laser induced fluorescence (LIF) experimental techniques—developed by Hilderman (2004, Chapter 2). For these data sets, Hilderman (2004) showed that there was no measurable effect of the source type on plume statistics—as long as data were selected from measurement positions sufficiently far from the source such that the plume has been sufficiently affected by the flow. The concentration probability distributions (PDFs), concentration spectra, and other higher order statistics were similar for all source types. This simplifies the process of selecting appropriate experimental data for use in testing the odour annoyance model. Data from any of the many point source experimental configurations in the water channel sufficiently far from the source can be used. The criteria used to select the specific data sets are the conditional (in-plume) concentration fluctuation intensity, i_p , and the intermittency factor, γ , pairs based on the shear corrected full-scale values calculated as described in the Section 3.3. The data will then be stretched in concentration to match the full-scale mean concentrations and stretched in time to match the full-scale integral time scales.

3.5.1 Water Channel Experiments

LIF Data

The laser induced fluorescence (LIF) experimental techniques summarized here are discussed in more detail in Hilderman (2004, Chapter 2). Data were acquired by injecting disodium fluorescein dye solutions into a rough surface boundary-layer shear flow in the 680 mm wide by 470 mm deep by 5240 mm long test section of the recirculating water channel in the Mechanical Engineering Department at the University of Alberta. A Dalsa (model CLC6-2048T), 12-bit, gray-scale CCD linescan camera was used to take high spatial and temporal resolution concentration measurements along a line illuminated by an argon-ion laser. An approximate measurement volume of 0.5 mm x 1 mm x 1 mm was measured by each of the 1024 pixels of the linescan digital camera, at a rate of 500 samples per second. Figure 3.13 is a schematic of this measurement set-up and shows the linescan camera positioned on top of the channel to capture the light emitted by the fluorescing dye passing through the laser line entering the channel from the side.

Concentration fluctuation data was collected using two different dye source types:

1. The horizontal jet was made up of a 4.3 mm OD and 3.25 mm ID stainless steel tube, suspended from a streamlined support (to reduce wake disturbances in the flow). The source was placed on the cross-stream centreline of the channel, at heights between 7 and 50 mm above the channel bottom. The source flow rates were iso-kinetic with the surrounding flow.
2. The small and large vertical ground level jets were positioned on the cross-stream centreline of the channel, flush with the ground, and measured 3.25 mm ID and 11 mm ID respectively. These sources had very low momentum, producing insignificant plume rise.

In all LIF linescan experiments, concentration measurements were made at downstream positions greater than 500 mm where source configuration and release rate effects were negligible.

Shear Flow Field

The flow in the water channel was designed to mimic neutrally stable conditions in the full-scale atmosphere. The well-developed, rough surface, turbulent boundary layer shear flow was created using several flow conditioning devices shown in Figure 3.13

- The rough surface on the bottom of the channel was created using 4 mm thick $\frac{1}{2}$ " x 18 gauge raised surface stainless steel expanded metal. This resulted in a measured $z_0 = 0.52$ mm roughness height.
- A 4 x 4 array of 19 mm (nominal $\frac{3}{4}$ ") stainless steel square bars was used to redistribute the turbulent flow at the channel inlet.
- A 70 mm high trip fence with 40 mm high by 60 mm wide "shark's teeth" was used to generate mid to large scale turbulent eddies.

The boundary layer profile was measured using a TSI Inc. two-component Laser Doppler Velocimeter (LDV). The water channel was run at a depth of $H = 400$ mm controlled with throttling valves and a weir gate. The mixing layer, H , extended the full depth of the channel. The mean downstream velocity at H was measured as $U_H = 232$ mm/s. The vertical velocity profile U was measured using the LDV and found to fit a log-law profile of Equation (3.22), shown in Figure 3.14. (If you take out any of the log-law stuff above like I suggested that you might, then 3.24 may not be there. In that case just put the log-law Equation in here somewhere.) with friction velocity $u_* = 14$ mm/s, von Karman constant $\kappa = 0.4$, zero-plane receptor height $d = 1.7$ mm and the roughness height $z_0 = 0.52$ mm. The cross-stream mean velocity U was found to deviate by less than $\pm 5\%$ across the channel.

Sampling Limitations in Water Channel Data

The data series used in this study are from experiments lasting 500 seconds at each measurement position; with a sampling rate of 500 samples / second this is 250000 samples per time series. As the intermittency factor, γ , decreases at the edges of the fluorescent dye plume, the number of non-zero samples in decreases and limits the accuracy of the variance and the associated fluctuation intensities and time scales. In the extreme case, the model for the full-scale expected values predicts intermittency factors of $\gamma = 0.02$ at positions $y/\sigma_y = 3$, resulting in only 10 seconds of non-zero data in the total 500 second sample. In this case, there is a greater chance for uncertainty in the predicted concentrations, however, the 250000 samples were deemed to provide a reasonable prediction of the expected variability in concentration fluctuations at the plume edge.

3.5.2 Scaling Mean Concentration, C_{avg}

Concentration is a linear property of a dispersing plume, and can be scaled by simply multiplying by an appropriate factor to produce the desired full-scale mean concentration.

Figure 3.15(a) is an example of this concentration scaling between water channel data and full-scale expected normalized values. This type of scaling has no effect on the intermittency factor or the concentration fluctuation intensity, as γ , i and i_p are already normalized dimensionless parameters.

3.5.3 Scaling Time Scales

It is possible to stretch the time scales of the water channel data to match full-scale only by assuming that the flow in both the water channel and the atmosphere have no inertia. It is assumed that the turbulent flow characteristics within the mixing layer of the atmosphere and water channel follow a first order Markov process: that is, the flow has no memory of the change in velocity and concentration (d/dt) in previous time steps, i.e. it has no inertia.

Figure 3.16 (a) is an illustration of the autocorrelation of the streamwise fluctuating velocity for a flow with inertia, R_{uu} . Notice that R_{uu} remains a constant for the first few time delay lengths. This is indicative of a fluid with inertia. Compare this to Figure 3.16 (b), which is an illustration the autocorrelation of the streamwise fluctuating velocity for a flow without inertia. This graph does not have any constant periods of R_{uu} . The autocorrelation function for concentration fluctuations is comparable to that for fluctuating velocities as the dispersion of concentration is governed by the fluctuations in the flow. The autocorrelation of concentration for a time delay τ is defined in Equation (3.44), and can be approximated by:

$$R_c(t) = \exp\left(-\frac{t}{T_c}\right) \quad (3.67)$$

Recall, from section 3.3.3, that the definition of the concentration integral time scale, Equation (3.43) is the area under the autocorrelation function $R_c(t)$.

There are several possible methods of scaling time between the water channel and the full-scale atmosphere.

1. Scaling water channel to full-scale by assuming pure linear geometric scaling and using a mean travel time. It will be shown that this method assumes that time is identical for both the water channel and full-scale, which is not reasonable. This method will be included as an example of the inappropriate results that are obtained when a poor choice of scaling factor is used.
2. Scaling water channel data to full-scale by comparing the velocities in both scales. As with the first model, this type of scaling assumes that the water channel is a near perfect model of the full-scale, and therefore, the geometric limitation of the water channel are also scaled with the velocity.
3. Stretching water channel to full-scale by directly comparing the time scales which affect the concentration fluctuations. This method sweeps aside all limitations of the water channel, and allows for direct comparison between the experimentally measured T_c and the predicted full-scale T_c for each crosswind and downwind

position chosen. Assuming an inertia free flow, the water channel data can be stretched in time to match the predicted concentration time scales.

The three methods are explored in further detail; the first two methods are explained to build the argument for use of the shear integral time scale.

Time scale-up factor from mean travel time

The time stretching from the water channel to the full-scale atmosphere can be estimated by comparing the respective mean travel times. Mean travel time is a function of downstream distance and mean flow speed:

$$t_t = \frac{x}{U} \quad (3.68)$$

The only logical length scale available for scaling between the water channel and full scale is the surface roughness length scale, z_0 , used in the classic log-law velocity profile for atmospheric conditions driven by mechanically-generated turbulence. The surface roughness length scale is approximately 0.5 mm in the water channel used in this study. Table 3.5 shows the geometric scaling factors that can be used to scale water channel data depending on the full-scale z_0 used.

Table 3.5 – Length scaling factors based on roughness height z_0 and corresponding full-scale distances

$z_0 \text{ full}$	1 cm	10cm	100cm
$z_0 \text{ model}$	0.05cm	0.05cm	0.05cm
$L_{\text{scale}} \text{ Factor}$	20	200	2000

For this study, a surface roughness of $z_0 \text{ full} = 10 \text{ cm}$ was assumed. This is consistent with rural areas in southern Alberta, where agricultural practices are prevalent, and provides a conservative estimate of the dilution that would take place in urban areas. Using $z_0 \text{ full} = 10 \text{ cm}$ results in a 1:200 length scale between the water channel and the full-scale. For example, the assumed full-scale reference height $z_{\text{met}} = 10 \text{ m}$ is equivalent to a water channel height of $z = 50 \text{ mm}$.

A mean full-scale streamwise velocity of $U_{\text{met}} = 3.0 \text{ m/s}$ at a reference height of $z_{\text{met}} = 10 \text{ m}$ is assumed in this study. For a downstream distance of $x_{\text{full}} = 100 \text{ m}$, the travel time $t_{\text{full}} = 33.3 \text{ s}$ as calculated from (3.68). A $z_{\text{met}} = 10 \text{ m}$ and $x_{\text{full}} = 100 \text{ m}$ are equivalent to $z_{\text{channel}} = 50 \text{ mm}$ and $x_{\text{channel}} = 500 \text{ mm}$, respectively, in the water channel using the 1:200 length scale. Assuming that the velocity scales with the 1:200 geometric scale, $z = 50 \text{ mm}$ would correspond to a mean velocity of $U_{\text{channel}} = 15 \text{ mm/s}$ and a travel time $t_{\text{channel}} = 33.3\text{s}$.

Following the log-law profile in Equation (3.22), the mean velocity in the channel is $U_{\text{channel}} = 160 \text{ mm/s}$ at a height of $z_{\text{channel}} = 50 \text{ mm}$. This results in a mean travel time of $t_{t,\text{channel}} = 3.2 \text{ s}$. The mean velocity clearly does not scale with the geometric length

scale as 3.2 seconds is not 1/200th of 33.3 seconds so it is not appropriate to scale time like a length.

From a fluid dynamics point of view, it is not expected that that time should be unchanged from full-scale to water channel scale. In order to achieve comparable flow characteristics, i.e. Reynolds number, between the water channel model and the full-scale atmosphere the mean velocity in the channel is much faster than the geometric scale would predict. This large Reynolds number is required to obtain a good approximation of the scales of turbulence that are present in the atmosphere and are important to the outcome based problems such as human toxicology and odour annoyance.

Time scale using shear-free integral time scale

The concentration integral time scale, T_c , provides an indication of the rate of concentration fluctuations, and the time over which these fluctuations are correlated. The shorter T_c is, the faster the fluctuations occur. Typically, the velocity fluctuations or concentration fluctuations must be known in detail in order to calculate T_c using (3.47) or (3.46) respectively. Hilderman (2004, Chapter 3) made some simplifying assumptions, described earlier, to evaluate T_c based on mean flow statistics. Comparing water channel concentration fluctuation data to full-scale atmospheric measurements, Hilderman recommends the Equation (3.53) for $T_{c,no-shear}$ based on the mixing height H and the free stream velocity $U_{no-shear}$.

Using this relationship the shear-free concentration time scale was $T_{c,no-shear} \approx 0.04$ seconds in the water channel, for a boundary layer of $H = 400$ mm and free stream velocity of $U_{no-shear} = 232$ mm/s.

Assuming a mixing layer depth $H \approx 600$ m for neutrally stable atmospheric conditions (from Table 3.1 above, Counihan, 1975), and a free stream velocity $U_{no-shear} \approx 5.8$ m/s is calculated based on $U_{met} = 3$ m/s at $z_{met} = 10$ and using the power-law velocity profile (3.21) with $p = 0.16$ (Irwin, 1979). Using (3.53) a shear-free concentration time scale of $T_{c,no-shear} \approx 2.6$ seconds is calculated for full-scale.

The ratio of the shear-free concentration timescales from full-scale assumptions and water channel measurements is $2.6 / 0.04 = 65$. This ratio can be used to scale the time series for full-scale use:

$$T_{c,no-shear,full-scale} = 65 * T_{c,no-shear,water channel} \quad (3.69)$$

This scaling should work in the shear flow just as well as the free-stream as long as the entire boundary layer flow is similar between the full-scale and the water channel: $T_{c,shear}$ at say 2 m full-scale = $65 * T_{c,shear}$ water channel at 10 mm if the water channel is a perfect 1:200 scale model of the atmosphere. Simply comparing the mixing layer heights shows that the 1:200 geometric scale does not work. Counihan (1975) recommended a mixing layer depth of $H_{full-scale} \approx 600$ m, but using the 1:200 ratio to scale the water channel mixing height results in $H_{full-scale} \approx 80$ m.

This method of stretching time also scales the limitations of the water channel to the full scale, including velocity profile, averaging times, stability class and meteorological conditions.

Direct scaling between predicted full scale T_c and measured water channel T_c

In order to avoid scaling the limitations of the water channel experiments each water channel concentration time series is simply directly scaled to match the predicted T_c . For example, it was assumed that the full-scale atmosphere is neutral stability, has a $U_{met} = 3$ m/s at $z_{met} = 10$ m and a mixing layer height $H = 600$ m. For a typical rural roughness height of 0.1 m and a receptor distance 1 km downwind of the odorant source, the integral time scale was calculated to be $T_c = 14.2$ seconds for the full-scale using Equation (3.54), shown in Table 3.3a.

The concentration integral time scale for the water channel data was calculated using Equation (3.46). The calculated concentration time scales vary slightly across the plume. In order to minimize the effects of these errors, the time scales for all measurements made across the water channel plume from the centreline to twice the plume spread on either side were calculated and then averaged. The calculated water channel concentration time scale corresponding to the full-scale reference case used in this study (at $y = 0$ m, $x = 1$ km), was $T_c = 0.335$ seconds. Note that this position was chosen from the water channel data based on the required full-scale intermittency factor, γ , and conditional (in-plume) concentration fluctuation intensity, i_p . Comparing the T_c measured from water channel data and T_c calculated from the model for the full-scale results in a time scale of approximately **1:42** for this particular case (at $y = 0$ m, $x = 1$ km full-scale).

Following this procedure to calculate a time scale factor is much more realistic and flexible when trying to scale the instantaneous concentration fluctuations measured in the model water channel environment to the full-scale atmosphere. The time scale factor varies for each full-scale position, surface roughness, atmospheric stability class, and water channel data set that is used. This variable ratio is then used to calculate the equivalent full-scale time step for each water channel data set which has the effect of stretching the data in time. An illustration of the time stretch is found in Figure 3.15 (b), where, as an example, the ratio between full-scale time scales and water channel time scales is 1:10. (The typical ratio between the full-scale and water channel times scales is closer to 1:50, but this large ratio is difficult to draw legibly.)

The temporal resolution of the water channel data was set by the camera speed at $1/500^{\text{th}}$ of a second. Using a typical time scale ratio of 1:50 this represents an equivalent full-scale measurement every 0.1 second which is sufficient to accurately examine the effects of all the time constants in the odour annoyance model, including the uptake time constant $\tau_{up} = 1$ sec.

3.6 Summary

Following the odour model development of Chapter 2, it is clear that the use of the mean concentration is not appropriate for evaluating human annoyance to odour. The instantaneous concentration fluctuations in a dispersing plume govern the physiological

and psychological processes involved in human olfaction. The concentration fluctuations in a dispersing plume can be described by the following five characteristics

- mean concentration C_{avg}
- fluctuation intensity i
- intermittency factor γ
- conditional fluctuation intensity i_p
- integral time scale of concentration fluctuations T_c

All five of these factors were used to characterize selected downwind and crosswind positions in a steady-state dispersing plume. The shear-corrected conditional fluctuation intensity and intermittency factors evaluated for each full-scale position were used to select time series of concentration fluctuations from a library of experimental water channel data. This data was then scaled in concentration to match the expected normalized mean concentrations at the respective full-scale positions. The mean concentrations of downwind and crosswind positions were normalized with the concentration at a reference position 1.0 km downstream of the source along the cross-stream plume centreline. The time of the water channel data series was also scaled by assuming inertialess flow and comparing the measured concentration integral time scale at for each experimental data set to the expected concentration integral time scale for the full scale positions.

These downwind and crosswind time series will be used in Chapter 4 to evaluate the model for human odour annoyance developed in Chapter 2.

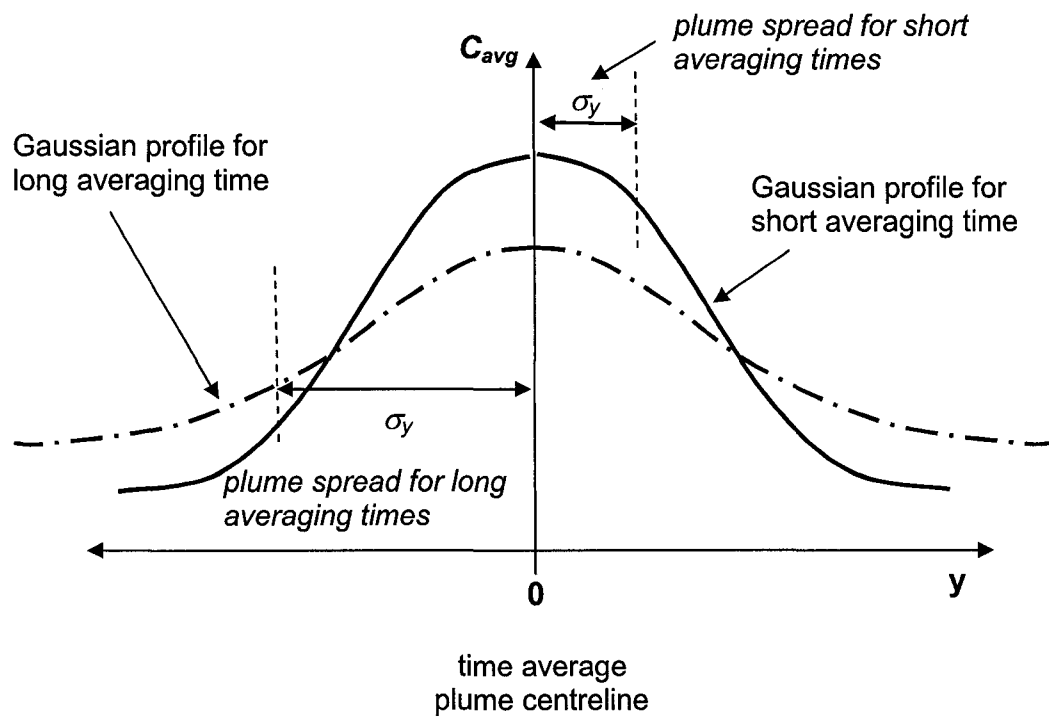


Figure 3.1: Gaussian distributions with variable averaging times. Longer averaging times result in larger plume spreads, smaller centreline mean concentrations, C_{avg} , and larger mean concentrations at the plume edges.

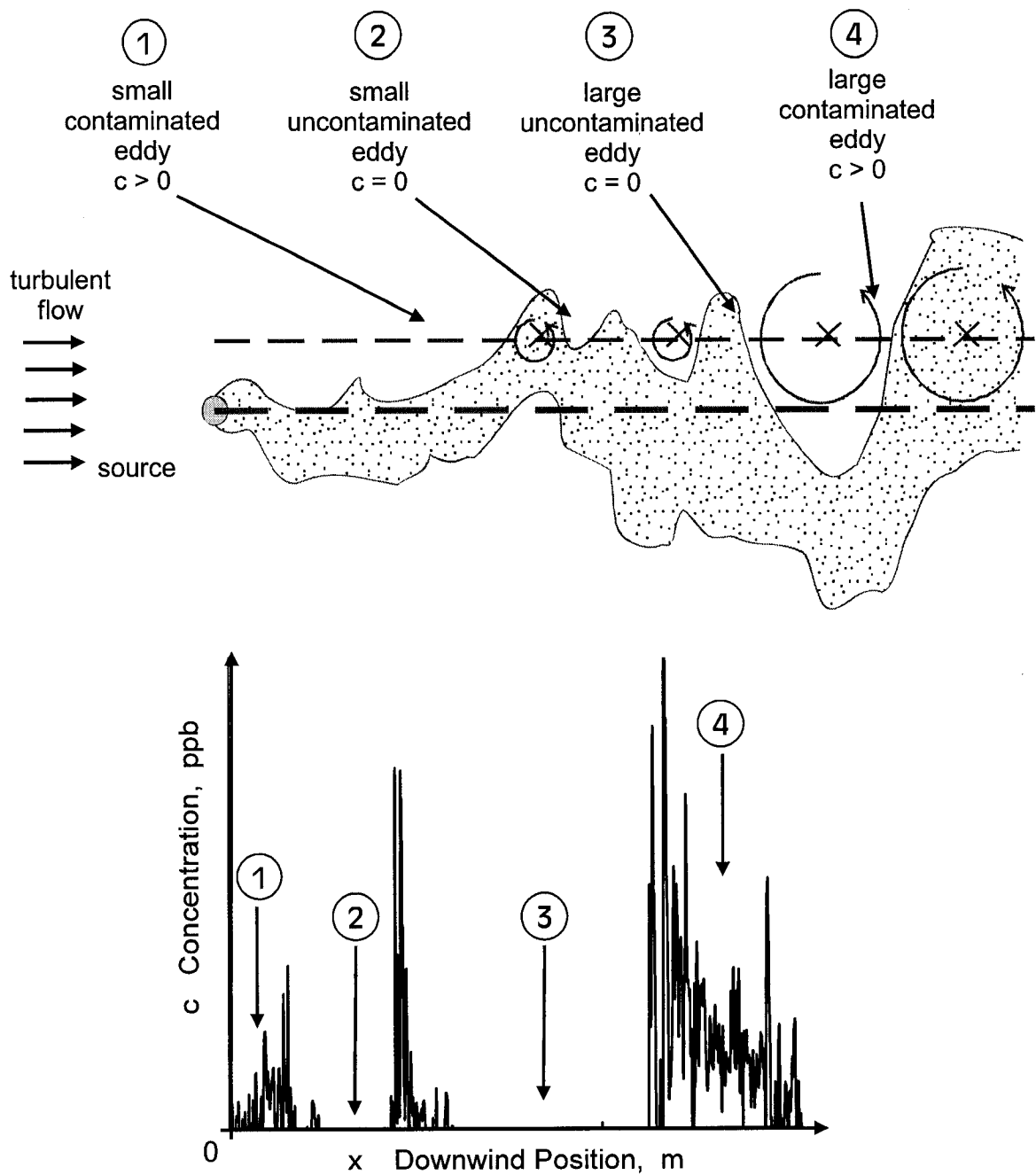
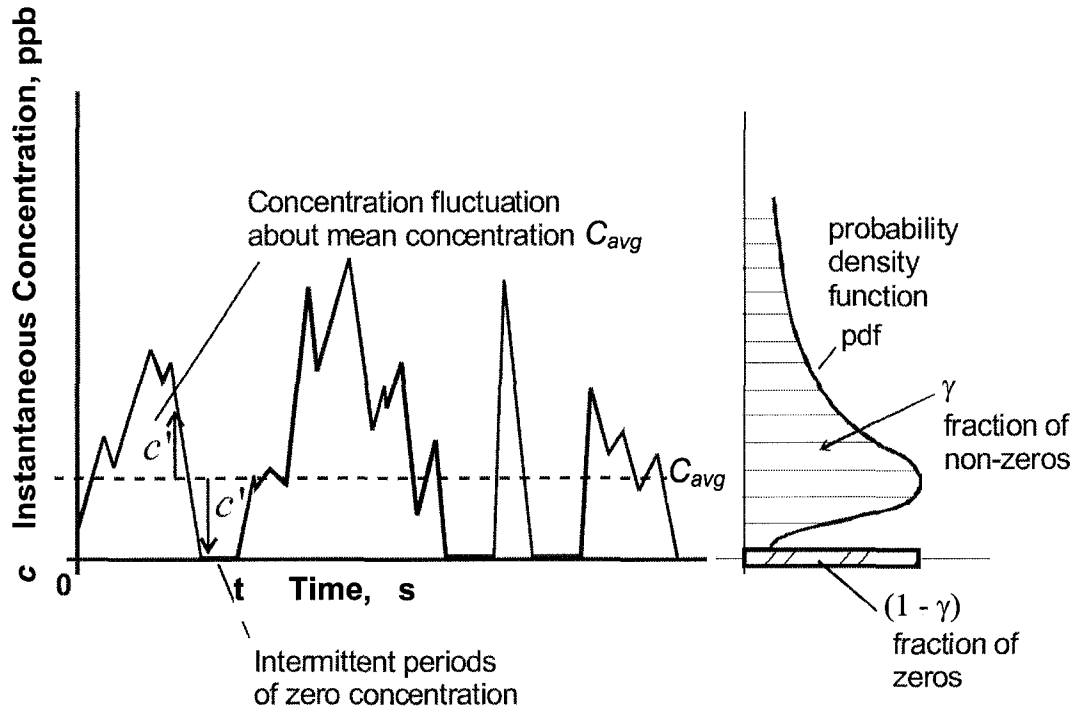


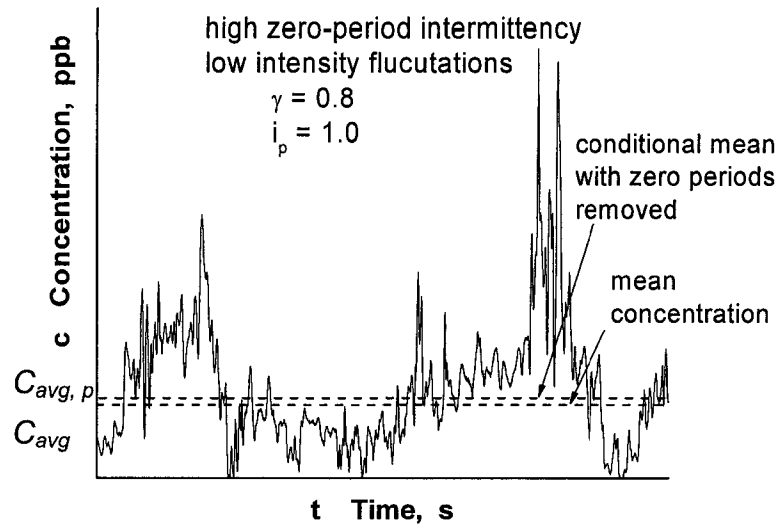
Figure 3.2: Cross-section through instantaneous dispersing plume. Large eddies meander plume about plume centreline, resulting in long durations of zero and peak concentrations, shown at positions three and four respectively, following Hilderman and Wilson (1999).



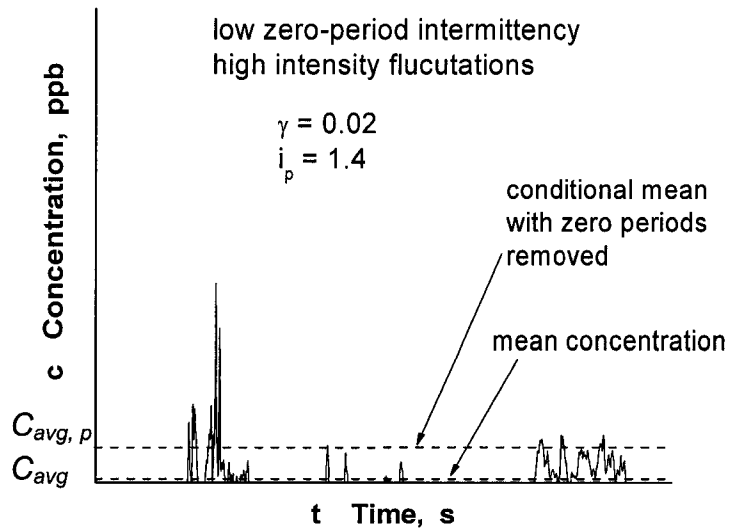
$$\text{Intermittency Factor} = \gamma = \frac{\text{Time } c > 0}{\text{Total Time}}$$

$$\text{Fluctuation Intensity} = i = \frac{c_{rms}}{C_{avg}}$$

Figure 3.3: Parameters describing concentration fluctuations.



(a)



(b)

Figure 3.4: Typical experimental concentration fluctuation time series. The smaller the intermittency factor, γ , the larger the difference between the conditional (zeros removed) mean concentration, $C_{avg,p}$, and the total mean concentration, C_{avg} .

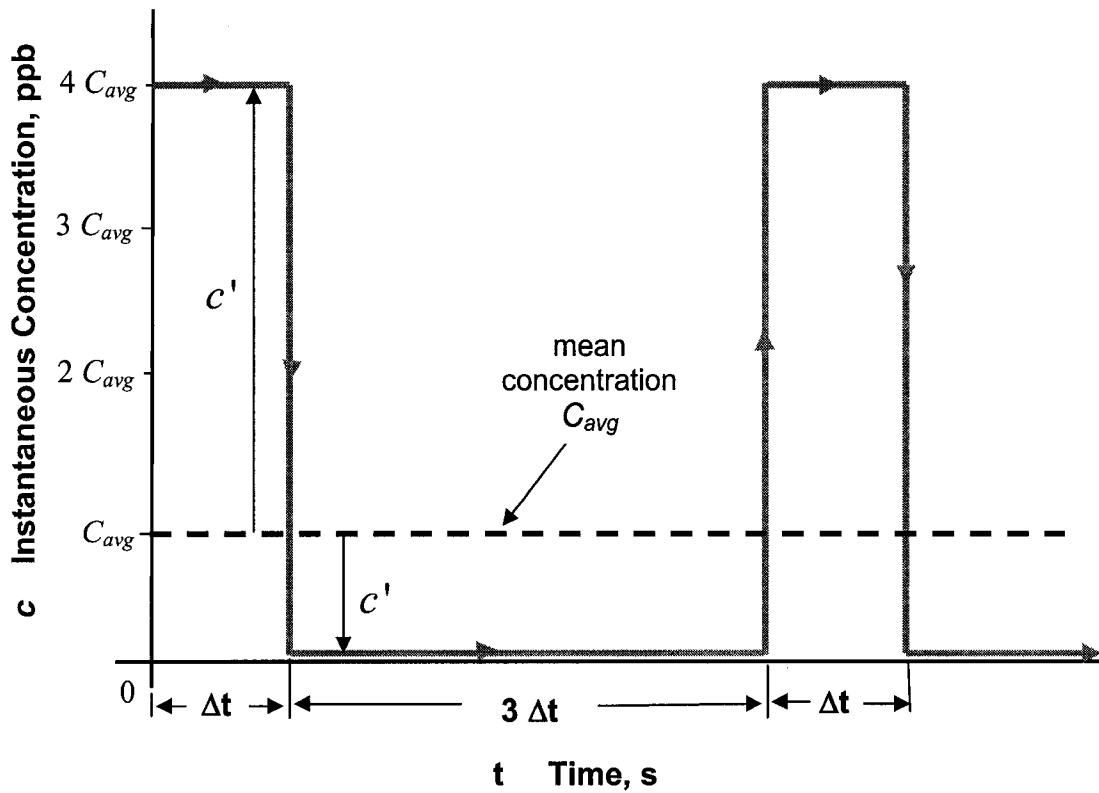


Figure 3.5: A concentration exposure made up of simple step functions, where the non-zero concentrations are four times the mean concentration, $c = 4C_{avg}$, and peak fluctuations are present 25% of the time, $\gamma = 0.25$.

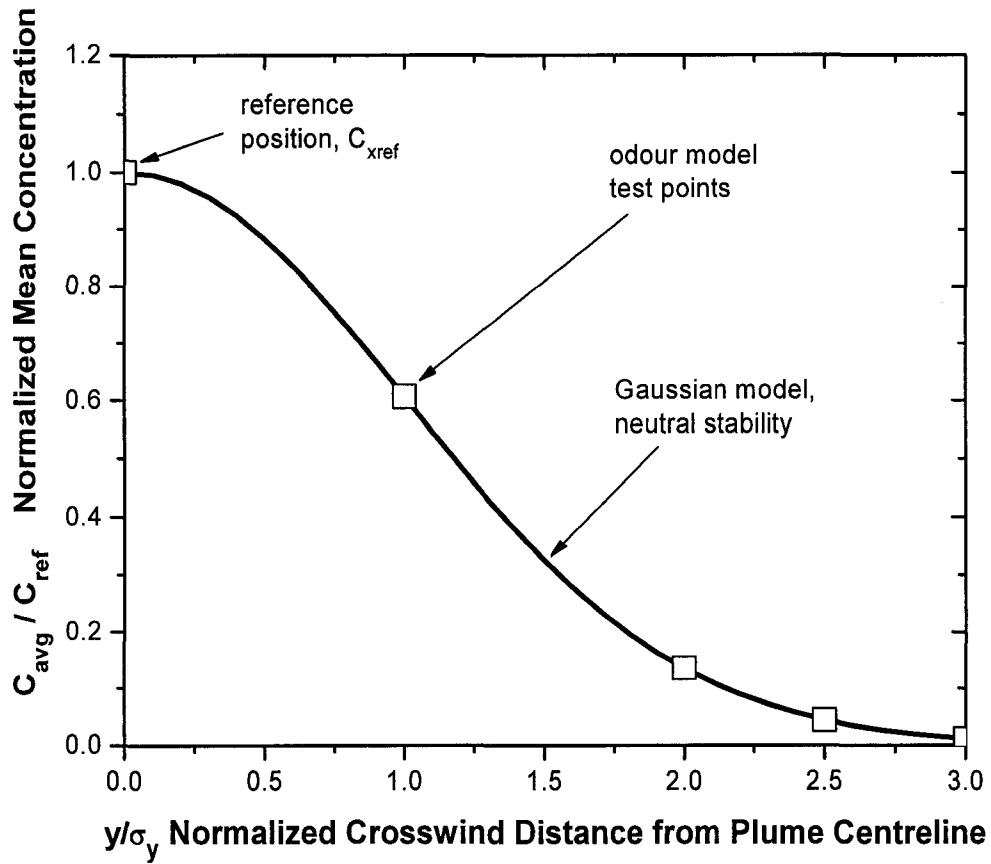
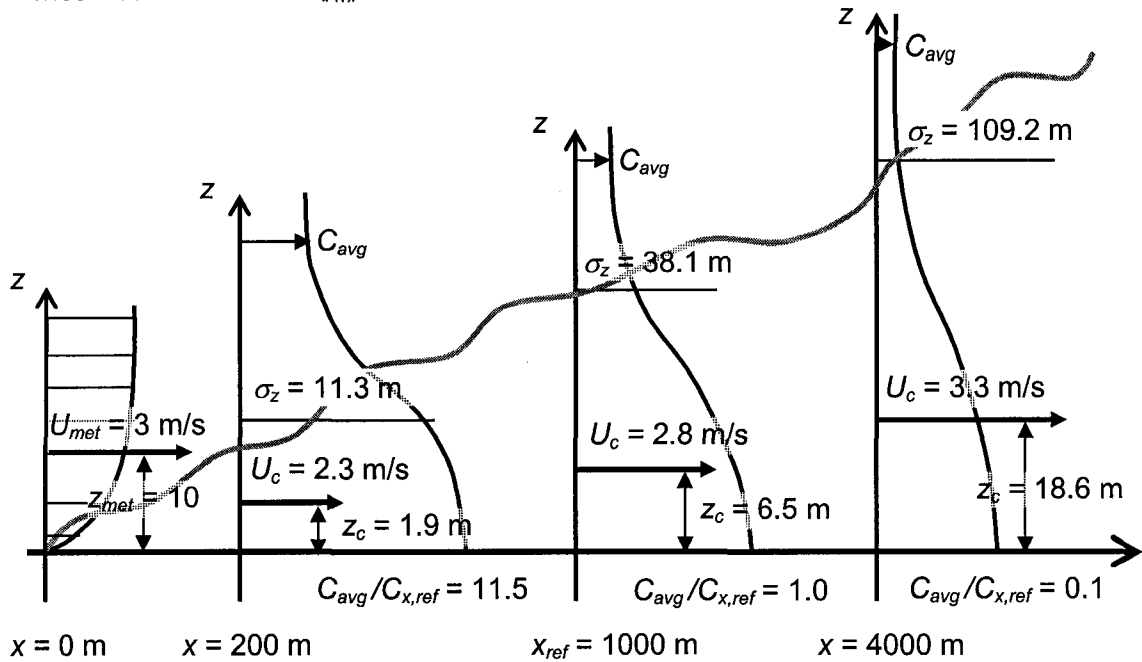


Figure 3.6: Variation in crosswind mean concentration normalized with concentration at full-scale reference position 1.0 km downwind from odorant source, on plume centreline. Following a Gaussian, mean concentration decays with crosswind position away from plume centreline ($y = 0$), for neutral stability and 180 min averaging time.

Stability Class D

reference position $x_{ref} = 1000\text{m}$ on plume centreline, $y/\sigma_y = 0$, where the mean concentration $C_{x,ref} = 1.0$



not to scale

Figure 3.7: Change in mean concentration profile, C_{avg} , plume spread, σ_z , and convection velocity, U_c , for a ground level source in atmospheric stability class D.

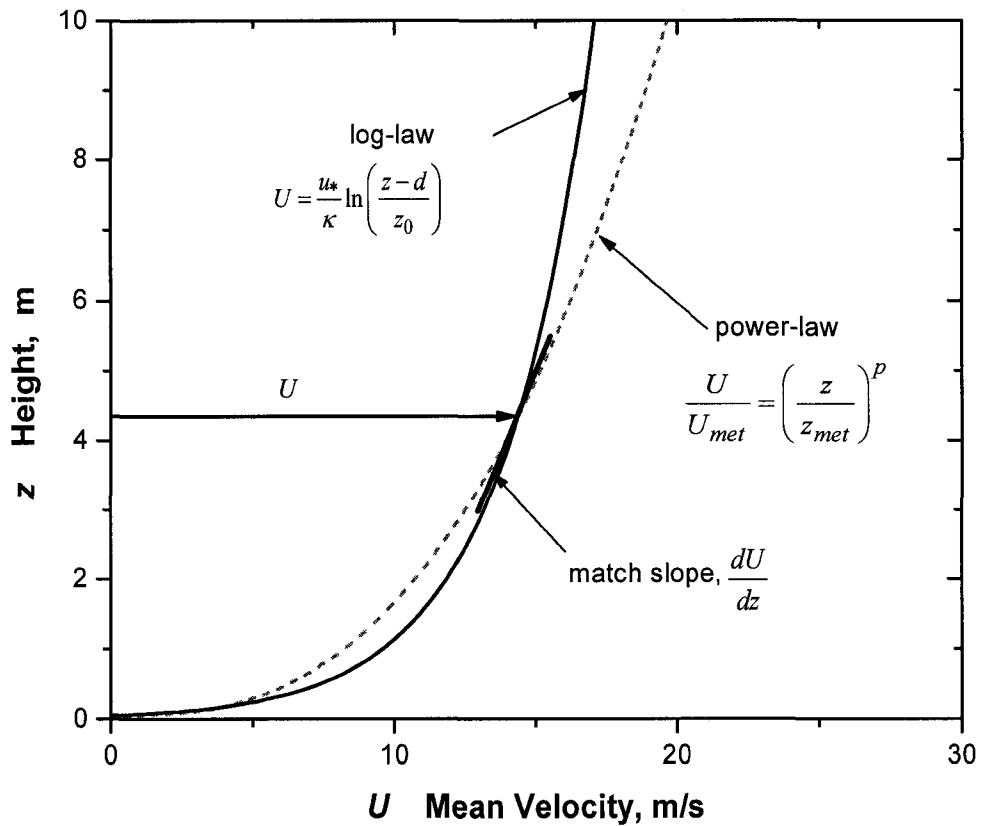


Figure 3.8: Comparison of log-law velocity profile, for neutral stability, with power-law velocity profile. Power p evaluated by matching slopes of both profiles at desired height. For neutral stability class, Irwin (1979) found $p = 0.16$ based on a match height of $z = 50$ m.

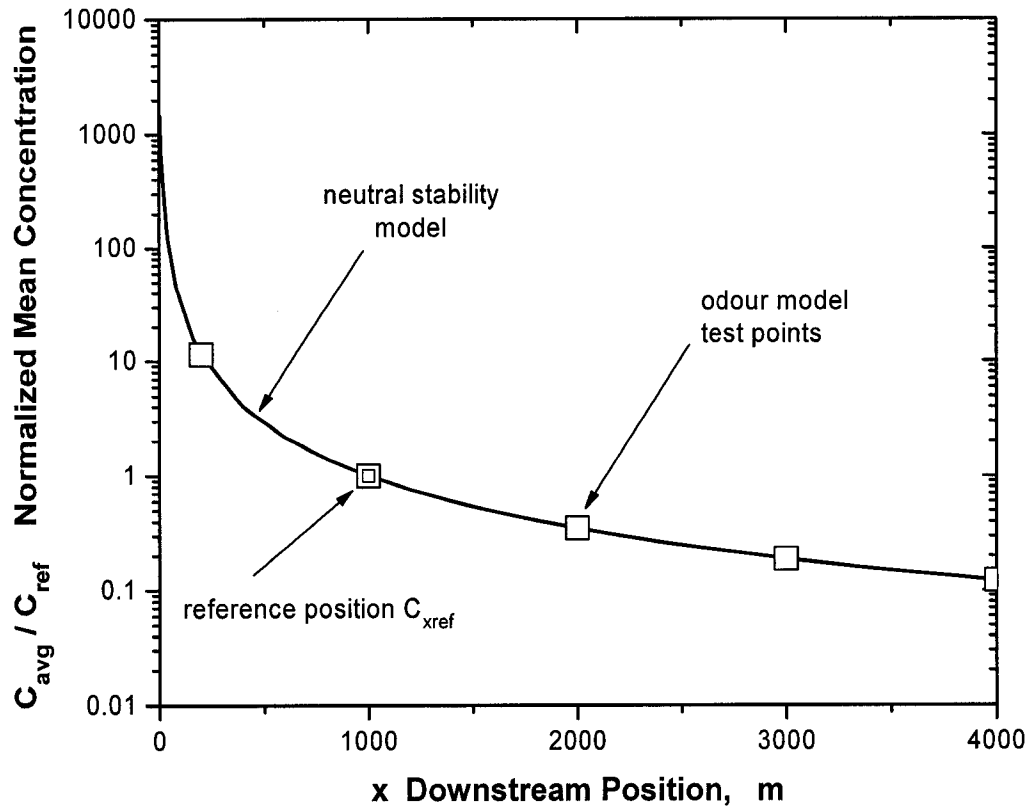


Figure 3.9: Downwind variation in mean concentration, caused by vertical and crosswind plume spreads for neutral stability and 180 min averaging time.

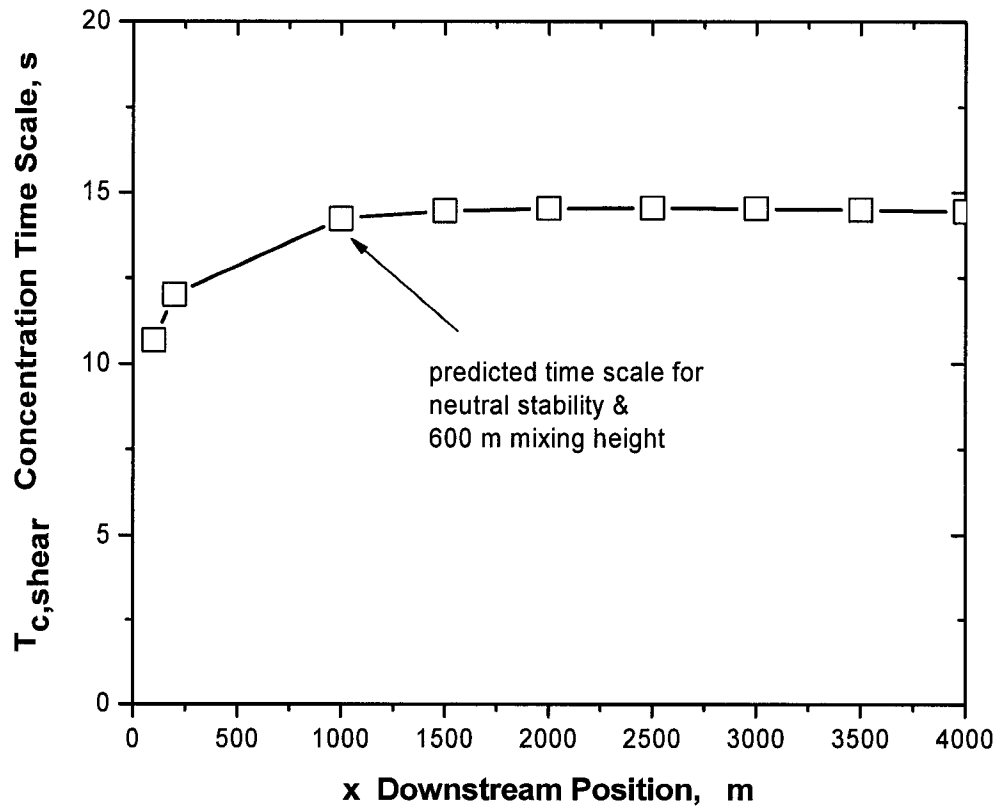
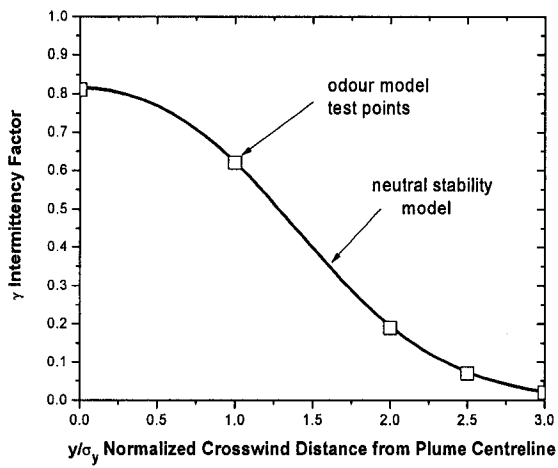
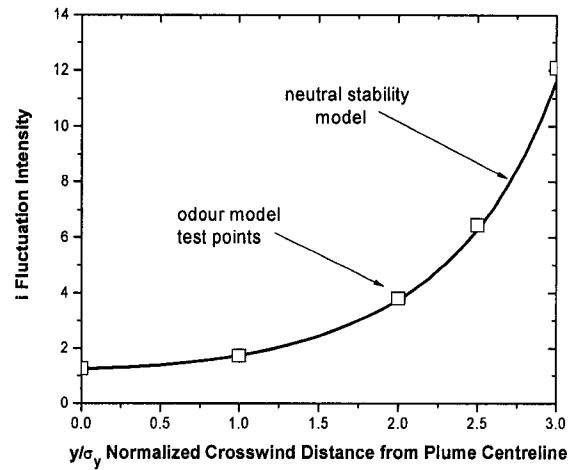


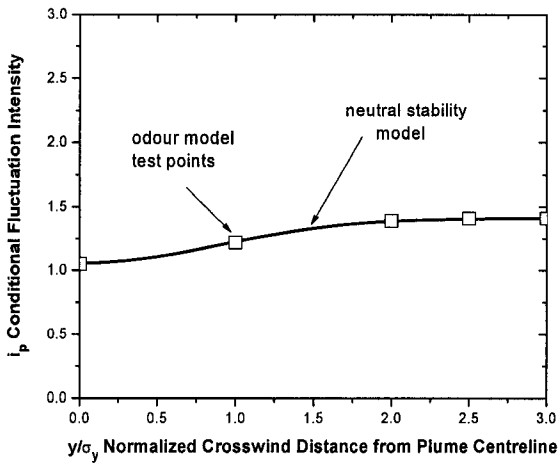
Figure 3.10: Concentration integral time scale, $T_{c,shear}$ levels-off beyond 2.0 km downwind of odorant source. Levelling-off is driven by decreasing shear $\partial U/\partial z$ as z_{ref} grows with downstream position, see Figure 3.7.



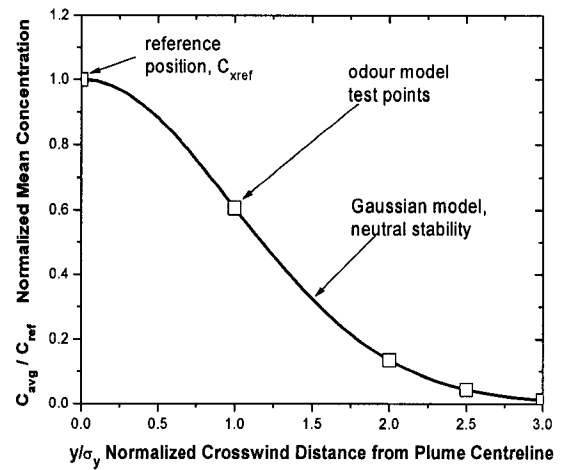
(a)



(b)

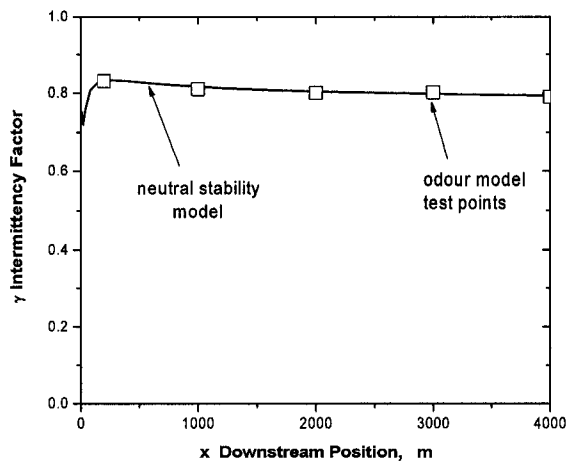


(c)

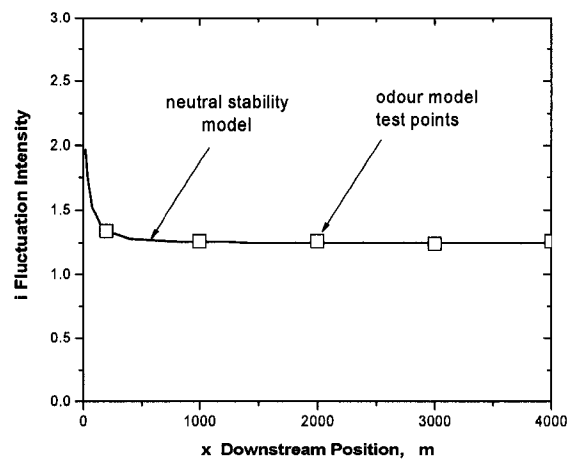


(d)

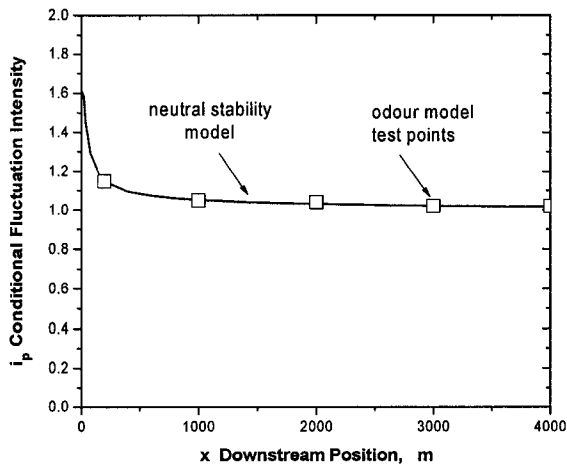
Figure 3.11: Crosswind variation in plume concentration parameters. Mean concentration normalized with respect to full-scale reference position at $y = 0$ and $x = 1000$ m.



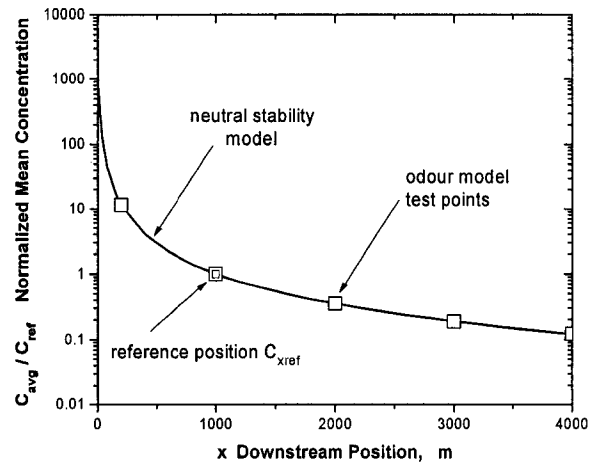
(a)



(b)



(c)



(d)

Figure 3.12: Downwind variation in plume concentration parameters. Mean concentration normalized with respect to full-scale reference position at $y = 0$ and $x = 1000$ m.

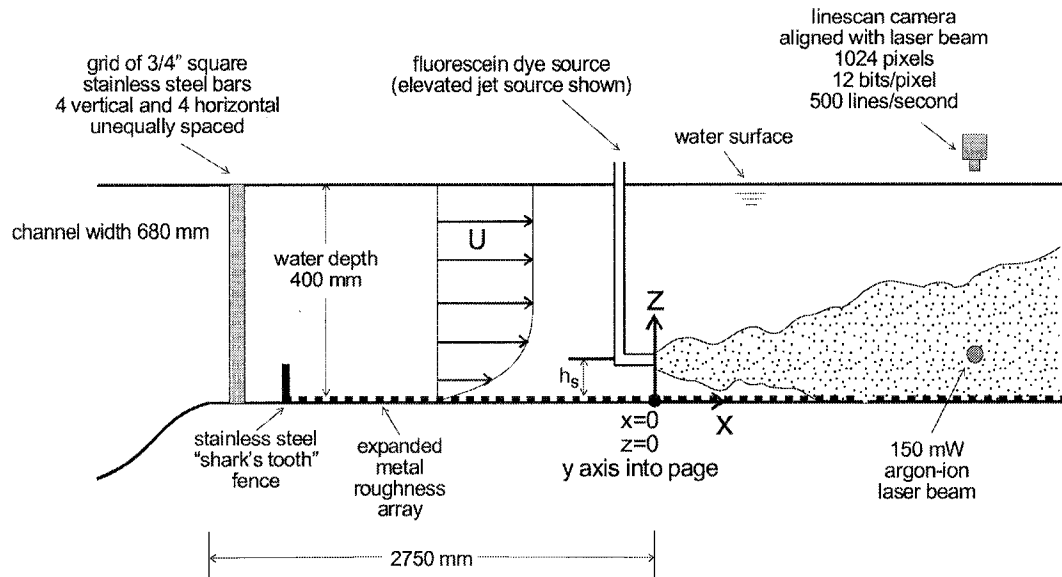


Figure 3.13: Side-view schematic used in the set-up of water channel measurements for the experimental data used in this study. Linescan camera positioned on top of channel to capture light emitted by fluorescing dye from laser line, which enters channel from side, following Hilderman (2004, Chapter 3).

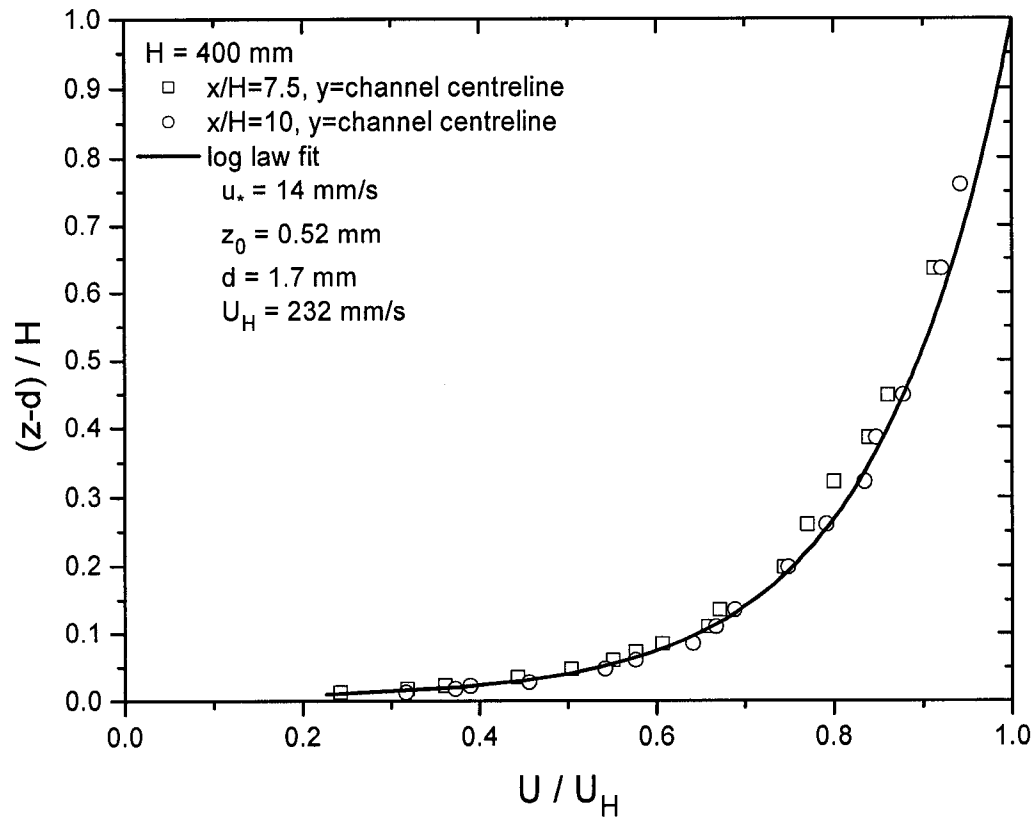
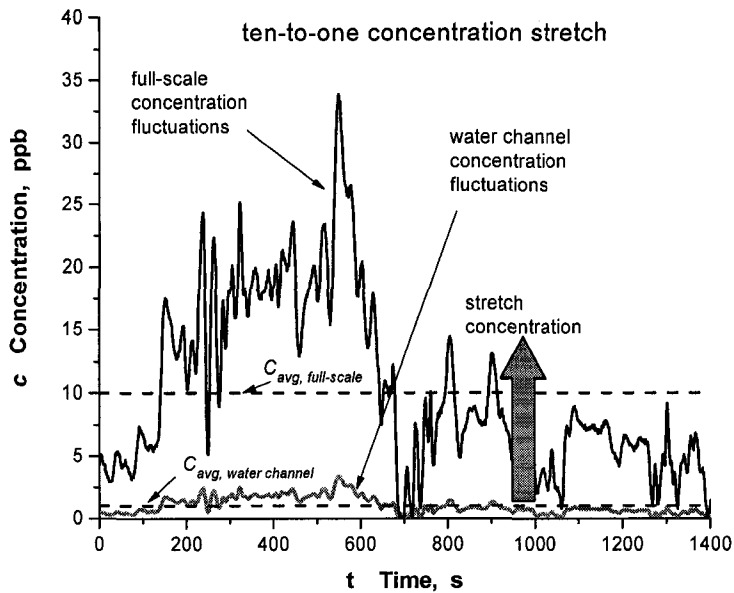
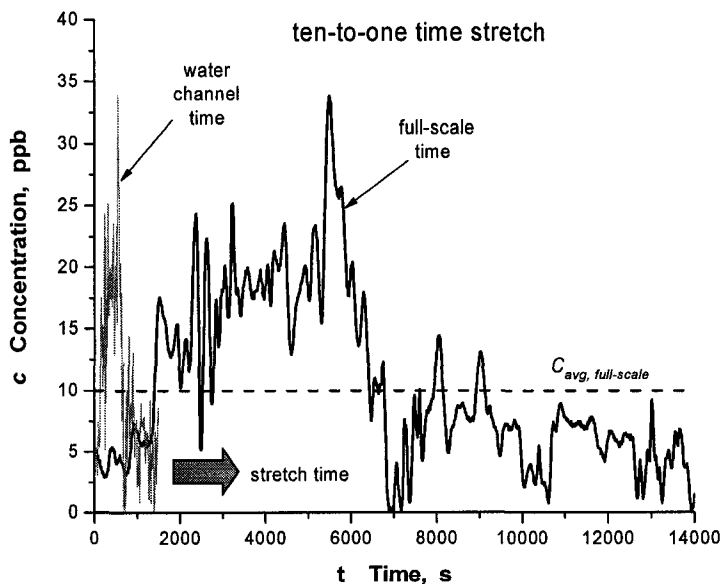


Figure 3.14: Normalized vertical velocity profile, U/U_H , for water channel LDV data taken along channel centreline at positions $x = 3000 \text{ mm}$ and 4000 mm downstream from the water channel inlet, for mixing layer height $H = 400 \text{ mm}$ (shown in Figure 3.13), following Hilderman (2004, Chapter 3).

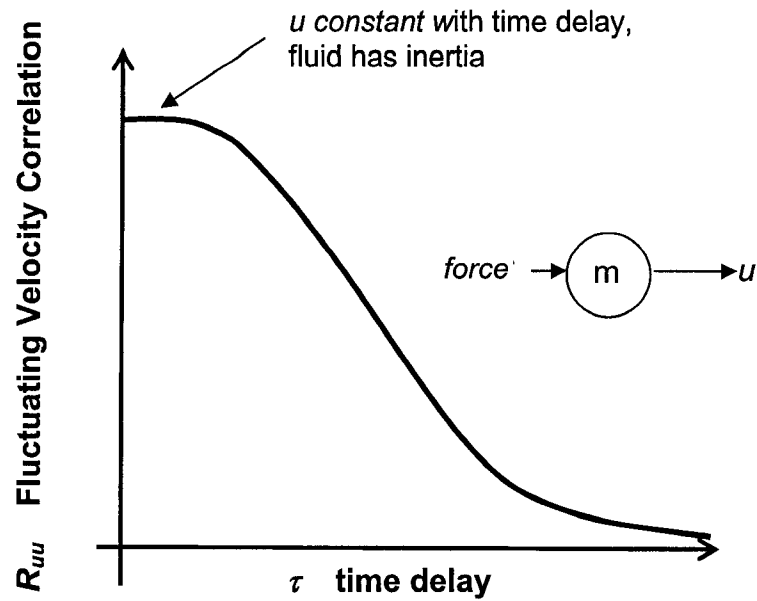


(a)

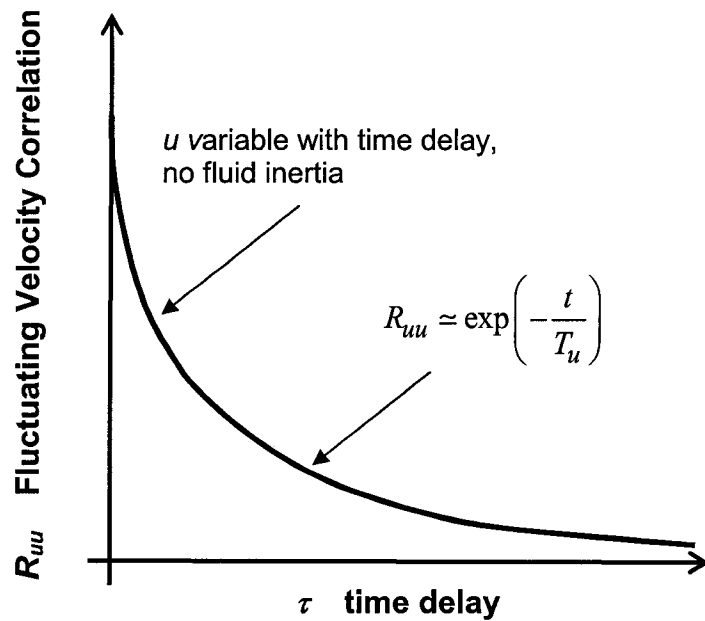


(b)

Figure 3.15: Illustration of scaling approach from water channel data to full-scale concentration and time by stretching mean concentrations (a) and concentration integral time scale (b).



(a)



(b)

Figure 3.16: (a) Autocorrelation of streamwise fluctuating velocity for a flow with inertia, R_{uu} , compared to flow without inertia (b). Note that R_{uu} remains a constant for first few time delay steps in (a), indicative of fluid with inertia.

Chapter 4

Evaluation of Odour Annoyance Model for Neutral Atmospheric Stability

4.1 Introduction

The purpose of this chapter is to examine quantitatively the psychophysical odour annoyance model developed in Chapter 2 using simulated full-scale exposure concentration fluctuation time series obtained from dispersion modelling and laboratory-scale data, as discussed in Chapter 3.

Section 4.2 is a parametric study of the sensitivity of predicted odour annoyance levels to variations in the input psychophysical parameters. Base detection thresholds, desensitization and resensitization time constants, odour intensity exponents, and memory window durations are subject to high levels of uncertainty which are coupled with the large variability in exposure concentrations during a typical release event. The parametric study will help determine which psychophysical parameters are most important to predicting the outcome and ensure that the odour model is robust enough to tolerate errors and uncertainty in these parameters while producing consistent realistic results.

The second part of this chapter (Sections 4.3 through 4.6) focuses on the mechanics of atmospheric dispersion by examining the mean concentration and concentration fluctuation effects on the odour annoyance outcome. As described in Chapter 3, scaled-up concentration time series from a library of water channel data will be used to simulate full-scale concentration fluctuation time series for five crosswind positions at 1.0 km downwind of the source, and an additional four downwind positions along the plume centreline. These nine locations are used to determine whether mean concentration or fluctuation characteristics are the most important factors for odour annoyance and to explore crosswind and downwind trends in memory load. It was hypothesized at the outset of this study that the concentration, duration and frequency of odour events contribute to the annoyance of human receptors, and that a frequently occurring event is just as annoying as an infrequent event of larger magnitude. The crosswind and downwind trends will be compared against this hypothesis and the current regulatory method that uses fluctuation-free odour units to predict and evaluating human annoyance to airborne odorants.

The downwind and crosswind variation of odour annoyance will be compared with toxic effects. Toxicity modelling has a longer history of regulation and is fairly well understood while odour annoyance modelling is still in its infancy. In section 4.6, a

comparison between the downwind decay of odour annoyance and toxic effects will show that odour annoyance is far more persistent than toxic effects.

Section 4.7 will examine the effect of indoor sheltering. As a self-preservation technique, people try to reduce their exposure to odours that are perceived as having hazardous health effects by either leaving the affected area or sheltering. An air filtration time constant will be used to model the air change rate of a building to predict indoor concentration fluctuations based on simulated outdoor exposure. Five indoor time series were created from the five crosswind positions of interest, and will be tested to determine human annoyance to indoor airborne odorants.

4.2 Parametric Study of Psychophysical Functions of Odour Annoyance Model

The model for human annoyance to airborne odorants developed in Chapter 2 incorporates six psychophysical parameters based on current knowledge of human olfaction.

- first-order uptake time constant, $\tau_{up} = 1.0$ s
- base detection threshold, $c_{th,base}$
- desensitization and resensitization first-order time constants, τ_{de} and τ_{re}
- odour intensity exponent, n
- A memory window of length t_{mem}

Excluding the uptake time constant, the five remaining parameters ($c_{th,base}$, τ_{de} and τ_{re} , n and t_{mem}) will be tested to determine their effect on the mean memory load, L_{avg} , for two simulated full-scale time series with three-hour averaging times, 1.0 km downwind of the source:

- plume centreline – exposure concentration fluctuations are relatively small ($i_p = 1.0$) and there are few intermittent (zero-concentration) periods ($\gamma = 0.8$)
- plume edge – exposure concentrations consist of many zero concentration periods with occasional bursts of measurable concentration during about 2% of the total event duration ($\gamma = 0.02$). The bursts are highly variable in strength so the fluctuation intensity is relatively large ($i_p = 1.4$)

These two time series cover a realistic range of intermittency factors, $0.02 < \gamma < 0.8$, and conditional concentration fluctuation intensities, $1.0 < i_p < 1.4$ that are expected for a dispersing plume. For the parametric study the mean exposure concentration at positions 1 and 2 were set equal to isolate the relationships between psychophysical parameters and realistic fluctuating concentration exposures. (In a real exposure the mean concentration at the edge of the plume would be much lower than on the centreline of the plume.)

Each of the five odorant- and receptor-dependent parameters was varied over a realistic range of values. Where parameter values were not available in current literature, a realistic estimated range was used. The base case values for all six psychophysical parameters are:

- $\tau_{up} = 1.0$ s
- $c_{th,base} = 0.1 C_{avg,ref}$

- $\tau_{de} = 180 \text{ s} = 3 \text{ min}$
- $\tau_{re} = 540 \text{ s} = 9 \text{ min}$
- $n = 0.4$
- $t_{mem} = 3600 \text{ s} = 1 \text{ hr}$

It will be shown that each of the five psychophysical parameters tested ($c_{th,base}$, τ_{des} , τ_{re} , n , and t_{mem}) monotonically and realistically affect the outcome of the odour annoyance model. For example, an increase in base detection threshold means that there are concentration fluctuations in a time series are less likely to be detectable and possibly annoying, resulting in lower mean memory loads. Each of these parameters behaves in realistic and predictable ways, so all that is required is a single set of psychophysical parameters to test how the odour annoyance model behaves over a large range of plume statistics.

4.2.1 Base Detection Threshold

The base detection threshold, $c_{th,base}$, is the minimum concentration of odorant which will elicit a detection response in 50% of the population, and no response in the remaining, less sensitive, 50%. Desensitization and resensitization processes were used to create the time and concentration dependent variable detection threshold, $c_{th,vary}$. The minimum $c_{th,vary}$ is $c_{th,base}$. The variable detection threshold is used to determine the concentration effective in producing a perceived intensity, c_{eff} , and the mean memory load, L_{avg} . For this reason, it is important to determine how sensitive L_{avg} , is to the base detection threshold.

The odour annoyance model developed in Chapter 2 was evaluated for very general test conditions to examine how it will behave over a large range of plume statistics while minimizing bias from parameters that are uncertain. The source concentration is unknown, so a reference position located at 1.0 km downwind of the source on the plume centreline was chosen as a basis from which to evaluate all concentrations. The mean concentration at the reference position is $C_{avg,ref} / C_{avg,ref} = 1.0$ (see Section 3.3.1). Because the base detection threshold is dependent on the type of odorant studied, but no particular odorant has been specified, $c_{th,base}$ will be specified in terms of $C_{avg,ref}$. For the purposes of the parametric study in Section 4.2, the mean concentrations for each time series used are equivalent, therefore, it is appropriate to evaluate $c_{th,base}$ as a fraction of the mean concentrations for both time series, C_{avg} .

By definition, a ratio of $C_{avg} / c_{th,base} = O_U = 1.0$ is detectable by 50% of the population, and ratios $C_{avg} / c_{th,base} < 1.0$ are detectable by fewer and fewer people. In addition, the odour unit intensity I_{OU} , evaluated using Equation (2.8), is only applicable to O_U greater than or equal to 1.0. As one of the goals of this study is to be able to compare this odour annoyance model with the current odour unit model, it is important to be able to evaluate I_{OU} for a range of C_{avg} within the dispersing plume. This requires the use of $C_{avg} / c_{th,base} \geq 1.0$, or equivalently $c_{th,base} \leq 1.0 C_{avg}$.

In order to evaluate how changes in the base detection threshold affect the outcome of the odour annoyance model, three values of $c_{th,base}$ were chosen:

- $c_{th,base} / C_{avg} = 0.03$
- $c_{th,base} / C_{avg} = 0.1$

- $c_{th,base} / C_{avg} = 0.3$

Figure 4.1 shows that the mean memory load decreases less than 10% for a tenfold increase in normalized base detection threshold for both crosswind positions. This result indicates that the odour annoyance model behaves in predictable ways to changes in the base detection threshold. Using Figure 2.5 as an example, it is expected that as the base detection threshold increases the effective concentration (shaded areas) will decrease, resulting in a decrease in mean memory load.

It is interesting to note that the mean memory load for the centreline time series is larger than that for the time series at the plume's edge, where concentration fluctuations are greater than zero only 2% of the time. This indicates that plume intermittency plays a larger role in predicting annoyance than mean concentration, and that the mean concentration alone can not be used to predict human annoyance to odours across a dispersing plume. The effects of both the mean concentration and fluctuation statistics, such as intermittency, will be explored in greater detail in Section 4.3.

The odour annoyance model was shown to behave in a predictable and realistic manner to changes in the base detection threshold, a reasonable selection for $c_{th,base}$ will provide reasonable results. Throughout the rest of this study, the base detection threshold will be assigned a value of 0.1 times the mean concentration at the full-scale reference position on the plume centreline, 1.0 km downwind of the source.

4.2.2 Desensitization and Resensitization Time Constants

For the purposes of this study, adaptation and habituation are treated as a single desensitization process that allows receptors to ignore constant concentrations in their environment, while recognizing and responding to changing odour concentrations or new odours. Desensitization was taken into account in the Chapter 2 odour model with an increasing detection threshold that is assumed to follow a first order decay function with a time constant, τ_{de} .

Just as people are able to adapt and habituate to odour, they are also able to recover from odour exposures to allow their olfactory systems to become sensitive to the original detection concentration. Resensitization is assumed to be a first order process governed by a time constant τ_{re} that only acts during a decreasing or zero-concentration exposure, as explained in Chapter 2.

The desensitization and resensitization time constants are not necessarily equal. In fact, it is assumed in this study that τ_{re} is larger (i.e. a slower process) than τ_{de} , as is apparent in the base case described above where $\tau_{de} = 180$ s and $\tau_{re} / \tau_{de} = 3$. The individual effects and the combined effect (where $\tau_{re} > \tau_{de}$) of these two time constants on the mean memory load were studied using the following test parameters:

- $60 \text{ s} < \tau_{de} < 1800 \text{ s}$ for $\tau_{re} = 180 \text{ s}$
- $60 \text{ s} < \tau_{re} < 1800 \text{ s}$ for $\tau_{de} = 180 \text{ s}$
- $60 \text{ s} < \tau_{de} < 1800 \text{ s}$ for $\tau_{re} / \tau_{de} = 3$
- $60 \text{ s} < \tau_{re} < 1800 \text{ s}$ for $\tau_{re} / \tau_{de} = 3$

These two sensitization time constant parameters were studied for the two simulated time series at the plume centreline and edge. Figure 4.2 illustrates the trends in

L_{avg} for the plume centreline data series. Notice in Figure 4.2 (a) that increasing only τ_{de} increases L_{avg} , whereas increasing only τ_{re} decreases L_{avg} . These two trends result in only a 70% change (i.e. less than a factor of 2) in L_{avg} over a factor of 30 increase in both time constants. These trends are interesting but are considered insignificant, especially for time constants greater than approximately 180 seconds, or 3 minutes. These differences may play more of a role when comparing between individuals and/or odorants, but will be left for future studies.

Figure 4.2 (b) shows the effect of increasing τ_{de} and τ_{re} for a constant ratio of time constants, $\tau_{re} / \tau_{de} = 3$, at the plume centreline. As with Figure 4.2 (a), the trends illustrated in this figure are negligible.

Figure 4.3 illustrates the variation in the mean memory load for increasing τ_{de} and τ_{re} for the plume centreline in Figure 4.3 (a), and plume edge in Figure 4.3 (b). The mean memory loads at the plume edge are slightly more sensitive to changing desensitization time constant than on the plume centreline. In both cases, L_{avg} varies less than a factor of two over a factor of 30 increase in sensitization time constant values.

These results of varying sensitization time constants are expected. Referring back to Figure 2.2, an increase in desensitization time constant, τ_{de} , increases effective concentration, c_{eff} , because desensitization takes longer to occur. This in turn increases mean memory load, L_{avg} , because L_{avg} is proportional to c_{eff} . Figure 2.2 also shows that an increase in resensitization time constant, τ_{re} , decreases c_{eff} because it takes longer to recover from an odour event, and therefore there is a decrease in L_{avg} .

Reported values of sensitization time constants are highly variable, as pointed out by Wang *et al.* (2002). Considering that the odour annoyance model behaves predictably and realistically to changes in τ_{de} and τ_{re} , a sensible choice of these two parameters is all that is necessary to insure reasonable predictions of crosswind and downwind variations in L_{avg} . For the remainder of this study, the desensitization time constant will be assigned a value of 180 seconds = 3.0 minutes, and the resensitization time constant will be assigned a value of 540 seconds = 9.0 minutes.

4.2.3 Odour Intensity Exponent

As discussed in Chapter 2, Stevens (1957) found that human odour responses are a non-linear function of the exposure concentration, and developed a power-law model for perceived odour intensity. Based on Stevens' law, the model for intensity, I , developed in this study is a function of the concentration effective in eliciting a response, c_{eff} , the variable detection threshold, $c_{th, vary}$, and odour intensity exponent, n . Receptors are highly sensitive to odorants with large values of n as opposed to odorants with small values of n . For this reason, it is important to understand the sensitivity of the mean memory load, or equivalently the level of odour annoyance, to the exponent n .

The odour intensity exponent was varied over the recommended range $0.2 < n < 0.8$ (NSW EPA, 2002) for the two simulated full-scale, ground-level positions in the plume, as shown in Figure 4.4. Figure 4.4 (a) shows that the plume centreline time series, where the intermittency factor is high and fluctuation intensity is low, is not very sensitive to changes in odour intensity exponent: with a factor of four increase in n , L_{avg}

varies by only 5%. Compare this to the sensitivity to the odour intensity exponent in the plume edge, where the exposure is highly intermittent and fluctuation intensity is high: L_{avg} increased by over 550% over only a factor of four increase in n .

Figure 4.4 shows that an incorrect exponent n produces large errors in the mean memory load. If n is too low, the annoyance at the edges of the plume could be drastically under-estimated. A careful study of the appropriate odorant-specific exponent n must be undertaken before the values of L_{avg} could be used to determine the accurate change in annoyance within a dispersing plume for any specific odorant, or to compare annoyance results between different odorants.

The overall goal of this study is to develop a robust model for human annoyance to odours, and to study the possible crosswind and downwind implications of this model in a dispersing plume. Even if a specific odorant was tested, the specifics of how people perceive odours, including appropriate exponent n , are not well known or documented in the scientific literature. For all further odour model testing the exponent n will be fixed at 0.4, as it is the geometric mean of the typical exponent range.

4.2.4 Memory Window Length

It is proposed that a person's level of annoyance is governed by the perceived intensity of both the current odour exposure and all previous odour exposures that they can recall. All of the events that an individual can recall within their memory window (of duration t_{mem}) add to the stress of the next offensive odour exposure. The perceived intensities of all remembered events are averaged over the entire memory window to determine the memory load, L . Recall from Chapter 2, Section 2.4.2, the mean memory load L_{avg} (averaged over an entire exposure) is normalized by the memory window length, t_{mem} , in order to compare events for receptors with different memory windows. Of all parameters used in this model, the psychological t_{mem} parameter has the most uncertainty and is the least amenable to engineering analysis. By normalizing the memory load with t_{mem} the complications of this psychological parameter are minimized.

As expected, t_{mem} was found to have negligible effects on the normalized L_{avg} . This implies that annoyance is a linear function of the memory window length. In order to determine the odour annoyance of an individual, the mean memory load, L_{avg} , must be multiplied by t_{mem} to determine the "real" un-normalized annoyance. The intricacies of choosing t_{mem} are beyond the scope of this engineering study, and are left for future work.

4.2.5 Summary of Psychological and Physical Parameters of Odour Annoyance Model

The purpose of the parametric study in Section 4.2 was to examine the psychophysical parameters that govern human response to odour stimuli in the proposed model for human annoyance, and determine how sensitive the model is to each of these parameters. A summary of the results of testing the six parameters of human response and the final values chosen for use in further parametric studies are presented below:

- The uptake time constant, τ_{up} , is used to determine the inhalation and response time of a receptor to an odorant. It is agreed in the literature that this value should be in the order of a one-second breath, or $\tau_{up} = 1.0$ s.
- The base detection threshold, $c_{th,base}$, is currently used to assess the minimum acceptable dilution of airborne odorants, and is used in this study as a minimum threshold for detection of an odorant. This parameter was found to have a predictable effect on the mean memory load: as expected, an increase in $c_{th,base}$ results in a decrease in odour annoyance. Without specifying a specific odorant and receptor, a reasonable value of the base detection threshold will be used, $c_{th,base} = 0.1 C_{avg}$.
- The desensitization time constant, τ_{de} , accounts for the human characteristic of habituation and adaptation to constant odour stimulus. As expected, an increase in τ_{de} results in an increase in odour annoyance. This parameter was found to have little effect on the mean memory load, and because detailed information of this parameter is not available in the literature, a realistic value of $\tau_{de} = 180$ s = 3.0 min will be used.
- The resensitization time constant, τ_{re} , accounts for the human ability to recover from desensitization to an odour when exposed to a decreasing or zero concentration. As expected, an increase in τ_{re} results in a decrease in odour annoyance. This parameter was found to have little effect on the mean memory load; therefore, any realistic value can be used. It is plausible that this resensitization time constant is longer than the desensitization time constant, so a realistic estimate of $\tau_{re} = 540$ s = 9.0 min was chosen.
- Odour intensity exponent, n , is used in an extension of Stevens' psychophysical power-law for the perceived intensity of a stimulus to describe the intensity, I , of an odour perceived by a receptor. This intensity is used to evaluate the end result of the model, the memory load, L . It was found that the mean memory load is very sensitive to this parameter for highly intermittent concentration time series at the edges of the plume, where an increase in n increases the effect of the concentration fluctuations resulting in an increase in odour annoyance, as expected. An exponent $n = 0.4$ will be used for further model testing. As L_{avg} is very sensitive to this parameter, further studies should be undertaken to accurately determine appropriate receptor and odorant based values.
- The memory window, t_{mem} , captures the effect of current exposure concentration and past odour events that can be remembered by a receptor, while assuming a linear decay of memory recall. As L_{avg} is normalized by the memory time, t_{mem} , the mean memory load is independent of t_{mem} . For the purposes of evaluating the normalized mean memory load, a reasonable memory window length of one hour will be used for the remainder of this study, i.e. $t_{mem} = 3600$ s = 1 hr.

This parametric study confirms that the odour model developed in Chapter 2 is well-behaved over a wide range of fluctuating concentration exposures. Changes in the psychophysical input parameters resulted in monotonic and predictable changes in the outcome of the odour annoyance model. With this information and a representative base case of psychophysical parameters, the downwind and crosswind odour annoyance trends

can be investigated for a dispersing plume without fear that any observed effects will be due to instabilities in the psychophysical model.

4.3 Predicted Odour Annoyance with Mean Memory Load for Full-scale Case Study

The remainder of this chapter focuses on odour annoyance trends that depend on the fluid mechanics of atmospheric dispersion, which determine event concentration, duration and frequency. In Chapter 3, the techniques used to predict full-scale characteristics of a dispersing plume were explained in detail. The five plume characteristics of interest are:

- mean concentration, C_{avg} , a function of averaging time and position within the dispersing plume
- fluctuation intensity, i , a measure of the magnitude of fluctuations about the mean concentration
- intermittency factor, γ , the fraction of exposure time that the odorant concentration is greater than zero
- conditional fluctuation intensity, i_p , a measure of the magnitude of fluctuations about the mean concentration when the plume is present (i.e. excluding the zero concentration intermittent periods.)
- integral time scale of concentration fluctuations, T_c , a measure of how quickly changes in concentration occur within the plume

Each of these five parameters were predicted for full-scale downwind and crosswind positions, under neutrally stable (Pasquill-Gifford class D), atmospheric conditions ($U_{met} = 3$ m/s at $z_{met} = 10$ m), for rural type surface conditions ($z_{o\ full} = 10$ cm), and a power-law velocity profile with power $p = 0.16$ and mixing layer height $H = 600$ m. A three hour averaging time was used to determine the mean characteristics of the meandering plume, such as C_{avg} and crosswind plume spread σ_y . Time series of concentration fluctuations that fit predicted full-scale intermittency factor, γ , and conditional fluctuation intensity, i_p , were selected from a library of concentration fluctuation data acquired from water channel experiments. These laboratory-scale time series were then stretched in concentration and time to match the predicted full-scale mean concentrations and timescales of odour events.

Five crosswind positions, ranging from the plume centreline to the far edge of the plume, will be explored in this section to determine the predicted crosswind trends of the odour annoyance model. These crosswind positions are located at a full-scale position 1.0 km downwind of the source, which was chosen as a typical distance between rural neighbours in Alberta (a major source of odour complaints). Five downwind, plume centreline positions, ranging from near odorant source to far downwind, will also be explored in this section to determine the predicted downwind trends of the odour annoyance model. A position 1.0 km downwind from the source on the plume centreline is used as a reference and assigned a normalized mean concentration $C_{avg,ref} = 1.0$. The positions of each of these test points are shown relative to one another in Figure 4.5. The plume characteristics (C_{avg} , i , γ , i_p and T_c) are shown for the selected crosswind and

downwind positions in Figure 3.11 and Figures 3.12 and 3.10 respectively (recall from Section 3.3.3 that T_c is constant across the width of the plume).

There are no experimental data available to associate memory load to annoyance so the calculated odour loads will indicate trends and enable relative comparisons rather than predict absolute odour annoyance values. As explained in the Section 4.2, memory loads are calculated using the base case of psychophysical parameters, and are not specific to a particular odorant and receptor.

4.3.1 Variation in Mean Memory Load with Averaging Time

Averaging time is used to determine mean statistics of a meandering plume. As illustrated in Figure 3.1, the longer the plume statistics are averaged, the wider the crosswind plume spread, the smaller the centerline concentration, and the larger the plume edge concentrations. The assumed averaging time for the present case study is three hours. Three hours is typically the longest time over which meteorological statistics, such a mean wind speed and direction, can be assumed stationary.

The effect of averaging time on mean memory load was examined for the reference position on the plume centreline, 1.0 km downwind of the virtual odorant source. Figure 4.6 illustrates the mean memory load for the three averaging times: 3.0 minutes, 1.0 hour, and 3.0 hours. There is a less than 15% increase in odour load over a factor of 60 increase in averaging time, indicating that L_{avg} is very insensitive to t_{avg} on the plume centreline. This kind of outcome is, however, not expected for positions at the edge of the plume. Averaging time affects all plume statistics, mean concentrations, intermittency and intensity making it impossible to isolate as a variable. It is possible to say from the results shown in Figure 4.6 that this change in statistics has little bearing on the outcome of the odour annoyance model for positions on the plume centreline, but this conclusion cannot be extrapolated to the edge of the plume. Averaging time dictates the statistics of the plume, and, as it will be shown in the following sections, the roles each of these statistics play on the outcome of the odour annoyance model are not all together intuitive.

Figure 4.6 illustrates another very important aspect to this model, the competition between two very important parameters. Recall, from Chapter 3, that the mean concentration along the centreline is greater and the plume is less intermittent for shorter averaging times, therefore, it could be expected that a shorter averaging time would produce a larger mean memory load. Figure 4.6 shows that this expectation did not come to fruition. This difference can be explained through the variable detection threshold. As a person is exposed to a concentration of odorant, they adapt and habituate to the odour, and require an increasing concentration of odorant to enable detection. In the absence of odorant, people recover their sensitivity to odour. For a short averaging time, such as three minutes, the plume is present during almost 100% of the exposure. This means that the receptor has little time to recover, or resensitize, to the odorant, resulting in a lower mean memory load, even though the mean exposure odorant concentration is higher than for a longer averaging time. It is the competition between the mean concentration and intermittency through the desensitization and resensitization processes, which cause

counter-intuitive results. The competition between concentration and intermittency is further explored in the following sections covering the crosswind and downwind variation in memory loads and the effect of indoor sheltering.

4.3.2 Crosswind and Downwind Variation in Mean Memory Load

At the beginning of this study, it was anticipated that short intermittent concentration bursts with lots of time for resensitization (like exposures in the edges of the plume) might be just as annoying as steady larger events where there is more opportunity for the desensitization process to occur (like exposures near the centre of the plume). A possible outcome is that a balance between the decrease in mean concentration and the increase in intermittency towards the edge of the plume would produce a constant level of annoyance across the plume.

The competition between mean concentration and intermittency factor make it difficult to predict outcomes of the of the odour annoyance model. The mean concentration, C_{avg} , and the intermittency factor, γ , both decrease across the plume, while the total and conditional fluctuation intensities, i and i_p respectively, both increase across the plume, as illustrated in Figure 3.11. Figure 3.12 showed that the intermittency factor, γ , and the conditional and total fluctuation intensities, i_p and i , levelled off beyond 1.0 km downwind, but the mean concentration, C_{avg} , decayed by a factor of ten from 1.0 km to 4.0 km downwind from the source. For these reasons, it is necessary to test the odour annoyance model using simulated full-scale time series representative of nine selected crosswind and downwind positions, illustrated in Figure 4.5, to evaluate trends in odour annoyance, and to demonstrate the robustness and realism of the model over a wide range of conditions.

4.3.2.1 Crosswind Mean Memory Load

Predicted mean memory loads, L_{avg} , for the five crosswind positions, 1.0 km downwind of the source, are shown in Figure 4.7. The mean memory load varies little out to one plume spread, σ_y , and then declines out to the plume edge with a 90% reduction in L_{avg} from plume centreline to $3.0 \sigma_y$. It is not advisable to test the model with simulated full-scale time series beyond $y = 3.0 \sigma_y$ from the plume centreline because the intermittency factor gets very small so there is insufficient data to produce realistic results without a large ensemble of data sets.

The hypothesis at the outset of this study was that the effects of decreasing mean concentration and increasing intermittency would balance through the sensitization processes producing a uniform level of annoyance across the width of the plume. Figure 4.7 contradicts this original theory. This result could be explained considering that the mean concentration decreases by a factor of 100 from plume centreline to plume edge, and that the plume is highly intermittent at the edge ($\gamma = 0.02$) compared with the centreline ($\gamma = 0.8$). Even though a person will perceive an odour event at the plume edge

as more intense than if it occurred more frequently, the lack of detected odour events must be a larger factor than originally anticipated.

It is easy to assume that both the intermittent nature and the low mean concentration at the plume's edge, compared with the centreline, play a role in this result. What is not obvious is which of the two factors plays a dominant role. To test this, the results from this test were compared with those from Section 4.2.1, where the mean concentration at the plume edge was equivalent to that on the centreline. Surprisingly enough, there was only a factor of two increase mean memory load for a factor of 100 increase in mean concentration. This indicates that plume intermittency plays a larger role in predicting annoyance than mean concentration, and that the mean concentration alone can not be used to predict human annoyance to odours across a dispersing plume.

4.3.2.2 Downwind Mean Memory Load

Downwind variation in mean memory load for each of the five downwind, centreline positions is shown in Figure 4.8. Over a 3800 m downwind range, L_{avg} only decreases by 30%. Compare this to the factor of 100 decrease in mean concentration over the same range, and the results are remarkable. However, with only a 5% decrease in intermittency factor over the 100:1 change in concentration with downstream distance, the slow decay in odour annoyance is reasonable. Tests in the crosswind direction, in the previous section, indicated that the change in intermittency is the key factor for the change in odour annoyance. Periods between odour events allow a person to resensitize, and the longer those periods are the greater the recovery to their original sensitivity, as shown in Figure 2.5 (b). Just as returning to a kitchen full of garlic odorant, after periods of recovery, the odour is perceived to be more intense than if the person had remained in the kitchen. Odorant exposures that have very few zero-concentration periods, like those along the centreline of the plume, allow the receptor to desensitize to the odour. There is a very high frequency of odour events (large γ) along the plume centreline, and the decay in this intermittency factor is very slow. For this reason, desensitization plays a large role in decreasing the perceived intensity and odour annoyance levels of exposure concentrations, even close to the plume where mean concentrations are comparatively high. The slow decay in L_{avg} indicates that people will be annoyed by persistent emissions far downwind of the source. This result also suggests that even a large dilution of mean concentration would have little effect on levels of odour annoyance. This is bad news for industrial and agricultural odorant emitters.

4.4 Downwind and Crosswind Comparison with Current Practices

The objective of this section will be to show that without accounting for the complexities of both concentration fluctuations and sensitization processes, the odour unit method for predicting odour annoyance greatly underestimates the potential downwind area affected

by an odorous plume. As explained in Section 2.3.5, the effective concentration can be compared to the current concept of odour units by:

$$\frac{c_{eff}}{c_{th,vary}} \Leftrightarrow O_U - 1 = \frac{C_{avg} - c_{th,base}}{c_{th,base}} \quad (4.1)$$

In a similar way, the intensity I , defined in Equation (2.9), is comparable to odour unit intensity, I_{OU} , defined in Equation (2.8), as follows:

$$I = \left(\frac{c_{eff}}{c_{th,vary}} \right)^n \Leftrightarrow (O_U - 1)^n = I_{OU} \quad (4.2)$$

O_U is constant in time and therefore I_{OU} is also constant in time. The memory load for I_{OU} is calculated using Equation (2.12) as follows:

$$\begin{aligned} L_{OU} &= \int_{t=-t_{mem}}^{t=0} \frac{W_o(t)}{t_{mem}} I_{OU} dt \\ &= I_{OU} \int_{t=-t_{mem}}^{t=0} W_o(t) \frac{dt}{t_{mem}} \\ &= \frac{I_{OU}}{2} \end{aligned} \quad (4.3)$$

or

$$L_{OU} = \frac{(O_U - 1)^n}{2} \quad (4.4)$$

As O_U is constant over the sampling time, the memory load does not change over the sampling time, and therefore, the mean memory load is equal to the memory load:

$$L_{avg,OU} = \frac{(O_U - 1)^n}{2} \quad (4.5)$$

Odour units were defined in Chapter 2 as the ratio of the mean concentration to the base detection threshold (see Equation (2.1)). In this study, $c_{th,base} = 0.1 C_{avg,ref}$, therefore, $O_U = 10 C_{avg} / C_{avg,ref}$ and can be evaluated across the width of the plume.

Using Equation (4.5) to evaluate the odour unit mean memory load, a comparison between L_{avg} and $L_{avg,OU}$ is shown for crosswind and downwind positions in Figure 4.7 and 4.8 respectively. It is perhaps not appropriate to compare the resulting values for the

two mean memory loads, considering that L_{avg} is evaluated using a fluctuating time series and the complications of sensitization, whereas $L_{avg, OU}$ is evaluated using a mean concentration that does not vary in time. However, the trends between the two curves are certainly comparable.

In the crosswind direction (Figure 4.7), the odour unit method predicts a much more rapid decay in odour annoyance across the width of the plume: at a distance twice the plume spread away from the centreline, there is a 70% reduction in $L_{avg, OU}$ compared with only a 50% reduction in L_{avg} . The most dramatic difference between these two trends is that odour annoyance extends out to the far edges of the plume ($y = 3 \sigma_y$), whereas the odour units method predicts a rapid decay in odour annoyance that is no longer detectable beyond $y = 2.3 \sigma_y$ from the plume centreline. Depending on the size of plume, this could be the difference between whether or not an entire neighbourhood is affected and will be annoyed by the odour. This could have dramatic results on the acceptability of minimum separation distances between agricultural or industrial producers and neighbouring communities. The simplistic odour unit method does a poor job of predicting the extent to which an odorous plume has the potential to annoy people.

In the downwind direction (Figure 4.8), the difference in predicted odour annoyance decay between L_{avg} and $L_{avg, OU}$ is equally dramatic. Compared with the model developed in this study, the odour unit method predicts a much more rapid decay of odours in the atmosphere: there is a 96% reduction in $L_{avg, OU}$ compared with only a 30% reduction in L_{avg} over a 3.8 km range in downwind distances from the source. The odour unit method suggests that odour annoyance would disappear shortly after the 4.0 km mark, whereas the human odour annoyance model suggests that odorous plumes are much more persistent. Extending the results of this model beyond 4.0 km will be left to future studies.

4.5 Total and Detectable Memory Loads

The mean memory load results thus far include periods when the odour is both detectable and not detectable. The results of the crosswind and downwind tests are reasonable: the mean memory load decreases as both the mean concentration and intermittency factor decrease. However, it is of interest to determine how intense the mean memory load becomes and what trends dominate when only periods of detectable odour are considered. Considering times when the odorant can and can't be detected gives a picture of the level of annoyance over an entire exposure, which could be hours on end; whereas, considering only those times during an exposure when the odour can be detected gives a picture of the maximum level of annoyance an individual might experience in a few breaths. Assuming that people are just as likely to complain about odours as soon as they become annoying, as they are to wait to see if the odour persists before complaining, it is of interest to examine the worst level of annoyance a person might perceive in an odour event.

Recall the concepts of total and conditional plume statistics introduced in Chapter 3. Conditional statistics are representative of only times when the plume has non-zero

concentrations; these are also called in-plume statistics. Total statistics are representative of both non-zero and zero concentrations. For example, C_{avg} is the mean concentration (“total” is implied) and $C_{avg,p}$ is the conditional mean concentration. The relationship between C_{avg} and $C_{avg,p}$, like all total and conditional statistics, is governed by the intermittency factor, γ : where, $C_{avg} = \gamma \cdot C_{avg,p}$. This concept can also be applied to the mean memory load; however, instead of distinguishing between periods of non-zero and zero concentration, periods of detectable and non-detectable odour will be highlighted. Periods of detectable odour are indicated by periods of non-zero effective concentration, $c_{eff} > 0$.

The detectable mean memory load, $L_{avg,d}$, is calculated from the total mean memory load (including periods of zero effective concentration), L_{avg} as follows:

$$L_{avg,d} = \frac{L_{avg}}{\gamma_{odour}} \quad (4.6)$$

where γ_{odour} , odour intermittency factor, indicates the percent of exposure time when $c_{eff} > 0$, and the subscript d denotes “detectable odour” statistics.

4.5.1 Crosswind Comparison of Total and Detectable Memory Loads

Figure 4.9 (a) compares the crosswind variation in the detectable and total mean memory loads. The detectable mean memory load is larger than the total mean memory load, and unlike L_{avg} , $L_{avg,d}$ increases towards the edge of the plume.

This result can be explained by examining the desensitization and resensitization processes included in the variable detection threshold. When the exposure concentrations are mostly greater than zero, as is the case at the plume centreline, a receptor’s detection threshold grows above the base detection threshold, and the receptor becomes less sensitive to subsequent odour events. With little respite from the odour, the variable threshold is maintained at a high level, resulting in a lower effective concentration and therefore, lower detectable mean memory loads. Compare this to the edge of the plume, where the receptor is able to resensitize between odour events when intermittency is high. Despite the significant decrease in C_{avg} , the receptor is more sensitive to new odour events, due to the resensitization process, than if no respite was allowed, resulting in larger c_{eff} and therefore, larger $L_{avg,d}$. This is the battle between mean concentration and intermittency, desensitization and resensitization. The result is that when the odorant plume is present, it is more annoying at the edges of the plume than at the plume centreline, as indicated by the plot of $L_{avg,d}$. The detectable mean memory load is larger than L_{avg} all the way across the plume because even at the centreline, odour is not detectable all the time. However, considering that the plume is not frequently detectable at the edges of the plume it is overall more annoying at the plume centreline, as indicated by L_{avg} .

At the outset of this study, it was thought that a balance would be struck between mean concentration and intermittency to produce a constant level of annoyance across the plume. This is not far from model results when considering the times of odour detection, so infrequent odour events are less annoying than frequently occurring events, but slightly more annoying when considering only times when the odour is detected.

The odour intermittency factor, γ_{odour} , is shown with the (concentration) intermittency factor, γ , in Figure 4.9 (b). The odour intermittency factor follows a similar trend to γ , but is much smaller in magnitude. This result is not surprising considering that the desensitization process reduces the overall time that an odour is detectable.

The purpose of the odour annoyance model is to predict the frequency of annoyance a receptor may feel over a given period of time, from daily to annually. As such, the detectable memory load paired with the odour intermittency factor provides more descriptive measure of human annoyance than the mean memory load alone.

4.5.2 Downwind Comparison of Total and Detectable Memory Loads

Figure 4.10 (a) compares the downwind variation in the detectable and total mean memory loads. The detectable load is approximately three times larger than the total load for each downwind position, with a slight divergence between the two measures of load at positions farther downwind. This can be explained by an increase in intermittency, resulting in an increase in recovery time and a sensitization to subsequent odour events. This, in turn, results in a larger effective concentration and larger detectable mean memory load.

The odour intermittency factor, γ_{odour} , is shown with the (concentration) intermittency factor, γ , in Figure 4.10 (b). The odour intermittency factor is similar to γ , but is much smaller in magnitude. This result is not surprising considering that the desensitization process adds to the intermittency by reducing the overall time that an odour is detectable.

4.6 Comparison of Odour Load with Toxic Effects

The human ability to detect odours from sources far upwind is one that is shared with other animals as part of a survival technique which allows for the forewarning of predators and downwind tracking of prey. For many regulatory agencies, acceptable toxic limits were introduced long before acceptable odour limits and therefore toxicological effects are much more familiar. In fact, as pointed out by Dalton (2002) the distinction between toxicological effects (such as sensory irritation) and odour effects are sometimes not clearly defined. For these reasons, it is important to show the differences between downwind decay of odour annoyance and toxicity.

In a report on the effects of concentration fluctuations on allowable exposure times and emergency planning zones for hydrogen sulphide, Wilson (2003) showed that the allowable toxic load is a function of the mean concentration with a toxic load exponent q as follows:

$$\text{Allowable Toxic Load} = (K_{peak} C_{avg})^q \times \text{Allowable Exposure Time} \quad (4.7)$$

where K_{peak} is a measure of the effective “peak” concentration caused by concentration fluctuations about the mean concentration, C_{avg} , and the power q is a function of both the toxic compound and the toxicological effect of interest. Recall from Chapter 3 that the mean concentration is inversely proportional to $x^{a_z} x^{a_y}$, and that the exponents a_z and a_y are based on meteorological stability class and surface roughness. The case study chosen in this study was a neutral atmospheric stability and a surface roughness height of 0.1 m. These two characteristics result in exponent values of $a_z = 0.76$ and $a_y = 0.88$, therefore:

$$\text{Allowable Toxic Load} \propto C_{avg}^q \propto \left(\frac{1}{x^{1.64}} \right)^q \quad (4.8)$$

For hydrogen sulphide, Wilson (2003) indicates that the U.S. EPA “AEGL” toxic load exponent is $q = 4.36$ for fatalities (used for predicting 1.0% fatalities for example). Then,

$$\text{Allowable Toxic Load} \propto \frac{1}{x^{7.2}} \quad (4.9)$$

Using Equation (4.9), the decay in odour annoyance is compared with the expected decay in toxicity for hydrogen sulphide with downwind receptor position as shown in Figure 4.11. There is a clear separation between annoyance and toxicity. Downwind zones which may be free from toxic effects (such as fatalities) from a chemical release are not necessarily free from odour annoyance effects. As people are known to react to odours in adverse ways, similar to reactions to toxic levels of the odorant (Shusterman, 1998), psychosomatic effects could be felt far downwind from the source, much farther than toxic effects are predicted (and much farther downwind than odour effects are currently being predicted using O_U). The coupling of odour and toxicity models would be advantageous for regulatory agencies, however, this task would not be easy as they are governed by very different mechanisms as illustrated in Figure 4.11.

4.7 Indoor Sheltering

When exposed to unpleasant odours outdoors, a natural reaction is to flee indoors. For this reason, it is of interest to study the effect of sheltering on the predicted memory load of odour.

4.7.1 Predicting Time Series of Indoor Concentration Fluctuations

As with the rest of the study, a steady state is assumed, implying a continuous plume of odorant, with no start up time. The method for evaluating the indoor concentration

fluctuations parallels that for determining the available concentration for detection in the nose. An air filtration time constant $\tau_{up} = 1.0$ sec was used to filter the outdoor concentration fluctuations and determine the concentration available to the receptor through inhalation using a first order function, as described in Chapter 2. A parallel process occurs in indoor sheltering situations where cracks and ventilation systems allow outdoor air into and out of a building. Concentration fluctuations of indoor air can be modeled using a first order function and an air filtration time constant $\tau_{building}$ as follows:

$$\frac{dc_{indoor}}{dt} = \frac{c_{exp} - c_{indoor}}{\tau_{building}} \quad (4.10)$$

$$\tau_{building} = 3600 / ACH \text{ (sec)} \quad (4.11)$$

where c_{indoor} is the indoor air concentration and c_{exp} is the outdoor exposure concentration of odorant. This simple model assumes that the entire building is surrounded by the same exposure concentrations, which is an adequate assumption for a building that is much smaller in size than the plume. The air filtration time constant for a building is typically measured in terms of the number of air changes per hour (ACH). The Canadian Standards Association (1991) air quality for residential construction specifies a ventilation rate of 0.3 ACH in new construction. A “leaky” or “drafty” building might have 1.0 ACH, and a tightly sealed building might have 0.1 ACH.

Figure 4.12 illustrates the effect of this air filtration time constant on the outdoor concentration fluctuations at two full-scale positions: one at the plume centreline, and the other at the plume edge, both 1.0 km downwind of the source. Recall from Chapter 2 that the mean concentration at the plume edge is approximately 100 times smaller than at the plume centreline, which accounts for the concentration differences between figures (a) and (b). The time over which these figures are plotted is 300 seconds or 5.0 minutes. Notice that there is very little variation in the indoor concentration over this time. The fluctuations in indoor concentration are expanded to show the entire 7.0 hour exposure time for both of these crosswind positions in Figure 4.13. Assuming a continuous odorant plume, the indoor concentration never reaches zero while the plume surrounds the building. The ratios of concentration fluctuation intensity and mean concentration between the centreline and plume edge are maintained from outdoors to indoors; indoor fluctuations are 9.6 times more intense on the plume edge than on the centreline, while the mean concentration at the plume edge is only 1.0% of the centreline concentration.

Figure 4.14 illustrates the effect of 0.1 and 1.0 air changes per hour on indoor air concentration fluctuations. As could be expected, the fewer the air changes per hour the less sensitive the indoor air concentrations are to outdoor fluctuations and therefore, the slower the change in odorant concentration becomes (the longer the time scale of concentrations becomes). It is predicted that fewer concentration fluctuations, as a result of lower number of air changes per hour, will translate into lower levels of mean memory load.

4.7.2 Mean Memory Loads for Indoor Fluctuations

Figure 4.15 compares the total mean memory loads for indoor concentration fluctuations using 1.0 and 0.1 ACH to the outdoor total mean memory loads. As predicted, the indoor memory loads for 1.0 ACH are larger than those for 0.1 ACH, and the indoor memory loads for receptors in buildings along the plume centreline are smaller than those located at the plume edge. What might not be expected is that the model predicts larger memory loads indoors than outdoors at the edges of the plume. This can be explained by re-examining Figures 4.12 and 4.13 and noticing that these indoor time series are very similar to the time series expected outdoors along the plume centerline. The indoor time series, even those at the plume edge, are not intermittent. Desensitization decreases levels of odour annoyance, but large fluctuations are maintained at the plume edge that lead to resensitization and higher levels of annoyance. This is compared with the outdoor time series at the edge of the plume where the concentration fluctuations are highly intermittent; the periods of zero detectable concentration reduce the total memory load over an entire exposure. Intense concentration fluctuations indoors that are always greater than zero are more annoying than the infrequent odour events at the edge of the plume.

Figure 4.16 compares the indoor detectable mean memory loads and odour intermittency factors for 1.0 and 0.1 ACH to the outdoor detectable mean memory loads and intermittency factors. Considering the trends developed in the previous three sections, it is no surprise that, when detectable, the outdoor memory loads are larger than those indoors, and that, with no zero-concentration intermittent periods, the indoor odour intermittency factors are larger than outdoor factors. The detectable mean memory load is useful because it allows comparison of odour annoyances for the times when the odour is detected, which is what is ultimately informative of the true problem. The odour intermittency factor should be used in conjunction with $L_{avg,d}$ because it gives an indication of what fraction of the sampling time levels of annoyance can be expected. These two pieces of information are much more informative than the total mean memory load alone, and are only attainable from data series with concentration fluctuations, as opposed to steady mean (or peak) concentrations.

For long, continuous release exposures, a receptors inside a building located at the edge of a plume may be more annoyed indoors than outdoors. This is contrary to intuition and is bad news to regulatory agencies who may be tempted to tell those who are annoyed by outdoor airborne odorants to seek relief inside their homes.

4.8 Summary

The purpose of this study is to develop a model for human annoyance to airborne odours from agricultural and industrial sources using concepts of human response to odours and the atmospheric dilution of point source emissions. The problem of predicting human

reaction to a dispersing plume of odorant has two components: the psychophysics of human olfaction, and the mechanics of atmospheric dispersion.

A parametric study was conducted in the first section of this chapter to examine the psychophysical parameters of the proposed odour annoyance model that are related to human response to odour stimuli, and to develop a feel for sensitivity to each of these parameters. This parametric study confirmed that the odour model developed in Chapter 2 is well-behaved even over a wide range of fluctuating concentration exposures: changes in the psychophysical input parameters resulted in monotonic and predictable changes in the outcome of the odour annoyance model. A summary of the six parameters of human response utilized in this model for human odour annoyance and the sensitivity of the memory load to these parameters is presented below.

- The uptake time constant, which is used to determine the inhalation and response time of a receptor to an odorant. It is agreed in the literature that this value should be in the order of a one-second breath, or $\tau_{up} = 1.0$ s.
- The base detection threshold, $c_{th,base}$, is currently being used to assess the acceptable dilution of airborne odorants, and is used in this study as a minimum threshold for detection of an odorant. This parameter was found to have a predictable effect on the mean memory load: as expected, an increase in $c_{th,base}$ results in a decrease in odour annoyance.
- The desensitization time constant, τ_{de} , is used in this study to account for the human characteristic of habituation and adaptation to constant odour stimulus. As expected, an increase in τ_{de} results in an increase in odour annoyance.
- The resensitization time constant, τ_{re} , is used in this study to account for the human ability to recover from desensitization to an odour when exposed to a decreasing or zero concentration of the specific odorant. As expected, an increase in τ_{re} results in a decrease in odour annoyance.
- The odour intensity exponent, n , is used in an extension of Stevens' psychophysical power-law for the perceived intensity of a stimulus to describe the intensity, I , of an odour perceived by a receptor. This intensity is used to evaluate the end result of the model, the memory load, L , because people perceive odours as intensities from not as concentrations. It was found that the mean memory load is very sensitive to this parameter, especially for highly intermittent concentration time series at the edges of the plume. More work must be conducted to accurately determine this parameter for odorant and receptor groups of interest.
- The memory window is used to capture the effect of the current exposure concentration and the odour events that can be remembered by a receptor, while assuming a linear decay of memory recall. As L_{avg} is normalized by the memory time, t_{mem} , the mean memory load is independent of t_{mem} .

The second part of this chapter focused on effects that mean concentration and concentration fluctuations have on the outcome of the odour annoyance model in order to fully explore the impact of atmospheric dispersion processes. A summary of the findings of these studies is presented below.

- The human odour annoyance model developed in this study predicted a slower crosswind and downwind decay of memory load, implying a much larger

footprint of affected area than predicted using the odour unit method. It was also shown that intermittency dominates predicted levels of odour annoyance. Current odour unit methods, which use constant concentrations, do not adequately predict the atmospheric and human complexities of odour annoyance, and therefore underestimate the effects of a dispersing plume of odorant.

- Considering an entire exposure, the level of annoyance is predicted to decay towards the edge of the plume; however, considering only the times when the odorant plume is detected, this model predicts that annoyance levels are nearly constant across the plume. This last result agrees with hypothesis of this study, and is due to the complicated relationship between plume intermittency and the sensitization processes.
- Compared with the total exposure time, downwind trends in odour annoyance are maintained when only odour detection times are considered. This is due to the slow downwind decay in intermittency factor.
- It was concluded that it is more informative to report annoyance levels for times when the odour is detected and the percent time this average level of annoyance is expected, rather than an overall mean annoyance level. How predicted odour loads compare to complaint-inducing annoyance levels is left for future work.
- In a comparison of downwind decay of odour perception to toxicity, it was predicted that odour annoyance decays much more slowly than toxicity, implying that odour annoyance will be experienced much farther downwind than irritation from the odorant. This comparison also showed that results from toxic effects cannot be extrapolated to evaluate odour annoyance, as the two are governed by much different mechanisms. This is important information to those who regulate acceptable limits for both toxicity and odour annoyance, and is informative to those who try to separate annoyance and irritation effects.
- Using predicted full-scale outdoor concentration fluctuations and an indoor air filtration time constant, Equation (4.10) was used to predict indoor fluctuations and odour annoyance. Five crosswind positions were used to show that, assuming steady state, indoor sheltering did not always provide relief from annoyance, particularly at the edges of the plume.

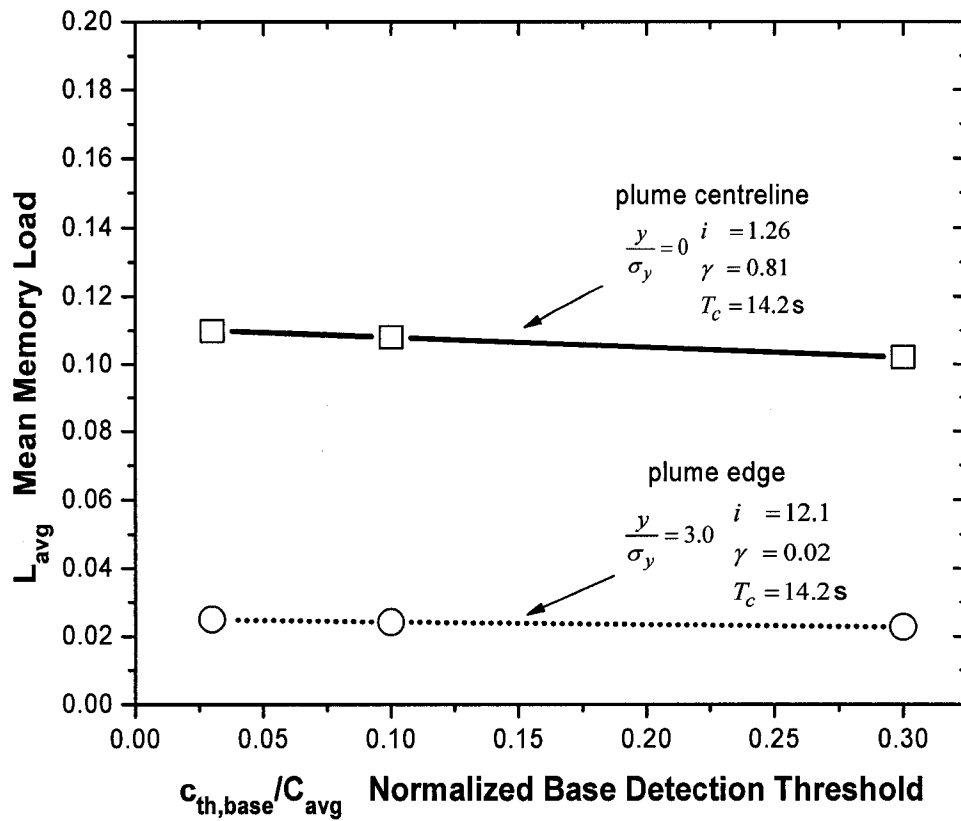
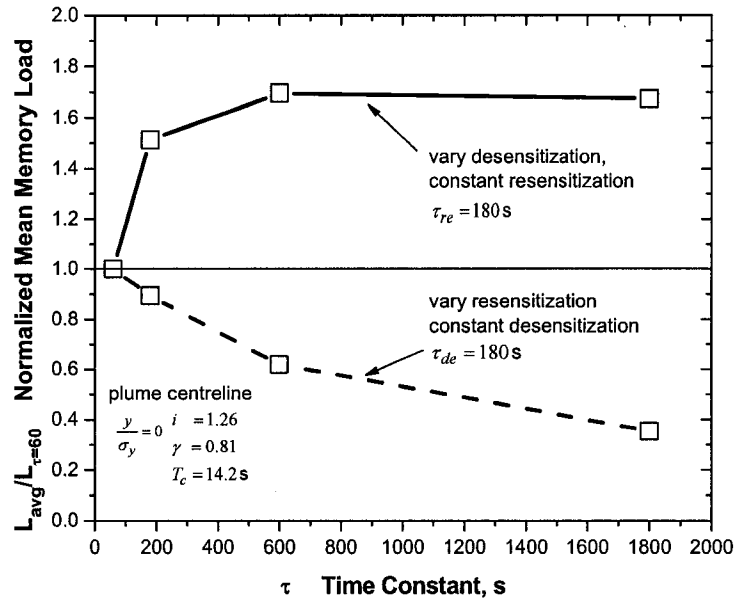
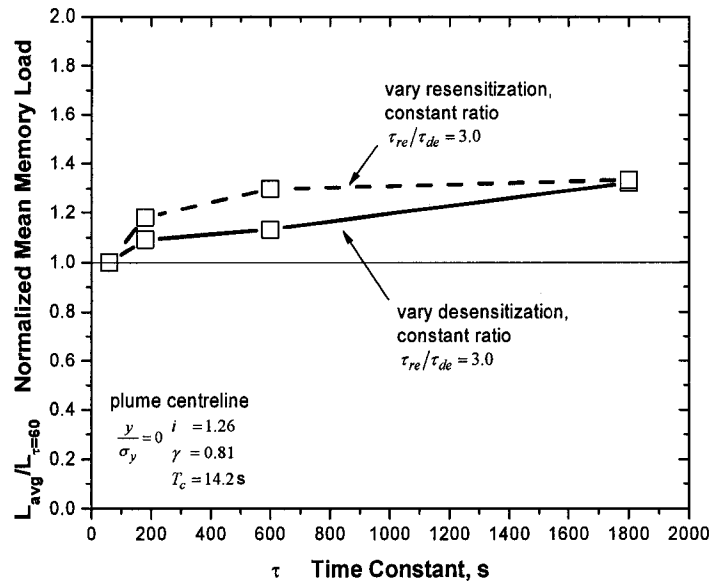


Figure 4.1: Insensitivity of mean memory load to base odour detection threshold for full-scale simulations at plume centerline and edge, 1.0 km downwind.

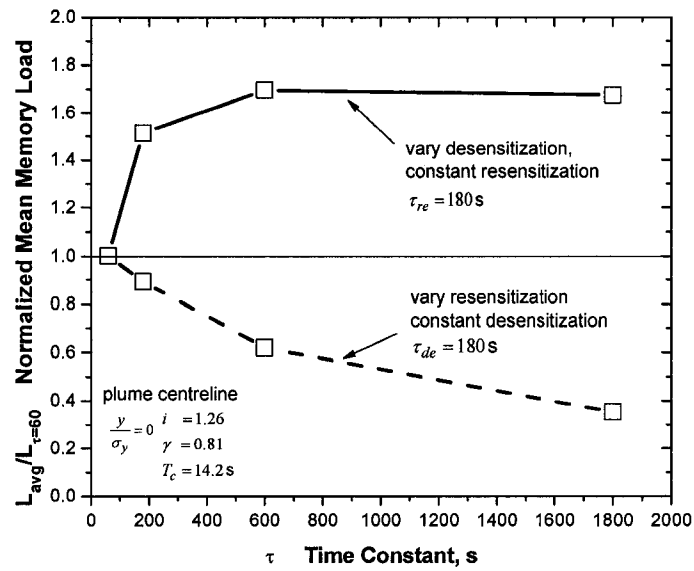


(a)

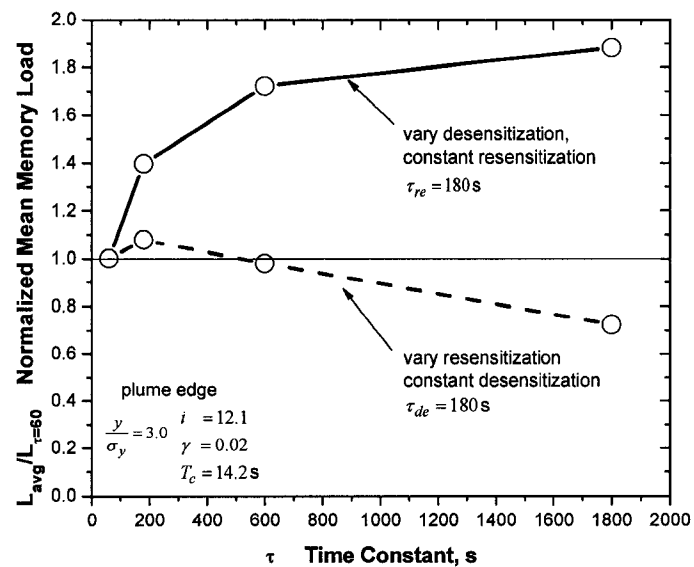


(b)

Figure 4.2: Sensitivity of mean memory load, L_{avg} , to desensitization (a) and resensitization (b) time constants, τ_{de} and τ_{re} for full-scale simulation on plume centreline, 1.0 km downwind.

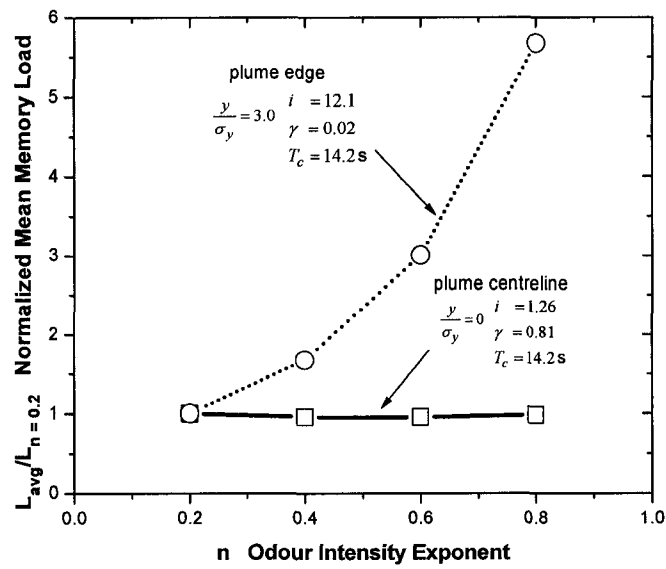


(a)

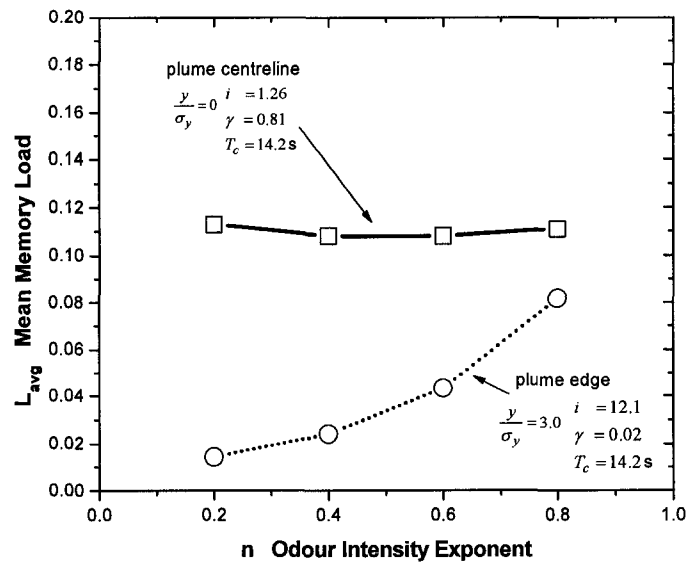


(b)

Figure 4.3: Sensitivity of mean memory load, L_{avg} , to desensitization and resensitization time constants, τ_{de} and τ_{re} for full-scale simulation on plume centreline (a) and on the plume edge (b), 1.0 km downwind. The mean memory load is equally affected by τ_{de} and τ_{re} along the plume centreline, but τ_{de} has a greater effect on L_{avg} than τ_{re} at the edge of the plume.



(a)



(b)

Figure 4.4: More than a 550% variation in mean memory load, L_{avg} , for a factor of 4.0 variation in perceived intensity exponent, n , for full-scale simulation at plume edge; compared with less than 5% variation in L_{avg} at plume centreline.

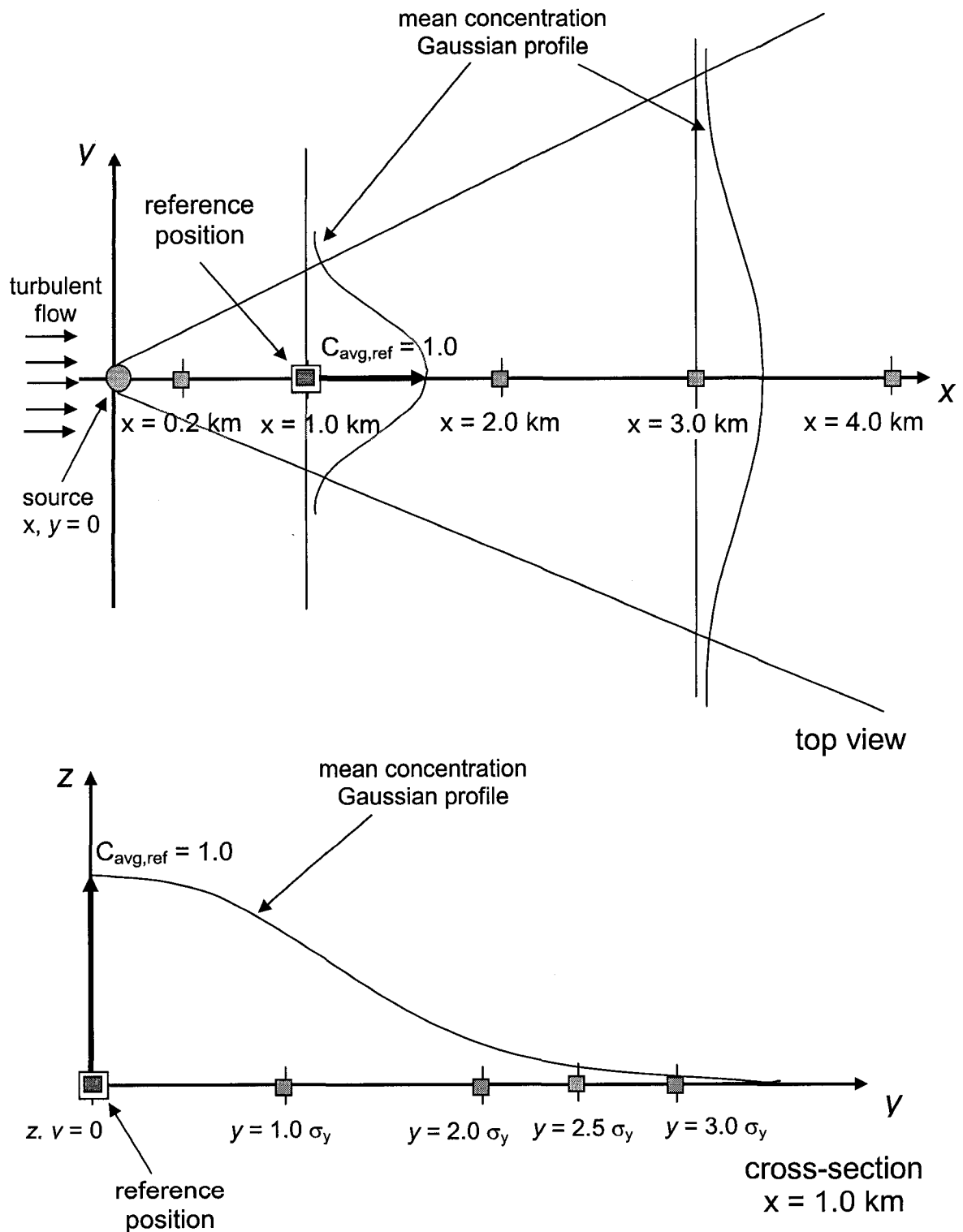


Figure 4.5: Schematic of simulated full-scale crosswind and downwind time series used to evaluate odour annoyance model.

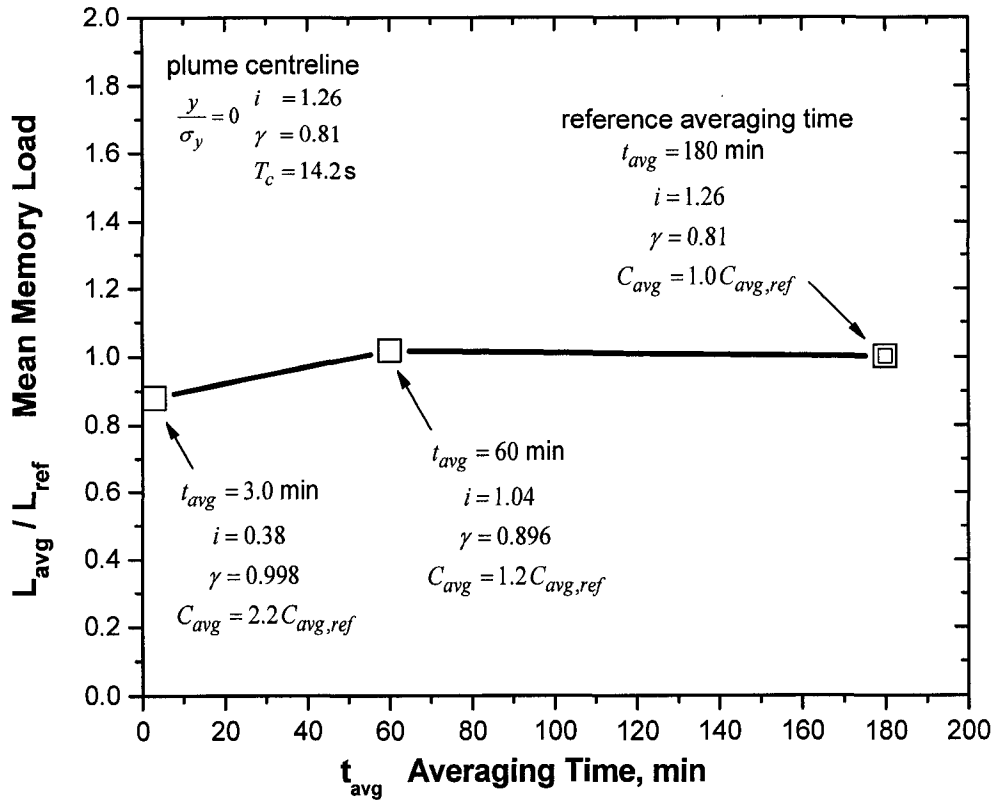


Figure 4.6: Less than 15% variation in mean memory load for a factor of 60 increase in averaging time on simulated full-scale plume centreline, 1.0 km downwind of the odorant source.

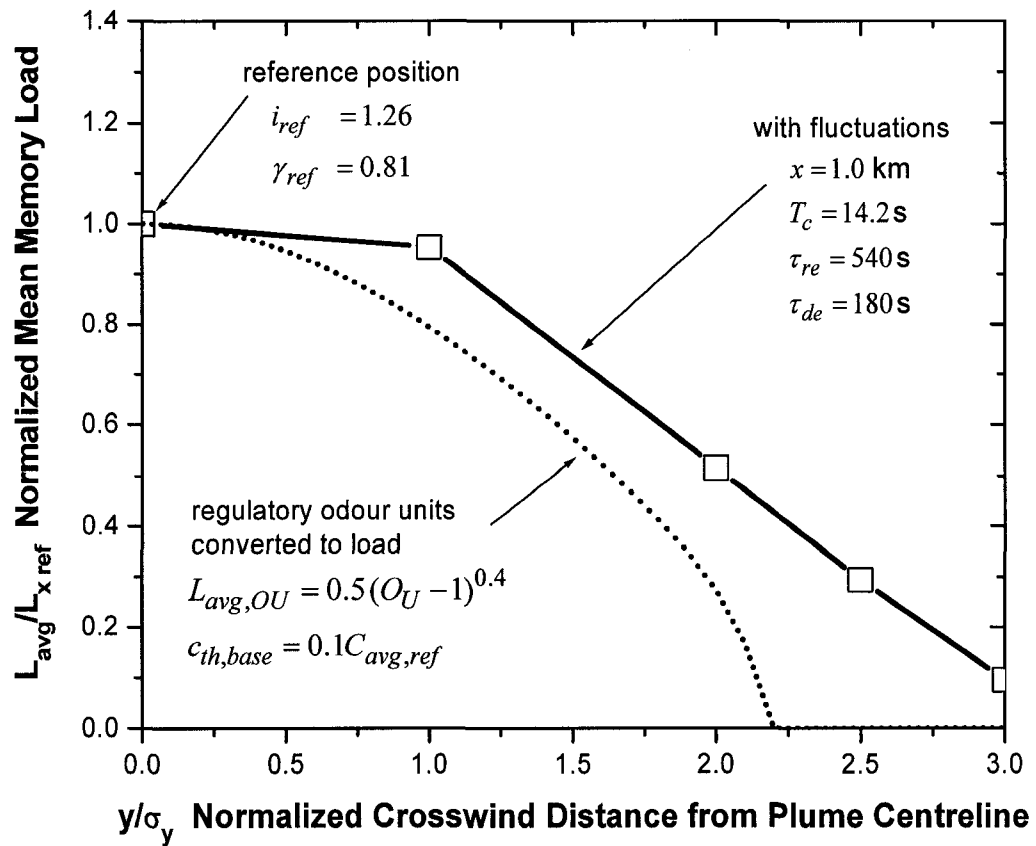


Figure 4.7: Perceived memory load changes gradually across the plume; compared to rapid decrease in regulatory odour load at plume edge.

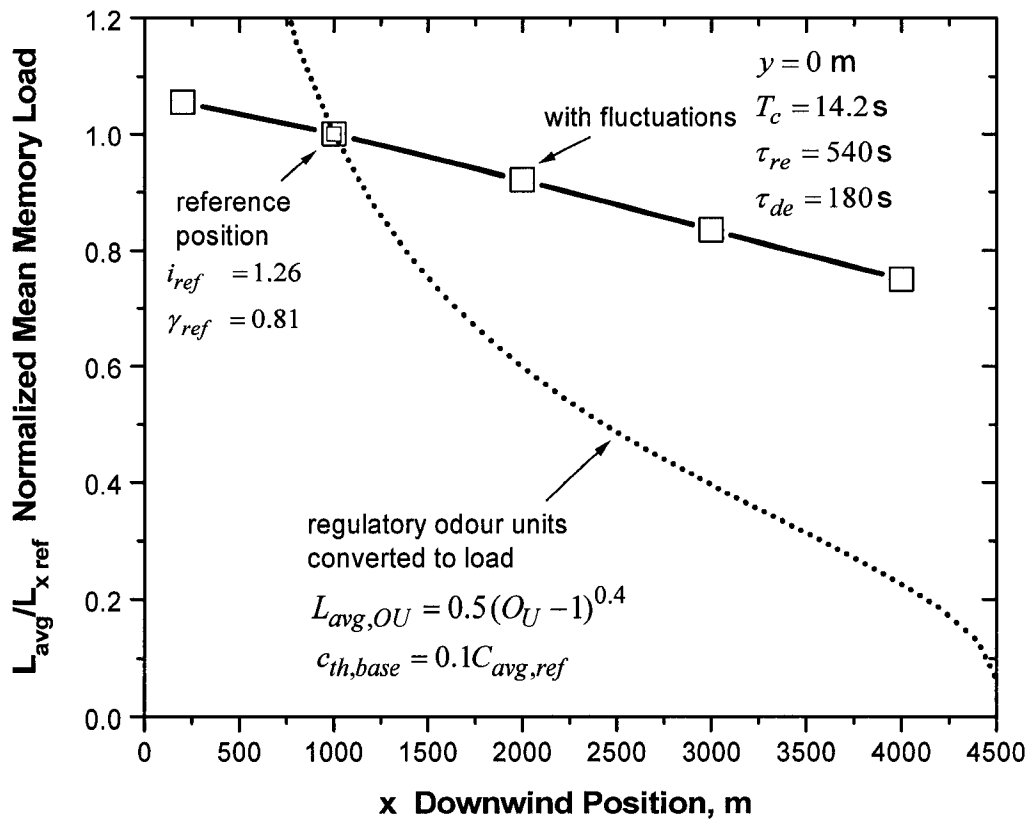
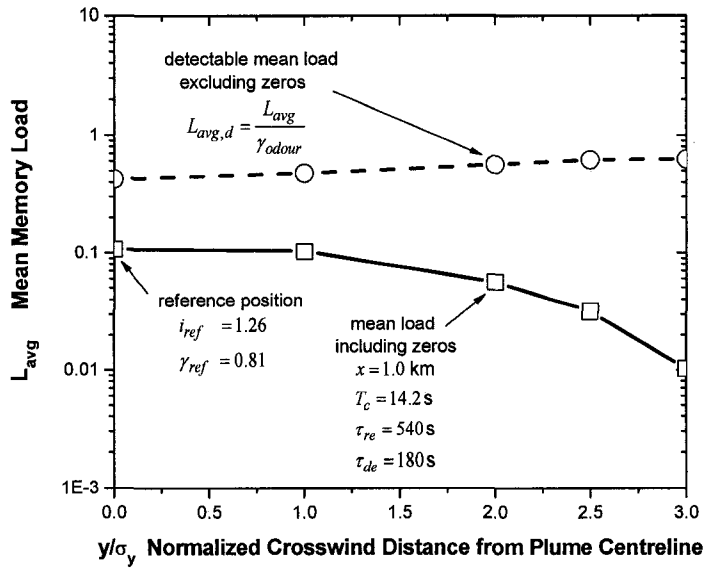
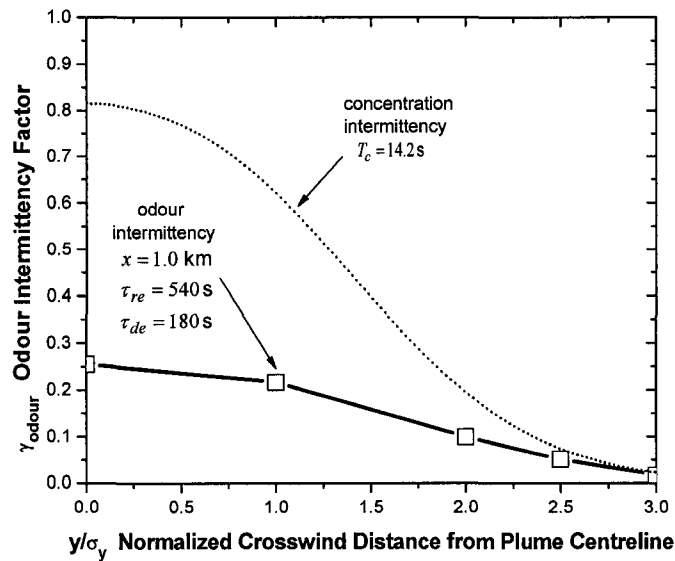


Figure 4.8: Perceived odour changes gradually downwind; compared with rapid decrease in regulatory odour load.

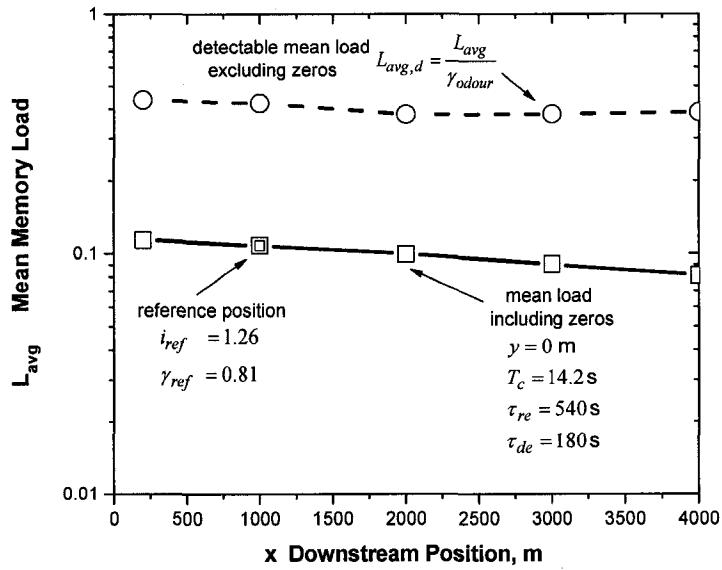


(a)

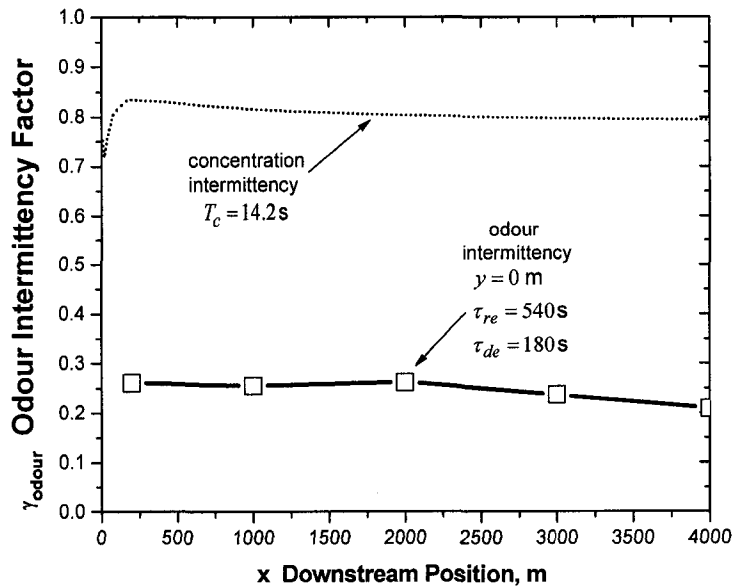


(b)

Figure 4.9: Crosswind comparison of total and detectable (zero effective concentrations removed) mean odour loads (a), and (b) between odour and concentration intermittencies. Conditional mean odour load increases from the plume centreline across the width of the plume due to resensitization between infrequent odour events. When the odour is present, it is perceived to be more intense when it occurs less frequently at the fringes of the plume.



(a)



(b)

Figure 4.10: Downwind comparison of total and detectable (zero effective concentrations removed) mean odour loads (a), and (b) between odour and concentration intermittencies. Detectable (zeros-removed) mean odour load follows general trend of the total load, but perceived intensity is larger for times when the odour is detected than perceived intensity for all times (including zero detection periods).

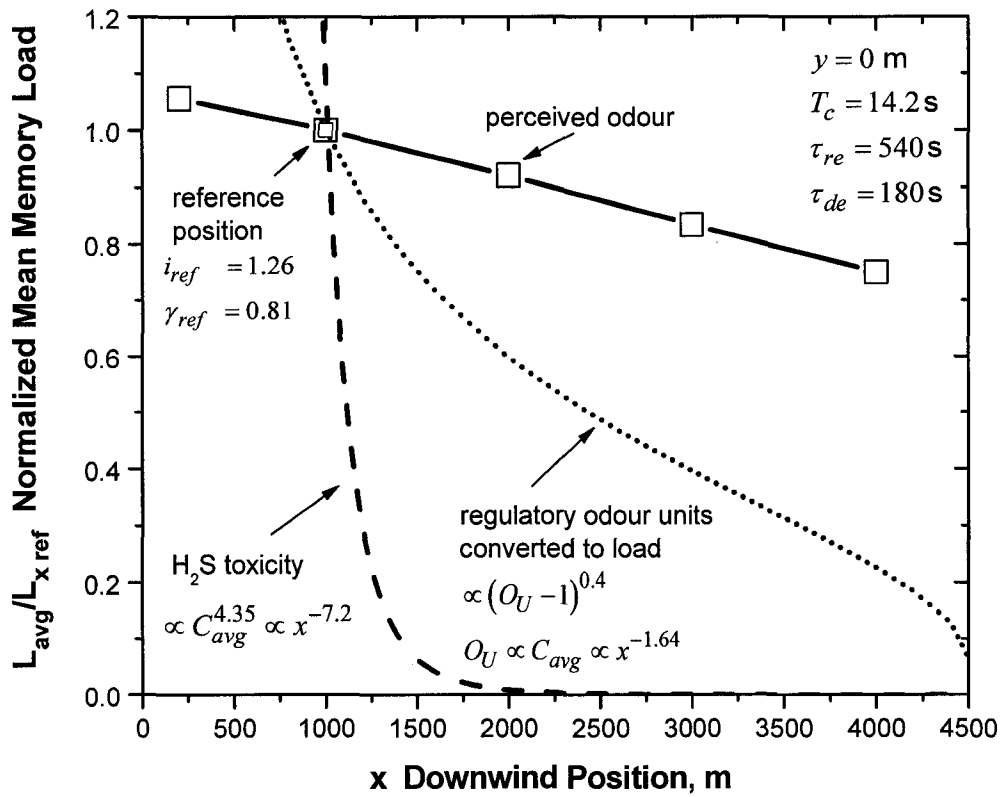
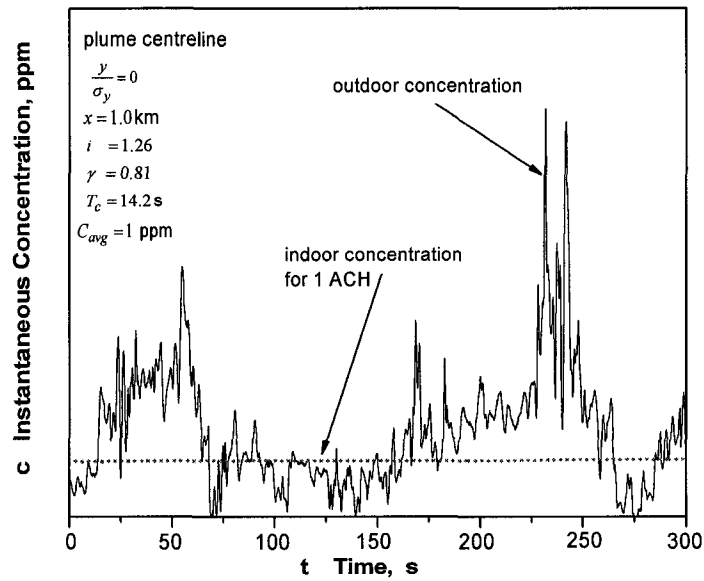
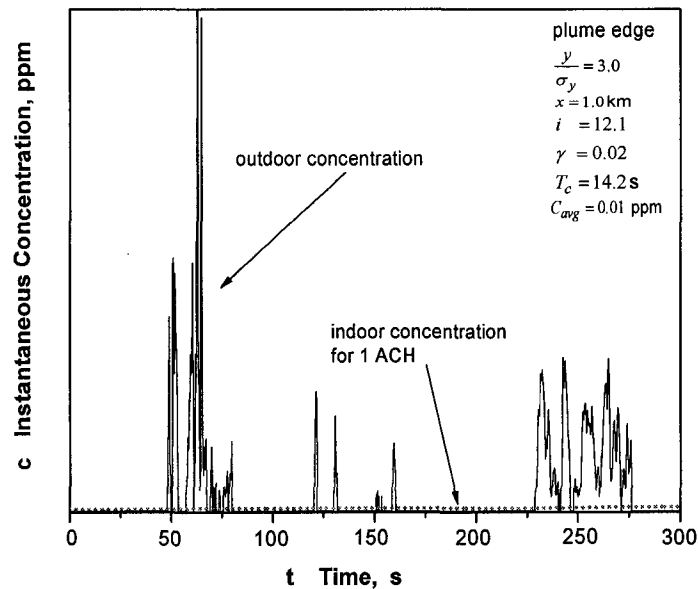


Figure 4.11: Perceived odour is virtually constant downwind; compared with rapid decrease in toxicity and regulatory odour load.

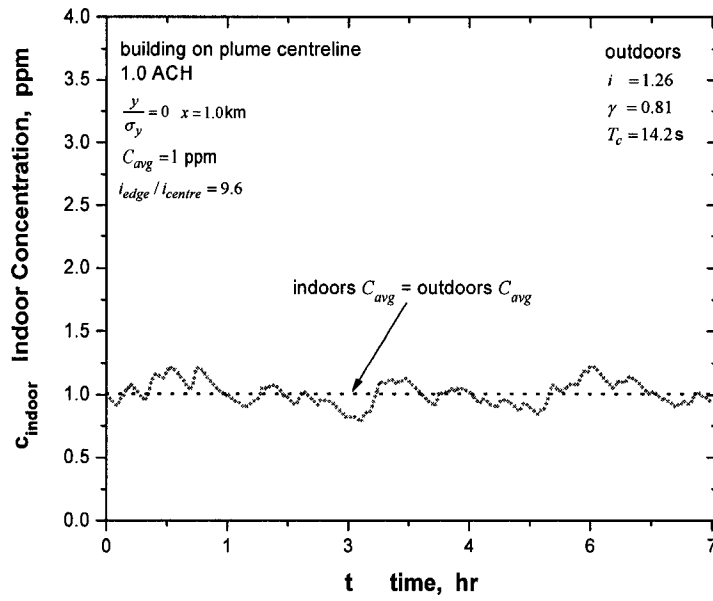


(a)

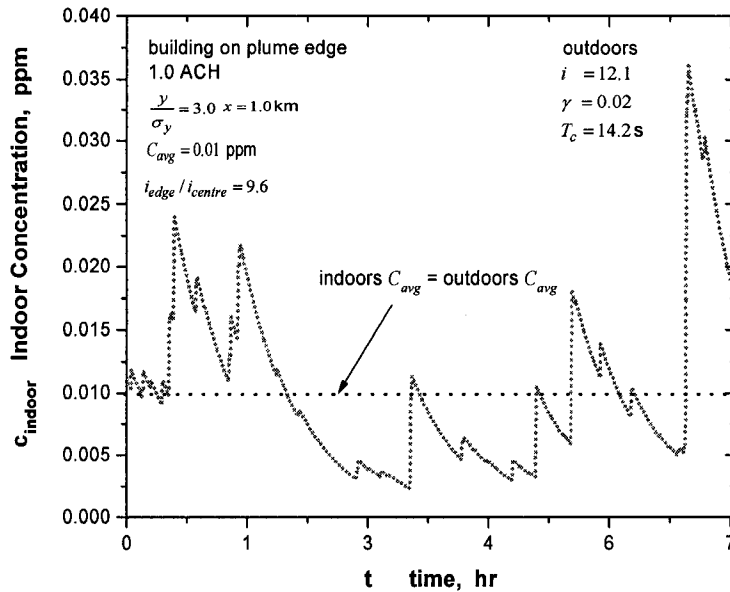


(b)

Figure 4.12: Comparison between outdoor and indoor concentration fluctuations for full-scale positions along the plume centreline (a) and at the plume edge (b), assuming one air change per hour. Outdoor high frequency fluctuations are attenuated indoors, but mean concentrations outdoors are equivalent to those indoors assuming steady state.



(a)



(b)

Figure 4.13: Ratio of concentration fluctuation intensity between centreline and plume edge is maintain from outdoors to indoors; indoor fluctuations are 9.6 times more intense on the plume edge than on the centreline, while plume edge mean concentration is only 1.0% of centreline mean concentration.

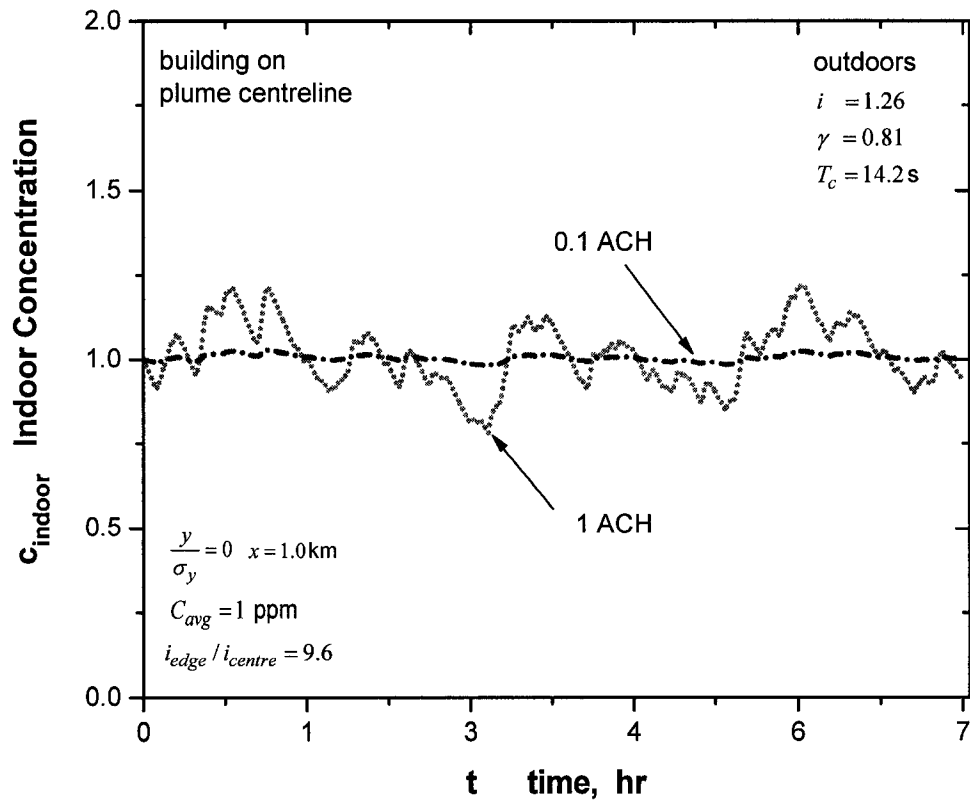


Figure 4.14: Decreasing air changes per hour (ACH) results in decreasing fluctuation intensities.

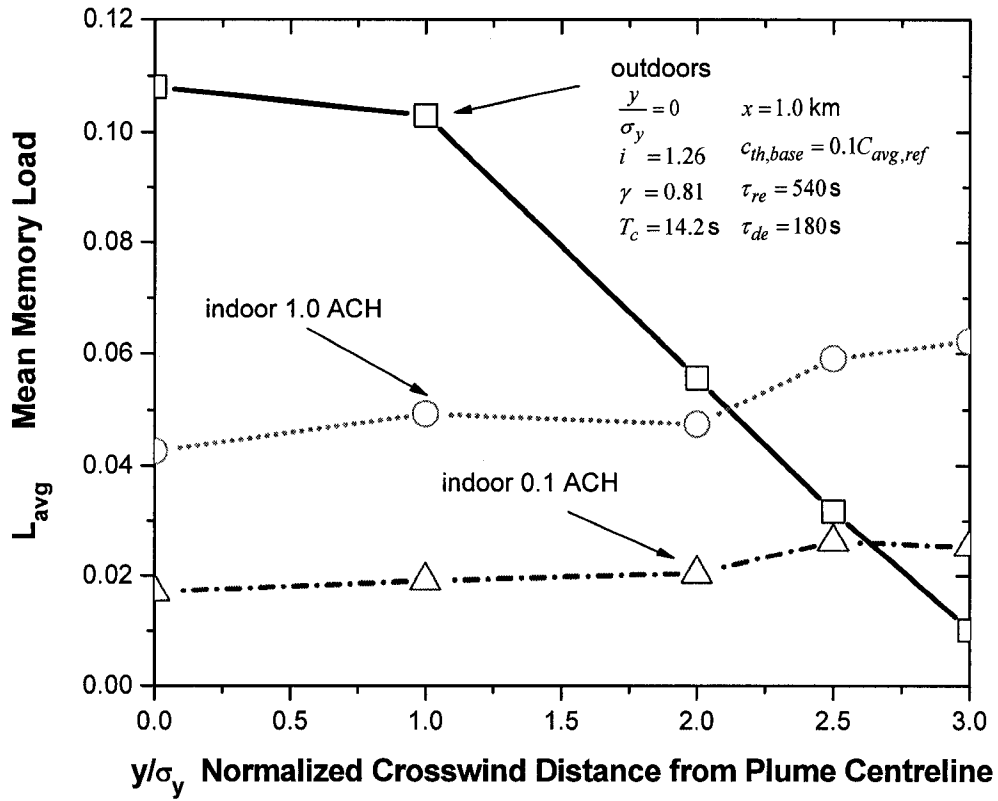
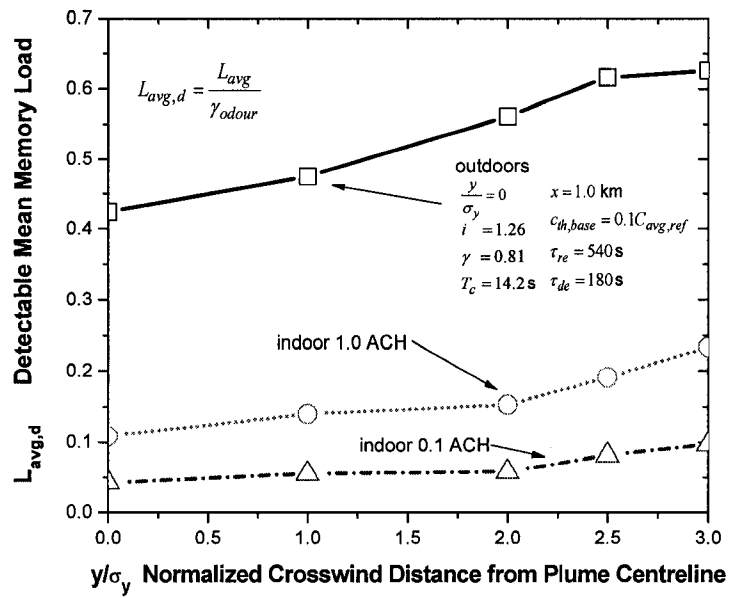
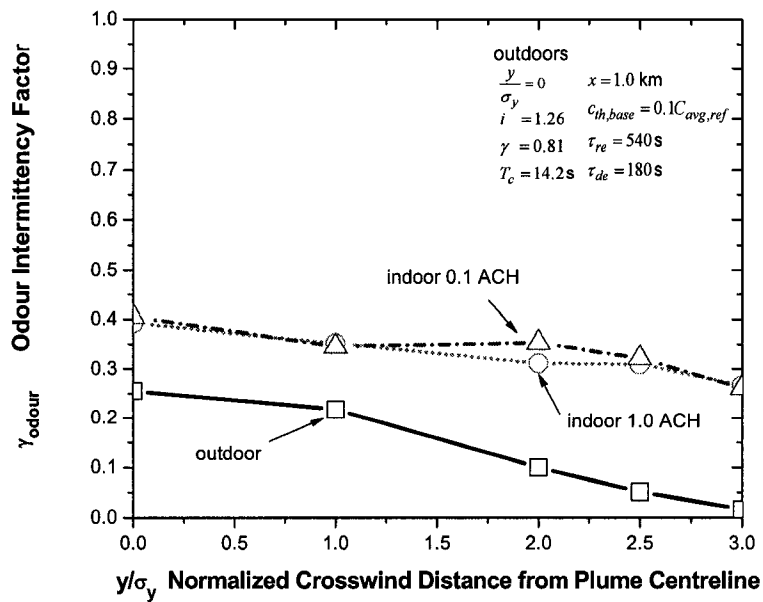


Figure 4.15: Comparison between mean memory loads for simulated outdoor and indoor concentration fluctuations shows that a person may be more annoyed indoors at the edge of the plume than outdoors.



(a)



(b)

Figure 4.16: Comparing only times when odour is detectable, mean memory loads are larger outdoor than indoors.

Chapter 5

Conclusions

The new odour annoyance model developed in this study takes into account the complexities of atmospheric dispersion and of human perception of odours. It uses current knowledge of odour perception and instantaneous concentration fluctuations to create an engineering model capable of predicting how odour perception, and therefore odour annoyance, will change from breath to breath based on exposure history, odorant type and individual people's sensitivities. This model uses a history of odorant fluctuations in conjunction with the newly developed model for how people detect, desensitize, resensitize and perceive odours to evaluate current and mean levels of odour annoyance. Readers familiar with the model can skip directly to Section 5.2.

5.1 Summary of Odour Annoyance Model

The key components of the new odour annoyance model are:

- An uptake time constant was incorporated into this model to remove the high frequency fluctuations in concentration that are averaged over one breath; fluctuations that occur faster than one breath are not important to how people perceive odours.
- Odour perception is a non-linear function of concentration that depends on both the odorant and sensitivity of an individual in question. A modified version of Stevens' power-law for perceived intensity was used in this model to measure odour annoyance, rather than concentration as is traditionally done in regulatory models.
- People are known to adapt and habituate to repeated or constant exposure to odours which leads to a decrease in sensitivity; people are also able to recover their sensitivity when the odorant is no longer present. This complex change in sensitivity means that the same concentration of odorant can be perceived differently depending on an individual's history of exposure. These desensitization and resensitization processes were accounted for in this model through a variable detection threshold, the minimum concentration of odorant required for detection. Concentrations above this threshold are those that are detectable and have the potential to cause annoyance, so these concentrations were used to evaluate the perceived intensity of odour.
- It is assumed that levels of annoyance are based on all exposure concentrations, present and past; to capture this idea, a linearly-fading memory window was used in this model. The variation in odour sensitivity within a population was

accounted for through a variable memory window length, t_{mem} , where more sensitive people can recall odour events over a longer time.

Full-scale time series of concentration fluctuations of a dispersing plume in a neutral atmosphere were simulated using laboratory-scale data taken in a water channel. Methods for predicting full-scale plume statistics were described in Chapter 3, along with the methods by which selected data were stretched in time and concentration to match predicted time scales and mean concentrations of full-scale exposures. Simulated time series at full-scale crosswind and downwind positions were designed to cover a realistic range of intermittency factors, $0.02 < \gamma < 0.8$, and conditional concentration fluctuation intensities, $1.0 < i_p < 1.4$ that are expected for a dispersing plume.

In Chapter 4, two time series of concentration fluctuations were used to evaluate the psychophysical parameters that govern the odour annoyance model: the base detection threshold, the desensitization and resensitization time constants, the odour intensity exponent, and the odour memory time. Changes in the psychophysical input parameters resulted in monotonic and predictable changes in the outcome of the odour annoyance model. This result provided confidence that crosswind and downwind trends in odour annoyance were the result of variations in concentration fluctuation statistics rather than uncertainties in the psychophysical parameters.

5.2 Conclusions

The fundamental reason for differences between current models and the model developed in this study is the complex relationship between intermittency and the processes of desensitization and resensitization. Based on this the conclusions are:

- Airborne odorants are far more persistent than are currently being predicted by models used by regulatory agencies; consequently the size of the odour annoyance area is being underestimated.
- Considering only the times intervals when an odour is detected, odour annoyance levels are almost constant across a dispersing plume of odorant.
- Comparing downwind trends, odour annoyance was shown to be more persistent than toxic effects. The difference in trends shows that separate models must be used to evaluate toxic effects and odour annoyance.
- Using the odour annoyance model developed in this study, a comparison between indoor and outdoor annoyance levels showed that people at the edge of the plume may experience higher levels of annoyance indoors than outdoors.

5.3 Future Work

This study showed that a more complicated model for odour annoyance that accounts for instantaneous concentration fluctuations and the complications of odour perception is an improvement over current regulatory models. This study offers new and important

information about human perception of airborne odorants, but it does not offer a solution that can be immediately incorporated as a regulatory model.

- In order to reduce uncertainties, more work must be done to determine the correct values of each psychophysical parameter included in this model.
- It is not clear whether a mean odour load that accounts for the average annoyance level over an entire exposure, or the detectable odour load that accounts for mean annoyance only when the odour is detected is more appropriate for use in a regulatory model. Both measures can be supported, but I feel that the detectable odour load, in combination with the percent time the odour is detectable, is more appropriate.
- By definition, odour loads greater than zero have the potential to annoy; however, future studies must be conducted to determine which odour loads will be tolerated, and which will result in a complaint.
- The odour annoyance model developed in this study should be tested over the range of sensitivities that can be expected in a population.
- This model should also be tested to evaluate crosswind and downwind trends for different environmental conditions, including atmospheric stability and wind speed.

Finally, it is demonstrated that it is the competition between the decreasing mean concentration and increasing periods of zero concentration that is fundamental to understanding the spatial persistence of odour annoyance.

References

Alberta Agriculture, Food and Rural Development, 2002. *The Application of the Minimum Distance Separation (MDS) for Siting Confined Feeding Operations in Alberta*, (A review of the current and past Agricultural Operations Practices Act for Alberta as approved by the Natural Resources Conservation Board (NRCB).), (http://www.agric.gov.ab.ca/engineer/mds_application_in_alberta.html.)

Alberta Health, 1988. Report on H₂S Toxicity, 65 pages.

Amoore, J.E., 1985. The perception of hydrogen sulfide odor in relation to setting an ambient standard. Olfacto-Labs, Berkeley, CA: prepared for the California Air Resources Board.

Amoore, J.E, Hautala, E., 1983. Odor as an aid to chemical safety: odor thresholds compared with threshold limit values and volatilities for 214 industrial chemicals in air and water dilution. *Journal of Applied Toxicology*, 3, pp. 272-90

Best, P.R., Lunney, K.E., Killip, C.A., 2001. Statistical elements of predicting the impact of a variety of odour sources, *Water Science and Technology*, 44(9), 157-164.

Berglund, U., 1974. Dynamic properties of the olfactory system, *Ann. N.Y. Acad. Sci.*, 237, pp. 17-27

Best, P.R., Lunney, K.E., and Killip, C.A, 2001. Statistical elements of predicting the impact of a variety of odour sources, *Water Science and Technology*, 44(9), pp. 157-164.

Canadian Standards Association, CAN/CSA A440.2M 1991

Cain, W.S., 1974. Perception of odor intensity and the time-course of olfactory adaptation. *ASHRAE Trans.*, 80, 53-75.

Committee Europe de Normalisation (CEN), 1998. Air quality – Determination of odour concentration by dynamic olfactometry, European Standard, CEN TC264/WG2 draft prEN for translation, WG2 prEN9805

Counihan, J., 1975. Adiabatic Atmospheric Boundary Layers: A Review and Analysis of Data from the Period 1880-1972, *Atmospheric Environment*, 9, pp. 871-905

Dalton, P., 2000. Psychophysical and Behavioral Characteristics of Olfactory Adaptation, *Chemical Senses*, 25, 487-492.

Dalton, P., 2002. Upper airway irritation, odor perception and health risk due to airborne chemicals, *Toxicology Letters*, 140-141, pp. 239-248.

Guyton, A. C., Hall, J. E., 2000. *Textbook of Medical Physiology, tenth edition*, pp. 616-619

Flesh, R.D and Turk, A., 1975. Social and economic effects of odors. In Cheremisinoff PN, Youn RA, Eds. *Industrial Odor Technology Assessment*. Ann Arbor, MI, Ann Arbor Science Publishers, pp. 57-74.

Gifford, F. A., 1959. Statistical Properties of a Fluctuation Plume Dispersion Model, *Advances in Geophysics*, 6, pp. 117-138.

Hanna, S. R., Drivas, P. J., and Chang, J. J., 1996. *Guidelines for Use of Vapor Cloud Dispersion Models*, Centre for Chemical Process Safety for the American Institute of Chemical Engineers, New York, New York, second edition.

Hilderman, T. L., 2004a. "Chapter 2: Plume Meandering and Averaging Time Effects from High Resolution One-dimensional Concentration Measurements" in unpublished PhD thesis, *Measurement, Modelling, and Stochastic Simulation of Concentration Fluctuations in a Shear Flow* University of Alberta, Department of Mechanical Engineering.

Hilderman, T. L., 2004b. "Chapter 3: Measurement and Prediction of Wind Shear Distortion of Concentration Fluctuation Statistics" in unpublished PhD thesis, *Measurement, Modelling, and Stochastic Simulation of Concentration Fluctuations in a Shear Flow*, University of Alberta, Department of Mechanical Engineering.

Hilderman, T. L., and Wilson, D. J., 1999. Simulating Concentration Fluctuation Time Series with Intermittent Zero Periods and Level Dependent Derivatives, *Boundary-Layer Meteorology*, 91, pg 451-482.

Hilderman, T. L., Hrudehy, S.E. and Wilson D.J., 1999. A model for effective toxic load from fluctuating gas concentrations, *Journal of Hazardous Materials*, A 64, pp 115-134.

Hinze, J., 1975. *Turbulence*, McGraw-Hill, Second Edition.

Irwin, J. S., 1979. A Theoretical Variation of the Wind Profile Power-Law Exponent as a Function of Surface Roughness and Stability, *Atmospheric Environment*, 13, pp. 13-20.

Jacob, T., 2003. Olfaction: A tutorial on the sense of smell, School of Biosciences, Cardiff University. (<http://www.cf.ac.uk/biosi/staff/jacob/teaching/sensory/olfact1.html>)

Jiang, J. K., and Sands, J. R., 2000. Odour and Ammonia Emission from Boiler Farms: A report for the Rural Industries Research and Development Corporation, Publication No 00/2, Project No UNS-11A

Kerschgens, M. J., Nolle, C., and Martens, R., 2000. Comments on Turbulence Parameters for the Calculation of Dispersion in the Atmospheric Boundary Layer, *Meteorologische Zeitschrift*, 9(3), pp. 155-163.

Mahin, T.D., 2001. Comparison of differing approaches used to regulate odours around the world. *Water Science and Technology*, Vol 44, No. 9, pp 87-102.

McGinley, C.M., McGinley, D.L., McGinley, K.J., 1995. Curriculum Development for Training Field Odor Investigators, *Proceedings of the Odors: Indoor and Environmental Air Specialty Conference of the Air & Waste Management Association*, Bloomington, Minnesota, September 13-15, 1995, pp. 121-130.

Mussio, P., Gnyp, A.W., Henshaw, P.F., 2001. A fluctuating plume dispersions model for the prediction of odour-impact frequencies from continuous stationary sources, *Atmospheric Environment*, 35, 2955-2962.

NSW EPA, 2002. Odour Control: Measuring Odours. New South Wales Environmental Protection Authority, Sydney, August 15, 2002.
(Found at: <http://www.epa.nsw.gov.au/mao/odourcontrol.htm#measuring%20odours>)

NSW EPA, 2001. *Draft Policy: Assessment and Management of Odour from Stationary Sources in NSW*. New South Wales Environmental Protection Authority, Sydney. ISBN 0 7313 2757 8

Omerod, R., 2001. Improving odour assessment by using better dispersion models: some examples. *Water Science and Technology*, Vol 44, No. 9, pp 149-156.

Pasquill, F. and Smith, F., 1983. *Atmospheric Diffusion*, John Wiley and Sons, third edition.

Ruth, J.H., 1986. Odor thresholds and irritation levels of several chemical substances: a review. *American Industrial Hygiene Association Journal*, 47(A), pp 142-51.

Savunen, T., and Rantakrans, E., 2000. The description and application of an odour dispersion model. *Air Pollution Modelling and Its Application XII*, pp 157-163.

Sawford, B. L. and Stapountzis, 1986. Concentration Fluctuations According to Fluctuating Plume Models in One and Two Dimensions, *Boundary-Layer Meteorology*, 37, pp. 89-105.

Schauberger, G., Piring, M., Petz, E., 2000. Diurnal and annual variation of the sensation distance of odour emitted by livestock buildings calculated by the Austrian odour dispersion model (AODM), *Atmospheric Environment*, 34, pp. 4839-4851.

Shusterman, D., 1992. Critical Review: The Health Significance of Environmental Odor Pollution. *Archives of Environmental Health*, 47, pp. 76-87.

Shusterman, D., 2001. Odor-associated health complaints: competing explanatory models. *Chemical Senses*, 26, pp. 339-343.

Smith, M. E., 1973. *Recommended Guide for the Prediction of Dispersion of Airborne Effluents*. ASME, New York.

Stevens, S.S., 1957. On the psychophysical law. *Psychol Rev*, 64(3), pp. 153-81.

Stevens, S.S., 1960. The psychophysics of sensory function. *American Scientists* 48, pp 226-253.

Sweeten, J.M., 1997. Separation Distances for Swine Odor Control in Relation to Manure Nutrient Balances. *International Symposium on Ammonia and Odour Control from Animal Production Facilities*. Vinkeloord, The Netherlands, October 6-10. pp. 659-665.

USEPA, 1995a. *User's Guide for the Industrial Source Complex (ISC3) Dispersion Models: Volume 1 - User Instructions*, U.S. Environmental Protection Agency, Research Triangle Park, North Carolina.

USEPA, 1995b. *User's Guide for the Industrial Source Complex (ISC3) Dispersion Models: Volume 2 - Description of Model Algorithms*, U.S. Environmental Protection Agency, Research Triangle Park, North Carolina.

van Ulden, A. P., and Holtslag, A. A. M., 1985. Estimation of Atmospheric Boundary Layer Parameters for Diffusion Application, *Journal of Climate and Applied Meteorology*, 24, pp. 1196-1207.

Wang, L., Walker, V. E., Sardi, H., Fraser, C., and Jacob, T. J. C., 2002. The correlation between physiological and psychological responses to odour stimulation in human subjects, *Clinical Neurophysiology*, 113, pp. 542-551.

Wilson, D. J., 1981. Along-Wind Diffusion of Source Transients, *Atmospheric Environment*, 15, pp 489-495.

Wilson, D. J., 1995. *Concentration Fluctuations and Averaging Time in Vapor Clouds*, Centre for Chemical Process Safety of the American Institute of Chemical Engineers.

Wilson, D.J., 2003. Dispersion, toxic load and odour calculations for transient releases from pipeline and gas well ruptures. Technical report for the Alberta Energy Utilities Board.

Wilson, D. J., Robins, A. G., and Fackrell, J. E., 1985. Intermittency and Conditionally-Averaged Concentration Fluctuation Statistics in Plumes, *Atmospheric Environment*, 19, pp. 1053-1064.

Wilson, D. J. and Zelt, B. W., 1990. Technical Basis for EXPOSURE-1 and SHELTER-1 Models for Predicting Outdoor and Indoor Exposure Hazards from Toxic Gas Releases, Engineering report 72, Department of Mechanical Engineering, University of Alberta.

Yamartino, R.J. and Strimaitis, D.G., 2000. Results of Extensive Evaluation of the Kinematic Simulation Particle Model Using Tracer and Wind Tunnel Experiments, In *11th joint AMS/AWMA Conference on the Applications of Air Pollution Meteorology*, Long Beach, CA, January 9-14, 2000.

Yamartino, R.J. and Strimaitis, D.G., Scire, J.S., Insley, E.M., and Spitzak, M.J., 1996. Final Report on the Phase I Development of the Kinematic Simulation Particle (KSP) Atmospheric Dispersion Model, Technical report, Institut fuer Meteorologie, Freie Universitaet Berlin, Carl-Heinrich-Becker Weg 6-10, D-12165 Berlin, Germany and Umweltbundesamt, Document No. 1274-3.